ELSEVIER

Coordination Chemistry Reviews
223 (2001) 117–216

COORDINATION CHEMISTRY REVIEWS

www.elsevier.com/locate/ccr

Tetraorganodichalcogenoimidodiphosphorus acids and their main group metal derivatives

Cristian Silvestru [a,*], John E. Drake [b]

[a] *Facultatea de Chimie si Inginerie Chimica, Universitatea Babes-Bolyai, RO-3400 Cluj-Napoca, Romania*

[b] *Department of Chemistry and Biochemistry, University of Windsor, Windsor, Ontario, Canada, N9B 3P4*

Received 8 November 2000; accepted 29 January 2001

Contents

---

* Corresponding author. Fax: +40-64-190-818.

PII: S0010-8545(01)00387-3

Abstract

The review is focused on the $(XPR_2)(YPR'_2)NH$ acids (X, Y = O, S, Se; R, R′ = alkyl, aryl, OR) and their main group metal derivatives. The methods of preparation, spectroscopic studies and molecular structures of known imidodiphosphorus acids and related derivatives as well as those of inorganic and organometallic main group metal complexes containing either protonated or deprotonated imidodiphosphorus ligand moieties are systematized and discussed. © 2001 Elsevier Science B.V. All rights reserved.

Keywords: Imidodiphosphorus acids; Metal complexes; Main group metals

1. Introduction

The coordination chemistry and uses of metal complexes of 1,1-dichalcogenophosphorus acids, e.g. diorganophosphinic acids (**1**), diorganophosphonic acids (**2**), diorganophosphoric acids (**3**) and their thio analogs, have been extensively investigated [1–10]. In contrast, imidodiphosphorus acids of the type **4**–**6** have received much less attention.

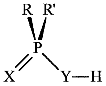

(1)

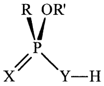

(2)

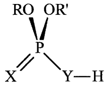

(3)

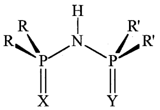

(4)

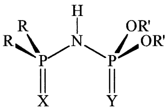

(5)

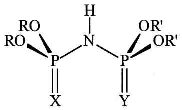

(6)

The preparation of some imidodiphosphoric acids, $[OP(OPh)_2][OP(OR'_2)]NH$ was described by Kirsanov and Zhmurova [11], and in the 1960s Schmidpeter and co-workers first reported the synthesis and spectroscopic studies of some imidodiphosphinic acids, $(XPR_2)(YPR'_2)NH$ (X, Y = O, S; R, R′ = Me, Ph), and their metal complexes [12–19]. In the next 20 years, the relatively few studies that were published were restricted mainly to the coordination properties of symmetric derivatives, i.e. those containing same organic groups and chalcogen atoms on both of the phosphorus atoms of a ligand moiety. The $[(XPR_2)(YPR'_2)N]^-$ anions were usually found to be coordinated to a metal center by both chalcogen atoms, thus leading to six-membered $MXYP_2N$ inorganic chelate (carbon-free) rings [20,21]. From this point of view, the imidodiphosphorus acids can be considered to be inorganic analogs of β-diketones. However, some important differences should be noted. The β-diketonato systems generally form planar rings due to the restricted sp^2 geometries at carbon atoms. In contrast, in the imidodiphosphorus systems the phosphorus atoms are sp^3 hybridized and the X–P–N–P–Y skeleton of the $[(XPR_2)(YPR'_2)N]^-$ anions are usually non-planar, although X-ray diffraction studies suggest considerable delocalization of the negative charge. However, in some cases the electron delocalization is limited to the P–N–P fragment or is even absent.

The last decade has seen a considerable increase in the investigations of both inorganic and organometallic compounds containing imidodiphosphorus ligands. There are several interesting fields of research being influenced by the chemistry of such complexes as summarized as follows:

1. inorganic chelate rings (metallacycles) of variable conformation due to the flexibility of the X–P–N–P–Y backbone [10,22–24];
2. metal extraction studies using mainly imidodiphosphates and their thio analogs [25–31];
3. the use of lanthanide tetraphenylimidodiphosphinates as NMR shift reagents for carboxylic acids, phenols and carboxylates [32–34];
4. potential industrial uses as catalytic systems [35];
5. the design of new materials, e.g. long-lived, highly luminiscent lanthanide complexes with potential applications in photonic devices and sensors [36];
6. potential biological activity of metal complexes since S-esters of tetraphenylmonothio- and dithioimidodiphosphinic acids, $R{-}S{-}PPh_2{=}N{-}PPh_2{=}X$ (X = O, S) were found to exhibit fungicidal activity [37].

In addition, structural chemistry [38,39] has illustrated a broad diversity of coordination patterns. The dichalcogenoimidodiphosphorus ligands exhibit a significantly larger bite than the 1,1-dichalcogenophosphorus ligands. Furthermore, coordination to a metal center may be possible through the nitrogen atom as well as through the chalcogens. Formation of supramolecular structures and heterogeometrism phenomena in metal complexes of phosphorus-based thio- and oxo-acids have also been recently reviewed [6,10].

This review will focus on imidodiphosphorus acids and their main group metal complexes. After a section dedicated to the synthesis, spectroscopic studies and structural aspects of known imidodiphosphorus acids and related derivatives, the organization of the review will be based on the protonated or deprotonated nature of the ligand in inorganic and organometallic main group metal derivatives. A second review will concern transition metal complexes.

Where possible, a table format is chosen to summarize the ligands belonging to a particular class or the metal complexes of the same group of the periodic system. References are included to the modes of synthesis and the spectroscopic methods used for characterization. Other tables contain some common structural features (e.g. monomeric, dimeric, or supramolecular associations) for compounds investigated by X-ray diffraction as well as important bond distances and angles. A search based on the original literature as well as the Cambridge Structure Database was used to collect all the available data concerning the title compounds. The structural diagrams were redrawn using the program DIAMOND [40], on the basis of reported atomic coordinates. The original atom numbering scheme was usually preserved. In some cases, for clarity and a better view of the structural pattern, only parts of the organic groups were represented.

2. Tetraorganodichalcogenoimidodiphosphorus acids, $(XPR_2)(YPR'_2)NH$ acids (X, $Y = O$, S, Se; R, $R' =$ alkyl, aryl, OR), and related derivatives

2.1. Synthesis

Several methods of synthesis [(i)–(v)] have been described so far for this type of phosphorus derivative. These are listed in Tables 1–4, along with the spectroscopic methods used for characterization.

(i) In an earlier work, Korshak and co-workers [94] first reported that a product identified as $Ph_4P_2O_2NH$ was formed in 60% yield when equimolar amounts of trichlorodiphenylphosphorane and ammonium chloride were boiled in chlorobenzene for 12 h. Obviously, water must have been present [95] and later [48] it was established that, under anhydrous conditions in dichlorobenzene, the tetraphenylimidodiphosphinic acid trichloride was formed according to Eq. (1); the latter being quantitatively converted into the corresponding acid by treatment with formic acid:

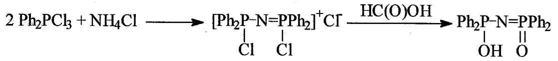

$$2\,Ph_2PCl_3 + NH_4Cl \longrightarrow [\underset{Cl}{Ph_2P}\text{-}N\text{=}\underset{Cl}{PPh_2}]^+Cl^- \xrightarrow{HC(O)OH} \underset{OH}{Ph_2P}\text{-}N\text{=}\underset{O}{PPh_2} \quad (1)$$

A similar reaction between Me_2PCl_3 and NH_4Cl failed to produce the analogous trichloride, and only $[Me_2PN]_n$ polymer was obtained [Eq. (2)] [18]:

$$n\mathrm{Me_2PCl_3} + n\mathrm{NH_4Cl} \rightarrow [\mathrm{Me_2PN}]_n + 4n\mathrm{HCl} \quad (2)$$

Tetraphenylimidodiphosphinic acid was also obtained by the hydrolysis of the reaction product of chlorodiphenylphosphine and ammonia-free chloramine in diethyl ether [Eq. (3)] [54]

Table 1
Tetraorganoimidodiphosphorus acids, $(OPR_2)(OPR'_2)NH$

Compound	Method of synthesis, yield (%)	M.p. (°C)	X-ray studies	Spectroscopic studies
$(OPMe_2)_2NH$	(i) [18]			^{31}P [41]
$(OPEt_2)_2NH$	(i), 57 [42]			
$[OP(C_3F_7)_2]_2NH$	(v), 65 [43]	–^{a}		IR, ^{1}H, ^{31}P [43]
$(OP^iPr_2)_2NH$	(iv.a), 54 [44]		[44]	IR, MS, ^{31}P [44]
$(OP^nBu_2)_2NH$	(ii.b), 54 [45]	136.5–137.5		IR [47]
	(iii) [46]	121–122		
$(OPPh_2)_2NH$	(i), 100 [48]	266.5	[52]	IR [53–55]
	(ii.b), 46 [45]	272–273		UV [53]
	(iv.a), 85 [49]	268–269		^{1}H, ^{13}C [56]
	(iv.a), 47 [50]	259–260		^{31}P [41,56]
	(iv.b), 100 [51]			
$(OPMe_2)(OPPh_2)NH$	(i), 60 [18]	217		^{1}H, ^{31}P [18,57]
	(i) [18]	216.5		IR, ^{13}C, MS [57]
$(OPEt_2)[OP(OEt)_2]NH$	(ii.b), 75 [45]	72–72.5		IR [47]
$(OPEt_2)[OP(OPh)_2]NH$	21 [58]	98	[59]	MS, ^{1}H, ^{31}P [58]
$(OP^nPr_2)[OP(OEt)_2]NH$	(ii.b), 47 [45]	–^{b}		IR [47]
$(OPPh_2)[OP(OEt)_2]NH$	(v), 67 [60]	170	[60]	IR, ^{13}C [60], ^{1}H, ^{31}P [58,60], MS [58]
	(v), 42 [58]	114		
$[OP(OMe)_2]_2NH$	(ii.a/b) [61]	–^{c}		IR, ^{1}H, ^{31}P [61]
$[OP(OEt)_2]_2NH$	(ii.b), 58 [62]	–^{d}		IR [47,61], ^{31}P [41,61]
	(ii.a/b) [61]			
$[OP(O^nPr)_2]_2NH$	(ii.a/b) [61]	–^{c}		IR [61]
$[OP(O^iPr)_2]_2NH$	(ii.b), 51 [45]	–^{e}		IR [47]
$[OP(O^nBu)_2]_2NH$	(ii.b), 34 [45]	–^{f}		IR [47], ^{1}H, ^{31}P [63]
$[OP(O^nHex)_2]_2NH$	(ii.b) [63]	–^{c}		
$[OP(O^nOct)_2]_2NH$	(ii.b) [63]	–^{c}		^{1}H, ^{31}P [63]
$[OP(OC_2H_4OC_2H_5)_2]_2NH$	(ii.b) [63]	–^{c}		
$[OP(OC_2H_4F)_2]_2NH$	(ii.b) [63]	–^{c}		
$[OP(OC_2H_4Cl)_2]_2NH$	(ii.b) [63]	–^{c}		
$[OP(OCH\{CH_2Cl\}_2)_2]_2NH$	(ii.b) [63]	–^{c}		
$[OP(OC_2H_2CF_2CF_3)_2]_2NH$	(ii.b) [63]	–^{c}		
$[OP(OEt)_2][OP(O^nBu)_2]NH$	(ii.b), 78 [45]	–^{g}		
$[OP(OMe)_2][OP(OPh)_2]NH$	(ii.a), 90 [11]			
$[OP(OEt)_2][OP(OPh)_2]NH$	(ii.a), 93 [11]			
$[OP(OPh)_2]_2NH$	(ii.a), [64]	113	[59,67]	IR [64], ^{1}H [64–66]
	(ii.a), 13 [64]	110–112		^{13}C [64,66]
	(ii.b), 57 [11]			^{31}P [41,61,64–66,68]
	(i), [65]	113		
	(v), 83 [66]	112		
$[OP(OC_6H_4CH_3\text{-}2)_2]_2NH$	(v), 74 [66]	85	[66]	^{1}H, ^{13}C, ^{31}P [66]
$[OP(OC_6H_4CH_3\text{-}3)_2]_2NH$	(v) [66]	Oil^{h}		
$[OP(OC_6H_4CH_3\text{-}4)_2]_2NH$	(v), 80 [66]	128		^{1}H, ^{13}C, ^{31}P [66]
$[OP(OPh)_2]\text{-}[OP(OC_6H_4CH_3\text{-}4)_2]NH$	(v), 81 [66]	102		^{13}C, ^{31}P [66]

[a] B.p. 130 °C/0.07 mmHg.

[b] B.p. 100–101 °C/10^{-4} mmHg.

[c] Colorless oil.

[d] B.p. 79–80 °C/10^{-3} mmHg.

[e] B.p. 109–110 °C/10^{-4} mmHg.

[f] B.p. 140–142 °C/9×10^{-5} mmHg.

[g] B.p. 118–122 °C/10^{-4} mmHg.

[h] Impure product.

Table 2
Tetraorganodithioimidodiphosphorus acids, $(SPR_2)(SPR'_2)NH$

Compound	Method of synthesis, yield (%)	M.p. (°C)	X-ray studies	Spectroscopic studies
$(SPMe_2)_2NH$	(iii), 71 [18]	177.5	[70]	IR [18,70,71]
	(iv.a), 99 [69]	177.5		Raman [71]
	(v), 55 [18]	178		^{1}H, ^{31}P [18,70], ^{13}C [70]
$(SPEt_2)_2NH$	(v), 34 [72]	111–112		
$(SP^iPr_2)_2NH$	(iv.a), 58 [73]	165–166	[73,74]	MS, ^{31}P [73]
$(SP^nBu_2)_2NH$	(v), 64 [75]	61	[75]	IR, Raman, MS, ^{1}H, ^{31}P [75]
$(SP^iBu_2)_2NH$	(v), 41 [75]	66–68	[75]	IR, ^{1}H, ^{31}P [75]
$(SP^sBu_2)_2NH$	(v), 52 [75]	93–95		IR, ^{1}H, MS, ^{31}P [75]
$(SPPh_2)_2NH$	(iii), 68 [76]	213	[52,77,78]	IR [13,71,77,79,80]
	(iv.a), 74 [49]	212–213		Raman [71,79]
	(v), 91 [13]	213.5–214.5		^{1}H, ^{13}C [56], ^{31}P [13,15,18,56,80]
$(SP^nBu_2)(SP^iBu_2)NH$	(v), 18 [75]	–[a]		IR, MS, ^{31}P [75]
$(SP^nBu_2)(SP^sBu_2)NH$	(v), 21 [75]	–[a]		IR, MS, ^{31}P [75]
$(SP^sBu_2)(SP^iBu_2)NH$	(v), 6 [75]	20–30	[75]	IR, MS, ^{31}P [75]
$(SPMe_2)(SPPh_2)NH$	(v), 32 [18]	156–157	[81]	IR, ^{1}H, ^{31}P [18,81]
	(v), 89 [81]	157–159		^{13}C, MS [81]
$(SPPh_2)[SP(OEt)_2]NH$	(v), 78 [82]	62	[82]	IR, ^{31}P [82]
$[SP(OPh)_2]_2NH$	(v), 61 [83]	112	[83]	MS [83], ^{1}H [66]
	(v) [66]			^{13}C, ^{31}P [66,83]
$[SP(OC_6H_4CH_3\text{-}2)_2]_2NH$	(v) [66]	Oil		^{1}H, ^{13}C, ^{31}P [66]
$[SP(OC_6H_4CH_3\text{-}3)_2]_2NH$	(v) [66]	Oil		^{31}P [66]
$[SP(OC_6H_4CH_3\text{-}4)_2]_2NH$	(v), 61 [66]	63–67		^{1}H, ^{13}C, ^{31}P [66]
$[SP(OPh)_2][SP(OC_6H_4\text{-}CH_3\text{-}4)_2]NH$	(v), 76 [66]	106		^{1}H, ^{13}C, ^{31}P [66]

[a] Very low temperature melting solid.

Table 3
Tetraorganodiselenoimidodiphosphinic acids, $(SePR_2)(SePR'_2)NH$

Compound	Method of synthesis, yield (%)	M.p. (°C)	X-ray studies	Spectroscopic studies
$(SeP^iPr_2)_2NH$	(iv.a), 48 [84]	172–173	[44]	IR, MS, ^{31}P [44,84]
	(iv.a), 65 [44]			^{1}H [84]
$(SePPh_2)_2NH$	(iv.a), 60 [49]	208–211	[85,87]	IR [49,86], MS, ^{1}H [86]
	(iv.a), 84 [85,86]			^{31}P [49,85,86]

Table 4
Mixed-chalcogen $(XPR_2)(YPR'_2)NH$ derivatives

Compound	Method of synthesis, yield (%)	M.p. (°C)	X-ray studies	Spectroscopic studies
$(OP^iPr_2)(SP^iPr_2)NH$	(iv.b), 25 [44]			IR, MS, ^{31}P [44]
$(OPPh_2)(SPMe_2)NH$	(v), 72 [88]	179–181	[88]	IR, ^1H, ^{13}C, ^{31}P [88]
$(OPMe_2)(SPPh_2)NH$	(v), 82 [88]	223–225	[88]	IR, ^1H, ^{13}C, ^{31}P [88]
$(OPPh_2)(SPPh_2)NH$	(i), 70 [16] (ii.b), 76 [16] (iv.b), 96 [89] (v), 89 [90]	172–174	[89,90]	IR [16,71,89,91] ^1H, ^{13}C [89,91] ^{31}P [15,16,89,91]
$[OP(OEt)_2](SPPh_2)NH$	(v), 74 [60] (v), 81 [92]	180 174	[60,92]	IR, ^{31}P [60,92] ^1H, ^{13}C [60]
$(OPPh_2)[SP(OEt)_2]NH$	(v), 73 [92]	84	[92]	IR, Raman, ^{31}P [92]
$[OP(OEt)_2][SP(OEt)_2]NH$	(ii.b), 35 [45]	–[a]		IR [47]
$[OP(OMe)_2][SP(OPh)_2]NH$	(ii.a), 90 [11]	115–117		
$[OP(OEt)_2][SP(OPh)_2]NH$	(ii.a), 81 [11]	67–69		
$[OP(OPh)_2][SP(OPh)_2]NH$	(ii.a), 87 [11] (ii.b), 53 [11] (v), 84 [66]	100–102 111		^1H, ^{13}C [66] ^{31}P [25,66]
$[OP(OC_6H_4Cl\text{-}4)_2][SP(OPh)_2]NH$	(ii.b), 34 [11]	144–146		
$[OP(OC_6H_4NO_2\text{-}4)_2][SP(OPh)_2]NH$	(ii.a) [11] (ii.b), 12 [11]	174–176		
$[OP(OC_6H_4CH_3\text{-}2)_2][SP(OC_6H_4CH_3\text{-}2)_2]NH$	(v), 85 [66]	95	[66]	^1H, ^{13}C, ^{31}P [66]
$[OP(OC_6H_4CH_3\text{-}3)_2][SP(OC_6H_4CH_3\text{-}3)_2]NH$	(v), 82 [66]	106	[66]	^1H, ^{13}C, ^{31}P [66]
$[OP(OC_6H_4CH_3\text{-}4)_2][SP(OC_6H_4CH_3\text{-}4)_2]NH$	(v), 78 [66]	126	[66]	^1H, ^{13}C, ^{31}P [66]
$(OPPh_2)(SePPh_2)NH$	(v), 74 [89]			IR, ^1H, ^{31}P [89]
$(SP^iPr_2)(SeP^iPr_2)NH$	(v), 37 [44]			IR, MS, ^{31}P [44]
$(SPPh_2)(SePPh_2)NH$	(v), 80 [93]			IR, ^1H, ^{31}P [93]

[a] B.p. 78–80 °C/10^{-4} mmHg.

$$2Ph_2PCl + 2NH_2Cl \rightarrow Ph_2P(NH_2)(Cl)\text{–}NH\text{–}PPh_2Cl_2 \xrightarrow{H_2O} (OPPh_2)_2NH \qquad (3)$$

or by the hydrolysis of $Ph_2P(O)\text{–}N{=}PPh_2Cl$, which was a secondary product (ca. 7%) in the reaction between equimolar amounts of $Ph_2P(O)N_3$ and Ph_2PCl [53].

The asymmetric trichloride, $[Me_2P(Cl)\text{–}N{=}PPh_2Cl]^+Cl^-$, was obtained by treating the corresponding dithio acid with gaseous chlorine. It can be hydrolyzed either directly to $(OPMe_2)(OPPh_2)NH$ in moist acetone or to the potassium salt by K_2CO_3 treatment in CH_2Cl_2 [18]. The methyl derivative, $(OPMe_2)_2NH$, was similarly prepared by hydrolysis of the corresponding acid trichloride, $[Me_2P(Cl)\text{–}$

$N{=}PMe_2Cl]^+Cl^-$, which was obtained by treatment of $(SPMe_2)_2NH$ with gaseous chlorine. However, in this case neither the potassium salt nor the free acid could be obtained as pure compounds [18].

The mixed chalcogen derivative $(OPPh_2)(SPPh_2)NH$ was prepared in a similar manner by hydrolysis of its monochloride (yield 70%), which in turn was obtained from the related dithio analog [Eq. (4)] [16]:

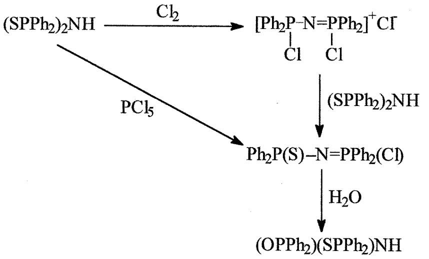

(4)

This monothio derivative has also been separated from the reaction mixture obtained by reacting Cu(II) salts with $Na[(SPPh_2)_2N]$, as a by-product of a redox process [71].

(ii.a) The tetraphenoxy derivative, $[OP(OPh)_2]_2NH$, as well as the asymmetric acids, $[XP(OPh)_2][OP(OR)_2]NH$ ($X = O, S$), were first obtained by Kirsanov and co-workers according to the following reaction sequence [Eq. (5)] [11]:

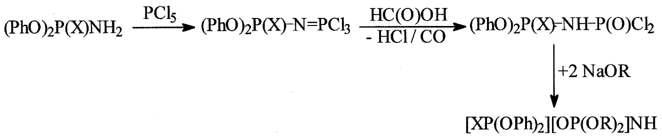

(5)

Alkolysis of $[Cl_2(O)P]_2NH$ with NaOR (R = alkyl, aryl) was also used to prepare the corresponding symmetric imidodiphosphoric acids, $[OP(OR)_2]_2NH$ [Eq. (6)] [61,64]:

$$Cl_2P(O)\text{–}NH\text{–}P(O)Cl_2 \xrightarrow[-4NaCl]{+4NaOR} [OP(OR)_2]_2NH \tag{6}$$

(ii.b) When the pentachloro derivative $Cl_2P(O)\text{–}N{=}PCl_3$ was treated with long-chain aliphatic alcohols in the presence of a HCl acceptor (amines or alkoxy derivatives), the symmetric $[OP(OR)_2]_2NH$ acids were formed directly [63]. Reaction of $Cl_2P(O)\text{–}N{=}PCl_3$ with sodium short-chain alkoxides (R = Me, Et, Pr) resulted in the formation of the 'pentaesters', $(RO)_2P(O)\text{–}N{=}P(OR)_3$, which can be converted to $[OP(OR)_2]_2NH$ derivatives by treatment with hydrochloric acid [Eq. (7)] [61,63]:

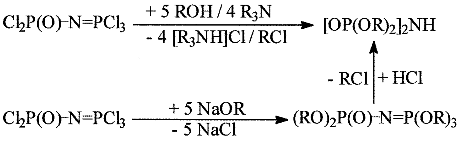

(7)

Asymmetric $[XP(OPh)_2][OP(OR')_2]_2NH$ acids can be prepared by this method if $(PhO)_2P(X)\text{–}N{=}P(OR')_3$ derivatives [obtained from $(PhO)_2P(X)\text{–}N{=}PCl_3$] are used as starting materials [11].

The reaction of diorganophosphorus azides with phosphinous esters followed by treatment of the resulting products with gaseous or alcoholic HCl also produced $(OPR'_2)(XPR_2)NH$ [Eq. (8)] [62,45]:

$$R_2P(X)N_3 + R'_2POR'' \rightarrow R_2P(X){-}N{=}PR'_2(OR'') \xrightarrow{H^+} (OPR'_2)(XPR_2)NH \tag{8}$$

This method was used mainly for the synthesis of dioxo compounds ($X = O$), but a monothio derivative ($X = S$, R, $R' = OEt$) was also prepared [45].

Similarly, the mixed chalcogen derivative $(OPPh_2)(SPPh_2)NH$ was prepared by hydrolysis of its O-methyl ester, obtained from the ammonium salt of the dithio acid [Eq. (9)] [16]:

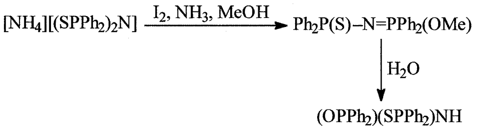

$$\begin{tikzcd}[NH_4][(SPPh_2)_2N] \arrow[r, "I_2,\ NH_3,\ MeOH"] & Ph_2P(S){-}N{=}PPh_2(OMe) \arrow[d, "H_2O"] \\ & (OPPh_2)(SPPh_2)NH\end{tikzcd} \tag{9}$$

The heating of triethyl- or triphenylphosphate, $(RO)_3P{=}O$, with $NaNH_2$ at 60–250 °C resulted in the sodium salts of the corresponding imidodiphosphoric acids [96], from which the free acid can be obtained by treatment with HCl.

(iii) The condensation of diorganophosphinyl amides, $R_2P(X)NH_2$, can be used for the synthesis of symmetric tetraorganodichalcogenoimidodiphosphinic acids [Eq. (10)]:

$$2R_2P(X)NH_2 \xrightarrow{\Delta} (XPR_2)_2NH + NH_3 \tag{10}$$

The formation of the $(OP^nBu_2)_2NH$ acid occurred simply on distillation of the corresponding amide, $^nBu_2P(O)NH_2$ [46]. Similarly, brief thermal treatment (260 °C, 15 min, N_2 atmosphere) of $Me_2P(S)NH_2$ resulted in condensation to $(SPMe_2)_2NH$ as the main product. Some evolution of H_2S and formation of small amounts of dimethylphosphazene oligomers, $[Me_2PN]_n$, was also noted [18].

When $Ph_2P(S)NH_2$ was heated in mesitylene (160 °C, 17 h) the starting material was recovered unchanged [13]. However, thermal treatment (280 °C) of thioamide in absence of any solvent resulted in formation of the corresponding dithioimidodiphosphinic acid, $(SPPh_2)_2NH$, as the main product [76]. Some side reactions also produced low yields of 2,2,4,4,6,6-hexaphenylcyclophosphazatriene (7%) and 2,4-diphenylcyclodiphosphazane-2,4-bisulfide (17%) as by-products [76].

(iv.a) A method of choice for the synthesis of symmetric $(XPR_2)_2NH$ (R = alkyl or aryl) is the oxidation of the bis(diorganophosphin)imine obtained by reacting R_2PCl ($R = {}^iPr$, Ph) with hexamethyldisilazane. Treatment of $(R_2P)_2NH$ [either isolated ($R = Ph$) or prepared in situ ($R = {}^iPr$)] with H_2O_2 (30%) [44,49], elemental sulfur [49,73] or selenium [44,84–86], or KSeCN (followed by treatment with HCl) [49] resulted in formation of the corresponding dichalcogenoimidodiphosphinates in good yields [Eq. (11)]:

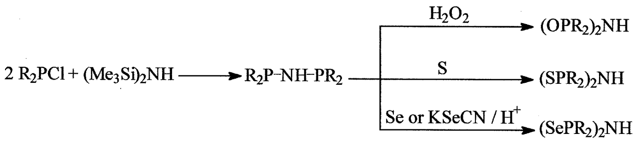

$$\begin{tikzcd}[column sep=small] & & (OPR_2)_2NH \\ 2\,R_2PCl + (Me_3Si)_2NH \arrow[r] & R_2P{-}NH{-}PR_2 \arrow[ur, "H_2O_2"] \arrow[r, "S"] \arrow[dr, "Se\ or\ KSeCN\,/\,H^+"'] & (SPR_2)_2NH \\ & & (SePR_2)_2NH\end{tikzcd} \tag{11}$$

Attempts to use ${}^{t}\mathrm{Bu_2PCl}$ as starting material in a similar reaction failed [49]. Treatment of $\mathrm{(Me_3Si)_2NH}$ with $\mathrm{Me_2P(S)Br}$ or $\mathrm{Ph_2P(S)Cl}$ in refluxing toluene also failed to lead directly to the corresponding dithio acids [49]. However, in the absence of a solvent, $\mathrm{Me_2P(S)X}$ ($\mathrm{X = Cl, Br}$) reacted rapidly with hexamethyldisilazane to produce $\mathrm{Me_2P(S){-}NH{-}SiMe_3}$, its subsequent treatment with $\mathrm{Me_2P(S)Br}$ resulting in the formation of the desired $\mathrm{(SPMe_2)_2NH}$ derivative [69]. It is probable that such reactions could also be useful for the synthesis of asymmetric $\mathrm{(XPR_2)(YPR'_2)NH}$.

Oxidation of either $\mathrm{(SPPh_2)_2NH}$ or $\mathrm{(OPPh_2)(SPPh_2)NH}$ with concentrated $\mathrm{HNO_3}$ also gave $\mathrm{(OPPh_2)_2NH}$ [16], thus indicating that both $\mathrm{P{-}C_{phenyl}}$ and P–N bonds are stable to strong oxidizing agents.

(iv.b) Mixed-chalcogen derivatives, $\mathrm{(XPR_2)(YPR_2)NH}$, can also be prepared by using a two-step oxidation procedure. Thus, partial oxidation of $\mathrm{(Ph_2P)_2NH}$ with $\mathrm{H_2O_2}$ (30%) afforded isolation of $\mathrm{Ph_2P{-}NH{-}P(O)Ph_2}$, which was then further oxidized using $\mathrm{H_2O_2}$ to yield the symmetric dioxo derivative quantitatively [51], or treated with elemental sulfur or selenium to give the corresponding mixed-chalcogen acids, $\mathrm{(OPPh_2)(YPPh_2)NH}$ ($\mathrm{Y = S, Se}$) [89]. Using a similar procedure, the thioseleno derivative, $\mathrm{(SPPh_2)(SePPh_2)NH}$, was prepared from $\mathrm{Ph_2P{-}NH{-}P(S)Ph_2}$ and Se [93]. The isolation of the P(III)/P(V) intermediate is not a strict requirement, and for $\mathrm{R} = {}^{i}\mathrm{Pr}$ the two-step oxidation process was carried out in situ leading to the $\mathrm{(XP^{i}Pr_2)(SP^{i}Pr_2)NH}$ acids ($\mathrm{X = O, Se}$) [44].

(v) A method of excellent versatility for the synthesis of both symmetric and asymmetric (different organic groups and/or chalcogen atoms at the two phosphorus atoms) $\mathrm{(XPR_2)(YPR'_2)NH}$ derivatives is the coupling reaction between an amide, $\mathrm{R_2P(X)NH_2}$, and a halide, $\mathrm{R'_2P(Y)Hal}$ ($\mathrm{Hal = Cl, Br}$), in the presence of a coupling agent, followed by $\mathrm{H^+}$ treatment to give the free acid.

In some cases, i.e. the synthesis of $\mathrm{[OP(C_3F_7)_2]_2NH}$ and $\mathrm{(SPEt_2)_2NH}$ derivatives, triethylamine [43] and sodium amide [72], respectively, have been used as coupling agents. Attempts to carry out the reaction between $\mathrm{Ph_2P(S)NH_2}$ and $\mathrm{Ph_2P(S)Cl}$ in pyridine as acid scavenger have failed to produce $\mathrm{(SPPh_2)_2NH}$, and only the pyridinium salt of diphenyldithiophosphinic acid could be isolated in low yield [13].

In earlier work, the best results in the preparation of dithioimidodiphosphinic acids using such coupling reactions were obtained using $\mathrm{KO^{t}Bu}$ followed by treatment of the resulting potassium salt with HCl [Eq. (12)] [13,18]:

$$\begin{array}{l}
\mathrm{R_2P(S)NH_2 + R'_2P(S)Hal \xrightarrow{KOBu^t} K[(SPR_2)(SPR'_2)N] \xrightarrow{HCl} (SPR_2)(SPR'_2)NH} \\
\qquad\qquad \mathrm{R = Me} \qquad \mathrm{R' = Me, Ph} \qquad \mathrm{Hal = Br} \\
\qquad\qquad \mathrm{R = Ph} \qquad \mathrm{R' = Ph} \qquad \mathrm{Hal = Cl}
\end{array} \tag{12}$$

Recently, methods of synthesis using LiBu or NaH as coupling agents have been developed for a large number of asymmetric $\mathrm{(XPR_2)(YPR'_2)NH}$ acids. The buthyllithium-based method was applied following an earlier report describing the use of LiMe in the preparation of $\mathrm{(SPPh_2)_2NH}$ [13]. LiBu is a cheaper reagent than LiMe and, since it is readily soluble in diethyl ether, its use instead of KO^{t}Bu allows better contact between the reactants and improves the yield of the $(XPR_2)(YPR'_2)NH$ final product considerably. A good yield was also found to be dependent on the use of a 2:1 molar ratio between the lithiated amide and the organophosphorus halide [Eq. (13)] [60,81,88,90]:

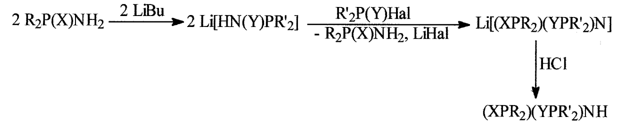

$$\begin{tikzcd} 2\,R_2P(X)NH_2 \arrow[r, "2\,LiBu"] & 2\,Li[HN(Y)PR'_2] \arrow[r, "R'_2P(Y)Hal", "-\,R_2P(X)NH_2,\ LiHal"'] & Li[(XPR_2)(YPR'_2)N] \arrow[d, "HCl"] \\ & & (XPR_2)(YPR'_2)NH \end{tikzcd} \quad (13)$$

Similarly, sodium hydride was also extensively used to deprotonate the organophosphorus amide in the first step of the synthesis of $(XPR_2)(YPR'_2)NH$ acids [13,66,75,82,83,92].

The large majority of imidodiphosphorus acids are crystalline solids, soluble in organic solvents and in some cases even in water, e.g. $(SPMe_2)_2NH$ can be recrystallized from water [18]. They are generally weak acids [45,63] and their acid strength can be tuned by changing either the organic groups or chalcogen atoms on phosphorus atoms [cf. $(SPR_2)_2NH$: R = Me, pK_a 8.7; R = Et, pK_a 9.6 (90% EtOH) [72]; $(OPEt_2)_2NH$: pK_a 7.65 (80% EtOH), 6.36 (H_2O) [45]; $[OP(OR)_2]_2NH$: R = Me, pK_a 2.6; R = Et, pK_a 3.7; R = ^{n}Pr, pK_a 4.3 (in aqueous solution) [61]).

2.2. Spectroscopic studies and structure

The spectroscopic methods used to investigate the structure of imidodiphosphorus acids are listed in Tables 1–4.

For symmetric and asymmetric imidodiphosphorus derivatives two (**7** and **8**, X = Y, same organic groups on phosphorus atoms) or three (**7**–**9**, X ≠ Y and/or different organic groups on phosphorus atoms) tautomeric forms are possible, respectively:

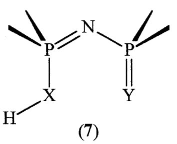

(**7**)

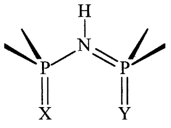

(**8**)

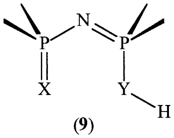

(**9**)

In earlier studies [13,16,19,71] it was suggested, at least for the solid state, that the acidic proton is linked to nitrogen (structure **8**). This was based on vibrational spectra including, in some cases, comparison with the spectra of alkali metal salts, O-esters, and S-esters. The presence of a strong IR band in the 950–900 cm^{-1} region [assigned to $\nu_{as}(P_2NH)$ stretching vibration] and the absence of strong bands around 1250 cm^{-1} supported the conclusion, which was confirmed by a large number of X-ray diffraction studies. Only in one case, i.e. the dioxo derivative containing phenyl groups on both phosphorus atoms, was it established by X-ray diffraction that the acidic proton is linked to oxygen instead of nitrogen (see subsequent discussion) [52].

The NMR spectra provided further evidence for the presence in solution of the tautomeric form **8** [13,16,19]. For example, in the case of the ^{15}N-containing $[OP(C_3F_7)_2]_2NH$ acid, the ^1H-NMR spectrum exhibited a doublet of multiplets at δ 7.39 ppm, with a $^1J(H–^{15}N)$ coupling constant of 73.5 Hz, which is consistent with the N–H structure [43]. The broad resonance observed at low field (δ 10.12 ppm) was assigned to an acidic proton, the consequence of partial dissociation in acetone-d_6 solution due to the strong electron withdrawing effect of the perfluorinated groups attached to phosphorus atoms. However, the N–*H* resonance is not usually observed in the ^1H-NMR spectra of the $(XPR_2)(YPR'_2)NH$ acids.

The parameters obtained from ^{31}P-NMR spectra (Tables 5–8) are of particular interest for the characterization of imidodiphosphorus acids and for comparative purposes in the investigation of their metal complexes.

For symmetric free acids at room temperature, only one ^{31}P resonance was observed in solution, consistent with equivalent chemical environments for the two phosphorus atoms of a molecule. In contrast, ^{31}P-NMR spectra of the asymmetric free acids in solution are usually of the AX type. As expected, they exhibited two resonances of equal intensity, generally as doublets due to phosphorus–phosphorus coupling. The assignment of these resonances for the seleno derivatives was facilitated by the presence of $^{31}P–^{77}Se$ satellites. For $(SePPh_2)_2NH$, the spectrum consists of a singlet of 92% intensity which is superposed with the AA′X spectrum of the $(SePPh_2)(^{77}SePPh_2)_2NH$ isotopomer [85,86]. In some cases the difference in the chemical shifts of the two ^{31}P resonances is quite small and their assignment was based on the $^{13}C–^{31}P$ coupling constants by comparison with the data obtained from the ^{13}C-NMR spectra.

The ^{31}P-NMR spectra failed to provide evidence for hydrogen bonding in solution. The solid state ^{31}P-NMR of $(SPR_2)_2NH$ ($R = {}^nBu$, ${}^iBu$) [75] and $(SPPh_2)[SP(OEt)_2]NH$ [82] also showed only the expected doublet resonances. In contrast, for the *sec*-butyl analog, the spectrum suggests the compound is present in two independent environments in the solid state, due to weak hydrogen bonding. This behavior was also supported by its solid state ^{15}N-NMR spectrum (two distinct resonances at 322 and 325 ppm) [75].

The solid state structure of several imidodiphosphorus acids have been investigated by single-crystal X-ray diffraction. Important interatomic bond distances and angles for all compounds of this class investigated so far are listed in Table 9.

With one exception, i.e. the tetraphenylimidodiphosphinic acid [52] (see subsequent discussion), some general features are common for all imidodiphosphorus acids investigated. Thus, the phosphorus–oxygen, phosphorus–sulfur and phosphorus–selenium bond distances (range 1.44–1.49, 1.89–1.96 and 2.08–2.10 Å) are typical for P=O, P=S and P=Se double bonds, respectively, as are the phosphorus–nitrogen bond distances (range 1.62–1.71 Å) for P–N single. The acid hydrogen atom is linked to the nitrogen atom, the P_2NH system is planar or close to planarity (thus suggesting considerable sp^2 character at nitrogen), and the P–N–P system is angular (range 122–133°). To date, in contrast, the tetraphenylimidodiphosphinic acid is unique in this class because the acid hydrogen is not attached to the

Table 5
^{31}P-NMR data for tetraorganoimidodiphosphorus acids, $(OPR_2)(OPR'_2)NH$

Compound	Solvent	$\delta(^{31}P)$ (ppm), $^nJ(PX)$ (Hz)			Ref.
$(OPMe_2)_2NH$			43.4s		[41]
$[OP(C_3F_7)_2]_2NH$	Et_2O		25.5m, $^2J(PF)$ 88		[43]
$(OP^iPr_2)_2NH$	$CDCl_3$		55.5s		[44]
$(OPPh_2)_2NH$			14.5s		[41]
	$CDCl_3$		19.4s		[56]
$(OPMe_2)(OPPh_2)NH$	CH_2Br_2	44.4s (P–Me)		21.3s (P–Ph)	[18]
	$CDCl_3$	44.7s (P–Me)		22.4s (P–Ph), $^1J(PC)$ 126.3	[57]
$(OPEt_2)[OP(OPh)_2]NH$	C_6D_6	51.9d (P–Et), $^2J(PP)$ 9.8		-8.8d (P–OPh), $^2J(PP)$ 9.8	[58]
$(OPPh_2)[OP(OEt)_2]NH$	$CDCl_3$	26.1s (P–Ph), $^1J(PC)$ 130.0		1.8s (P–OEt)	[60]
	C_6D_6	20.1d (P–Ph), $^2J(PP)$ 2.8		0.7d (P–OEt), $^2J(PP)$ 2.8	[58]
$[OP(OMe)_2]_2NH$			3.0s		[61]
$[OP(OEt)_2]_2NH$			2.5s		[41]
			-1.1s		[61]
$[OP(OPh)_2]_2NH$			-10.7s		[41,65]
			-11.3s		[68]
	$CDCl_3$		-9.9d, $^2J(PP)$ 7.6		[66]
$[OP(OC_6H_4CH_3\text{-}2)_2]_2NH$			-11.0s		[68]
	$CDCl_3$		-9.0s		[66]
$[OP(OC_6H_4CH_3\text{-}4)_2]_2NH$			-11.0s		[68]
	$CDCl_3$		-10.1s		[66]
$[OP(OPh)_2][OP(OC_6H_4CH_3\text{-}4)_2]NH$	$CDCl_3$	-9.9d (P–OPh), $^2J(PP)$ 5.8		-9.7d (P–$OC_6H_4CH_3$-4), $^2J(PP)$ 5.8	[66]

Table 6

^{31}P-NMR data for tetraorganodithioimidodiphosphorus acids, $(SPR_2)(SPR'_2)NH$

Compound	Solvent	$\delta(^{31}P)$ (ppm), $^{n}J(PX)$ (Hz)			Ref.
$(SPMe_2)_2NH$	CH_2Cl_2		59.6s		[18]
	$CDCl_3$		60.4s		[70]
$(SP^{i}Pr_2)_2NH$	$CDCl_3$		91.2s		[73,74]
$(SP^{n}Bu_2)_2NH$	$CDCl_3$		71.0s		[75]
$(SP^{i}Bu_2)_2NH$	$CDCl_3$		68.3s		[75]
$(SP^{s}Bu_2)_2NH$	$CDCl_3$		87.2s		[75]
$(SPPh_2)_2NH$	THF		55.1s		[13,15,18]
			55.7s		[80]
	$CDCl_3$		57.6d, $^{2}J(PP)$ 23.5		[66]
$(SP^{n}Bu_2)(SP^{i}Bu_2)NH$	$CDCl_3$	72.3d (P–^{n}Bu), $^{2}J(PP)$ 26.4		70.4d (P–^{i}Bu), $^{2}J(PP)$ 26.4	[75]
$(SP^{n}Bu_2)(SP^{s}Bu_2)NH$	$CDCl_3$	84.7d (P–^{s}Bu), $^{2}J(PP)$ 30.8		79.0d (P–^{n}Bu), $^{2}J(PP)$ 30.8	[75]
$(SP^{s}Bu_2)(SP^{i}Bu_2)NH$	$CDCl_3$	82.8d (P–^{s}Bu), $^{2}J(PP)$ 30.8		76.1d (P–^{i}Bu), $^{2}J(PP)$ 30.8	[75]
$(SPMe_2)(SPPh_2)NH$	CH_2Cl_2	64.1s (P–Me)		52.5s (P–Ph)	[18]
	$CDCl_3$	63.9d (P–Me), $^{2}J(PP)$ 22.8		51.3d (P–Ph), $^{2}J(PP)$ 22.8	[81]
$(SPPh_2)[SP(OEt)_2]NH$	$CDCl_3$	63.6d (P–OEt), $^{2}J(PP)$ 22.0		53.3d (P–Ph), $^{2}J(PP)$ 22.0	[82]
$[SP(OPh)_2]_2NH$	$CDCl_3$		51.8d, $^{2}J(PP)$ 24.3		[66]
$[SP(OC_6H_4CH_3\text{-}2)_2]_2NH$	$CDCl_3$		50.0s		[66]
$[SP(OC_6H_4CH_3\text{-}3)_2]_2NH$	$CDCl_3$		52.0s		[66]
$[SP(OC_6H_4CH_3\text{-}4)_2]_2NH$	$CDCl_3$		51.5s		[66]
$[SP(OPh)_2][SP(OC_6H_4CH_3\text{-}4)_2]NH$	$CDCl_3$	52.5d (P–$OC_6H_4CH_3$-4), $^{2}J(PP)$ 24.3		52.0d (P–OPh), $^{2}J(PP)$ 24.3	[66]

Table 7
^{31}P-NMR data for tetraorganodiselenoimidodiphosphinic acids, $(SePR_2)(SePR'_2)NH$

Compound	Solvent	$\delta(^{31}P)$ (ppm), $^{n}J(PX)$ (Hz)	Ref.
$(SeP^{i}Pr_2)_2NH$	$CDCl_3$	89.5s, $^{1}J(PSe)$ 757	[44]
	$CDCl_3$	90.8s, $^{1}J(PSe)$ 755	[84]
$(SePPh_2)_2NH$	CD_2Cl_2	53.0s, $^{1}J(PSe)$ 793	[85]
	$CDCl_3$	53.2s, $^{1}J(PSe)$ 786	[86]

Table 8
^{31}P-NMR data for mixed-chalcogen $(XPR_2)(YPR'_2)NH$ derivatives

Compound	Solvent	$\delta(^{31}P)$ (ppm), $^{n}J(PX)$ (Hz)		Ref.
$(OP^{i}Pr_2)(SP^{i}Pr_2)NH$	$CDCl_3$	90.9d (P=S), $^{2}J(PP)$ 21.9	54.8d (P=O), $^{2}J(PP)$ 21.9	[44]
$(OPPh_2)(SPMe_2)NH$	$CDCl_3$	63.0d (P=S), $^{2}J(PP)$ 19.5, $^{1}J(PC)$ 65.4	23.9d (P=O), $^{2}J(PP)$ 19.5, $^{1}J(PC)$ 124.8	[88]
$(OPMe_2)(SPPh_2)NH$	$CDCl_3$	47.9s (P=S)	50.8d (P=O), $^{2}J(PP)$ 6.9, $^{1}J(PC)$ 84.0	[88]
$(OPPh_2)(SPPh_2)NH$	CH_2Cl_2	54.2s (P=S)	22.1s (P=O)	[15,16]
	$CDCl_3$	56.1d (P=S), $^{2}J(PP)$ 17.5	23.1d (P=O), $^{2}J(PP)$ 17.5	[91]
$[OP(OEt)_2](SPPh_2)NH$	$CDCl_3$	53.2d (P=S), $^{2}J(PP)$ 8.2	1.3d (P=O), $^{2}J(PP)$ 8.2	[60]
		53.3d (P=S), $^{2}J(PP)$ 13.2	0.1d (P=O), $^{2}J(PP)$ 13.2	[92]
$(OPPh_2)[SP(OEt)_2]NH$	$CDCl_3$	64.1d (P=S), $^{2}J(PP)$ 17.6	19.7d (P=O), $^{2}J(PP)$ 17.6	[92]
$[OP(OPh)_2][SP(OPh)_2]NH$	$CDCl_3$	52.1s (P=S)	−11.1s (P=O)	[25]
		53.3d (P=S), $^{2}J(PP)$ 3.6	−11.1d (P=O), $^{2}J(PP)$ 3.6	[66]
$[OP(OC_6H_4CH_3\text{-}2)_2]$-$[SP(OC_6H_4CH_3\text{-}2)_2]NH$	$CDCl_3$	52.3s (P=S)	−9.9s (P=O)	[66]
$[OP(OC_6H_4CH_3\text{-}3)_2]$-$[SP(OC_6H_4CH_3\text{-}3)_2]NH$	$CDCl_3$	52.3s (P=S)	−11.0s (P=O)	[66]
$[OP(OC_6H_4CH_3\text{-}4)_2]$-$[SP(OC_6H_4CH_3\text{-}4)_2]NH$	$CDCl_3$	53.1s (P=S)	−10.3s (P=O)	[66]
$(OPPh_2)(SePPh_2)NH$	$CDCl_3$	52.4d (P=Se), $^{2}J(PP)$ 24, $^{1}J(PSe)$ 779	21.0d (P=O), $^{2}J(PP)$ 24, $^{1}J(PSe)$ 779	[89]
$(SP^{i}Pr_2)(SeP^{i}Pr_2)NH$	$CDCl_3$	92.1d (P=S), $^{2}J(PP)$ 35.2, $^{1}J(PSe)$ 747	89.2d (P=Se), $^{2}J(PP)$ 35.2, $^{1}J(PSe)$ 747	[44]
$(SPPh_2)(SePPh_2)NH$	$CDCl_3$	57.1d (P=S), $^{2}J(PP)$ 28, $^{1}J(PSe)$ 783	52.7d (P=Se), $^{2}J(PP)$ 28, $^{1}J(PSe)$ 783	[93]

nitrogen, but rather a symmetric O–H–O intermolecular bridge is established [52]. In this case the phosphorus–nitrogen bond distances [1.535(1) Å] are consistent with double bond character (cf. $S{=}PPh_2{-}N{=}PPh_2{-}SMe$ [97]: P–N 1.610(4), P=N 1.568(4) Å; $[(Me_3Si)_2N{-}P({=}N^{t}Bu)S]_2$ [98]: P–N 1.662(2), P=N 1.529(2) Å) and the P–N–P fragment is linear (180°).

The conformation of the X–P–N–P–Y skeleton exhibits a broad diversity in the free acids which reflects the high flexibility of this inorganic fragment. Basically it can be described in terms of *anti* (**10**) (X–P···P–Y torsion angle generally in the range 150–180°) and *syn* (**11** and **12**) (X–P···P–Y torsion angle smaller than 90°) with respect to the relative orientations of the phosphorus–chalcogen bonds.

Table 9
X-ray data [bond lengths (Å) and bond angles (°)] for $(OPR_2)(OPR'_2)NH$ acids

Compound	P–O	P–S	P–Se	P–N	P–N–P	Ref.
$(OP^iPr_2)_2NH$	1.486(2), 1.471(2)			1.671(2), 1.669(2)	130.0(2)	[44]
$(OPPh_2)_2NH$	1.519(2)			1.535(1)	180	[52]
$(OPEt_2)[OP(OPh)_2]NH$	1.482(2) (PEt), 1.454(2) (POPh)			1.683(3), 1.630(3)	129.7(1)	[59]
$(OPPh_2)[OP(OEt)_2]$-$NH \cdot 1/2HCl \cdot 1/4H_2O$	1.463(8) (PPh), 1.448(4) (POEt)			1.66(1), 1.62(1)	126.5(6)	[60]
$[OP(OPh)_2]_2NH$	1.458(4), 1.446(4)			1.632(2), 1.646(2)	130.9(1)	[59]
	1.474(5), 1.448(4)			1.639(6), 1.653(6)	130.0(3)	[67]
$[OP(OC_6H_4CH_3\text{-}2)_2]_2NH$	1.465(2), 1.453(2)			1.641(2), 1.645(3)	130.4(2)	[66]
$(SPMe_2)_2NH$		1.962(2), 1.939(2)		1.675(3), 1.679(3)	133.2(2)	[70]
$(SP^iPr_2)_2NH$		1.949(1), 1.941(1)		1.684(2), 1.682(3)	131.6(1)	[73,74]
$(SP^nBu_2)_2NH$		1.941(2), 1.929(2)		1.681(4), 1.686(3)	132.1(2)	[75]
$(SP^iBu_2)_2NH$		1.948(3), 1.932(3)		1.706(6), 1.657(5)	133.0(4)	[75]
$(SPPh_2)_2NH$		1.950(1), 1.937(1)		1.672(2), 1.683(2)	132.68(14)	[77]
		1.917(3), 1.915(3)		1.700(7), 1.652(7)	131.7(5)	[78]
		1.950(1), 1.936(1)		1.671(2), 1.684(2)	132.62(11)	[52]
$(SP^sBu_2)(SP^iBu_2)NH$		1.943(1) (P^iBu)		1.686(3)	133.1(2)	[75]
		1.935(2) (P^sBu)		1.695(3)		
$(SPMe_2)(SPPh_2)NH$		1.962(3) (PMe)		1.698(7)	126.1(4)	[81]
		1.946(3) (PPh)		1.692(6)		
$(SPPh_2)[SP(OEt)_2]NH$		1.920(2) (POEt)		1.667(3), 1.681(3)	129.9(2)	[82]
		1.937(1) (PPh)				
$[SP(OPh)_2]_2NH$ Mol. 1		1.912(1), 1.911(1)		1.650(2), 1.653(2)	129.3(1)	[83]
Mol. 2		1.892(1), 1.894(1)		1.670(2), 1.662(2)	130.4(1)	

Table 9 (*Continued*)

Compound		P–O	P–S	P–Se	P–N	P–N–P	Ref.
$(SeP^iPr_2)_2NH$				2.103(1), 2.096(1)	1.693(3), 1.686(3)	131.2(2)	[44]
$(SePPh_2)_2NH$				2.101(1), 2.085(1)	1.678(4), 1.686(3)	132.3(2)	[85]
$(SePPh_2)_2NH \cdot THF$				2.0942(7)	1.6757(12)	125.15(14)	[87]
$(SePPh_2)_2NH \cdot 2THF$				2.0990(7), 2.0967(7)	1.6804(19), 1.6896(19)	132.67(12)	[87]
$(OPPh_2)(SPMe_2)NH$	Mol. 1	1.480(5)	1.944(3)		1.662(7), 1.681(7)	126.5(4)	[88]
	Mol. 2	1.477(5)	1.925(3)		1.665(6), 1.681(6)	128.7(4)	
	Mol. 3	1.479(5)	1.941(3)		1.666(7), 1.669(8)	127.9(4)	
$(OPMe_2)(SPPh_2)NH$		1.48(1)	1.946(5)		1.66(1), 1.71(1)	123.0(9)	[88]
$(OPPh_2)(SPPh_2)NH$	Mol. 1	1.491(4)	1.935(2)		1.668(5), 1.694(4)	131.4(3)	[90]
	Mol. 2	1.514(4)	1.915(2)		1.683(5), 1.673(5)	132.9(3)	
$[OP(OEt)_2](SPPh_2)NH$		1.471(3)	1.940(2)		1.641(4), 1.697(4)	130.1(2)	[60]
$[OP(OEt)_2](SPPh_2)NH$		1.457(2)	1.931(1)		1.632(3), 1.679(3)	130.5(1)	[92]
$(OPPh_2)[SP(OEt)_2]NH$	Mol. 1	1.476(3)	1.895(3)		1.673(4), 1.662(4)	122.6(2)	[92]
	Mol. 2	1.484(3)	1.921(2)		1.661(4), 1.653(3)	127.2(2)	
$[OP(OC_6H_4CH_3\text{-}2)_2]\text{-}[SP(OC_6H_4CH_3\text{-}2)_2]NH$		1.465(2)	1.911(1)		1.653(2), 1.658(2)	132.0(1)	[66]
$[OP(OC_6H_4CH_3\text{-}3)_2]\text{-}[SP(OC_6H_4CH_3\text{-}3)_2]NH$		1.457(3)	1.902(2)		1.643(3), 1.654(3)	131.4(3)	[66]
$[OP(OC_6H_4CH_3\text{-}4)_2]\text{-}[SP(OC_6H_4CH_3\text{-}4)_2]NH$		1.459(2)	1.902(1)		1.635(2), 1.654(2)	133.0(1)	[66]

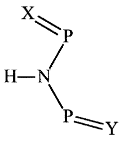

(10)

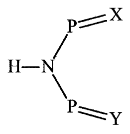

(11)

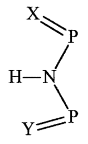

(12)

On the other hand, in both these cases the P=X and P=Y bonds can be situated on the opposite or same side of the PNP plane. To distinguish between different orientations of phosphorus–chalcogen bonds with respect to the PNP plane the following convention is proposed (**13**):

1. the triatomic PNP fragment is placed in the (x, y) plane; (x, y) coordinates for N, P_X and P_Y atoms are $(-x, 0)$, $(0, -y)$ and $(0, y)$, respectively (P_X is the phosphorus atom bearing the chalcogen involved in intermolecular hydrogen bonding);
2. the position of X and Y chalcogen atoms are codified in terms of (x, z) coordinates.

The data listed in Table 10 show that, according to this convention, for most X–P–N–P–Y skeletons with an *anti* conformation the chalcogen atoms are placed on opposite sides $[(-, -)/(+, +)$ or $(-, +)/(+, -)$ codes] of the PNP plane [e.g. for $(SPPh_2)_2NH$ (Fig. 1a)]. In a few cases, an *anti* conformation of the X–P–N–P–Y system with the chalcogens situated on the same side of the PNP plane are established. This is the case for two of the three independent molecules found in the crystal of $(OPPh_2)(SPMe_2)NH$ (Fig. 1b) [88] (the third exhibits *anti* conformation with the chalcogen atoms lying on both sides of the PNP plane). For $(OPEt_2)[OP(OPh)_2]NH$ [59], the X–P–N–P–Y skeleton is almost planar, with very small deviations of the two P=O bonds on the same side (Fig. 2). The perfect planarity of a X–P–N–P–Y backbone of *anti* conformation is found in the unique

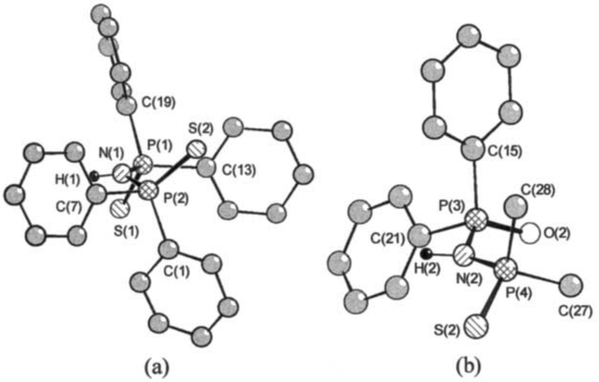

Fig. 1. The *anti* conformation of the X–P–N–P–Y skeleton in (a) $(SPPh_2)_2NH$ [77], code $(-, -)/(+, +)$, and (b) $(OPPh_2)(SPMe_2)NH$ [88], molecule 2 — code $(+, -)/(-, -)$.

Table 10
Conformation of the X–P–N–P–Y skeleton and association degree in the dichalcogenoimidodiphosphorus acids

Compound		X–P···P–Y torsion angle[a] (°)	Atom deviation from PNP plane[a]		X/Y code	N–H···X (°)	Association degree	Ref.
			X (Å)	Y (Å)				
Anti conformation								
$(SP^{n}Bu_2)_2NH$		179.0[b]	–[c]	–[c]	(−, −)/(+, +)	156	Dimer	[75]
$(SP^{i}Bu_2)_2NH$		179.8[b]	–[c]	–[c]	(−, ?)/(+, ?)	142	Polymer	[75]
$(SP^{s}Bu_2)(SP^{i}Bu_2)NH$		179.4[b]	–[c]	–[c]	(−, −)/(+, +)	152	Dimer	[75]
$(SPPh_2)_2NH$		155.7	S(1), −1.549	S(2), +1.635	(−, −)/(+, +)	178(3)	Dimer	[77]
$(SPMe_2)(SPPh_2)NH$		−171.0	S(1), −0.745	S(2), +1.263	(−, −)/(+, +)	156(6)	Dimer	[81]
$[SP(OPh)_2]_2NH$	Mol. 1	−166.5	S(1), −0.532	S(2), +1.144	(−, −)/(+, +)	126.0	Dimer	[83]
	Mol. 2	173.8	S(3), +0.227	S(4), −0.530	(−, +)/(+, −)	162.6		
$(SePPh_2)_2NH$		153.7	Se(1), −1.787	Se(2), +1.664	(−, −)/(+, +)	166	Dimer	[85]
$[OP(OC_6H_4CH_3\text{-}3)_2]\text{-}[SP(OC_6H_4CH_3\text{-}3)_2]NH$		179.5	O(1), −0.318	S(1), +0.560	(−, −)/(+, +)	170(3)	Dimer	[66]
$[OP(OC_6H_4CH_3\text{-}4)_2]\text{-}[SP(OC_6H_4CH_3\text{-}4)_2]NH$		−170.7	O(1), −0.343	S(1), +0.889	(−, −)/(+, +)	175(2)	Dimer	[66]
$(OPPh_2)(SPPh_2)NH$	Mol. 1	−176.8	O(1), −1.141	S(1), +1.728	(−, −)/(+, +)	173(5)	Polymer	[90]
	Mol. 2	−174.7	O(2), −1.166	S(2), +1.718	(−, −)/(+, +)	175(5)		
$[OP(OPh)_2]_2NH$		162.4	O(1), +0.080	O(2), −0.544	(−, +)/(+, −)	172.6	Dimer	[59]
$[OP(OC_6H_4CH_3\text{-}2)_2]_2NH$		−178.7	O(1), +0.117	O(2), −0.198	(−, +)/(+, −)	171(3)	Dimer	[66]
$(SPMe_2)_2NH$		177.3	S(1), +0.098	S(2), −0.005	(−, +)/(+, −)	175.9(4)	Polymer	[70]
$(SePPh_2)_2NH \cdot 2THF$		179.2	Se(1), +1.711	Se(2), −1.418	(−, +)/(+, −)	–[d]	Monomer	[87]
$[OP(OEt)_2](SPPh_2)NH$		173.1	O(1), +0.164	S(1), −0.535	(−, +)/(+, −)	159.3	Dimer	[60]
$(OPPh_2)(SPMe_2)NH$	Mol. 1	−179.7	O(1), −0.556	S(1), +0.507	(+, −)/(−, +)	161(7)	Polymer	[88]
	Mol. 2	−121.1	O(2), −0.933	S(2), −0.451	(+, −)/(−, −)	173(7)		
	Mol. 3	−172.0	O(3), −0.213	S(3), −0.007	(+, −)/(−, −)	164(9)		

Table 10 (*Continued*)

Compound		X–P···P–Y torsion angle[a] (°)	Atom deviation from PNP plane[a]		X/Y code	N–H···X (°)	Association degree	Ref.
			X (Å)	Y (Å)				
$(OPEt_2)[OP(OPh)_2]NH$		179.0	O(1), −0.007	O(2), −0.016	(−, −)/(+, −)	170.1	Dimer	[59]
$(OPPh_2)_2NH$		180	O(1), 0.0	O(2), 0.0	(−, 0)/(+, 0)	–[e]	Polymer	[52]
$(SPPh_2)[SP(OEt)_2]NH$		87.0[b]	–[c]	–[c]	(−, +)/(+, +)	–[c]	Dimer	[82]
Syn conformation								
$(OP^iPr_2)_2NH$		52[b]	–[c]	–[c]	(+, −)/(+, +)	174	Polymer	[44]
$(SP^iPr_2)_2NH$		79.4	S(1), −1.134	S(2), +1.330	(+, −)/(+, +)	170	Polymer	[73,74]
$(SeP^iPr_2)_2NH$		80[b]	–[c]	–[c]	(+, −)/(+, +)	173	Polymer	[44]
$(SePPh_2)_2NH \cdot THF$		81.8	Se(1), −1.367	Se(2), +1.367	(+, −)/(+, +)	–[f]	Monomer	[87]
$(OPMe_2)(SPPh_2)NH$		75.5	O(1), −0.839	S(1), +1.265	(+, −)/(+, +)	175(15)	Polymer	[88]
$(OPPh_2)[SP(OEt)_2]NH$	Mol. 1	79.5[b]	–[c]	–[c]	(+, −)/(+, +)	172	Polymer	[92]
	Mol. 2	69[b]			(+, +)/(+, −)	168		
$(OPPh_2)[OP(OEt)_2]$-$NH \cdot 1/2HCl \cdot 1/4H_2O$		27.0	O(1), −0.678	O(2), −0.019	(+, −)/(+, −)	–[g]	Polymer	[60]
$[OP(OC_6H_4CH_3\text{-}2)_2]$-$[SP(OC_6H_4CH_3\text{-}2)_2]NH$		2.7	O(1), −0.033	S(1), +0.019	(−, −)/(−, +)	171(3)	Dimer	[66]

[a] Calculated from published atomic coordinates.

[b] From original publication.

[c] Atomic coordinates not available in Cambridge Structure Database or original publications.

[d] N–H···O_{THF} 157°.

[e] P–O–H 124.12(15)°, O–H–O 180°.

[f] N–H···O_{THF} 180°.

[g] N–H···Cl 159.5°.

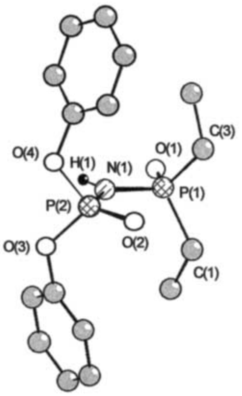

Fig. 2. The *anti* conformation of the almost planar X–P–N–P–Y skeleton [code (– , –)/(+ , –)] in the molecule of $(OPEt_2)[OP(OPh)_2]NH$ acid [59].

structure of the tetraphenylimidodiphosphinic acid [52]. The monothio derivative, $(SPPh_2)[SP(OEt)_2]NH$ [82], exhibits a conformation which can be considered as transitional between the *anti* and *syn* conformations (X–P···P–Y torsion angle of 87.0°).

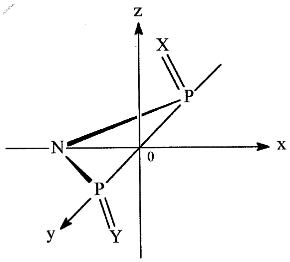

(13)

Most of the X–P–N–P–Y skeletons of *syn* conformation are of type **11** and code (+ , –)/(+ , +), i.e. with the chalcogens on opposite sides of the PNP plane [e.g. for $(SP^iPr_2)_2NH$ (Fig. 3a)]. For $(OPPh_2)[OP(OEt)_2]NH$ [60], the two P=O bonds are located on the same side of the PNP plane, while $[OP(OC_6H_4CH_3\text{-}2)_2][SP(OC_6H_4CH_3\text{-}2)_2]NH$ [66] is the unique example of type **12** with the almost planar X–P–N–P–Y fragment (Fig. 3b).

With few exceptions (see below), molecular crystals of the imidodiphosphorus acids have dimeric or polymeric associations through N–H···X=P hydrogen bonding. As common features one should note that:

1. in most cases only one chalcogen atom double bonded to phosphorus per molecular unit is involved in intra- or intermolecular hydrogen bonding;
2. regardless of the nature of the conformation of the X–P–N–P–Y skeleton, when an oxygen atom double bonded to phosphorus is present in the molecule, this atom is always involved in hydrogen bonding.

Most of the acids exhibiting an *anti* conformation are associated into distinct dimers, e.g. $(SePPh_2)_2NH$ (Fig. 4a) [85] or $[OP(OEt)_2](SPPh_2)NH$ (Fig. 4b) [60]. In the case of the asymmetric $(SPMe_2)(SPPh_2)NH$ derivative the dimers are further associated into polymeric chains through interactions between the second sulfur atom of the molecular unit and an aromatic proton of a neighboring acid molecule [S(2)···H(17a′) 2.869 Å] (Fig. 5) [81].

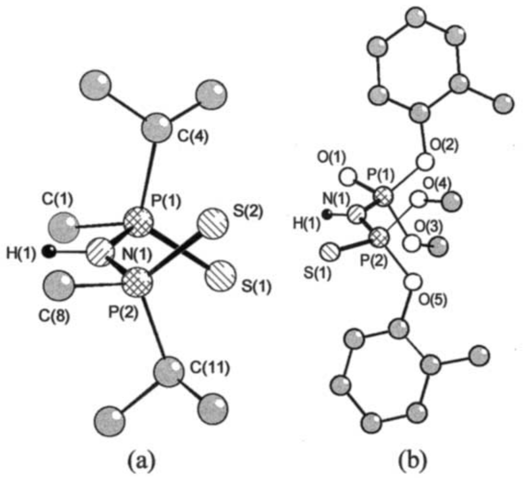

Fig. 3. The *syn* conformation of the X–P–N–P–Y skeleton in (a) $(SP^{i}Pr_2)_2NH$ [73], code (+ , −)/(+ , +), and (b) $[OP(OC_6H_4CH_3\text{-}2)_2][SP(OC_6H_4CH_3\text{-}2)_2]NH$ [66], code (− , −)/(− , +) (for clarity, some carbons of the isopropyl and phenyl groups are not shown).

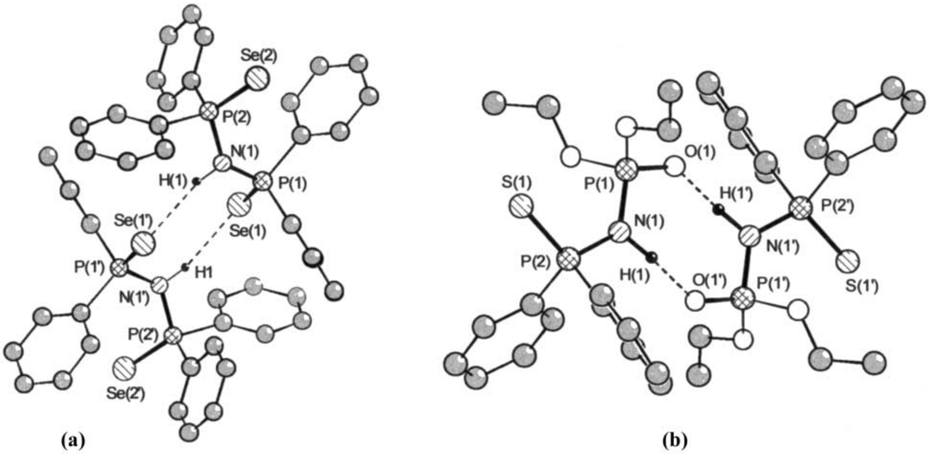

Fig. 4. The dimeric association in the crystal of (a) $(SePPh_2)_2NH$ [85], and (b) $[OP(OEt)_2](SPPh_2)NH$ [60].

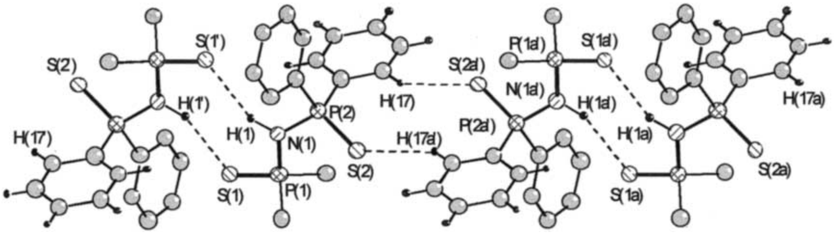

Fig. 5. The dimeric/polymeric association in the crystal of $(SPMe_2)(SPPh_2)NH$ [81].

Only in a few cases (Table 10) are the molecules of imidodiphosphoric derivatives with *anti* conformation of the X–P–N–P–Y skeleton associated into polymeric chains. Thus, the crystal of $(SPMe_2)_2NH$ (Fig. 6a) [70] contains molecules with basically planar S–P–N–P–S fragments associated through intermolecular N–H···S=P hydrogen bonds which involve only one chalcogen atom of a molecular unit. In contrast, the molecules of the tetraphenylimidodiphosphinic acid, which also contain planar O–P–N–P–O skeletons, are associated with a polymeric chain

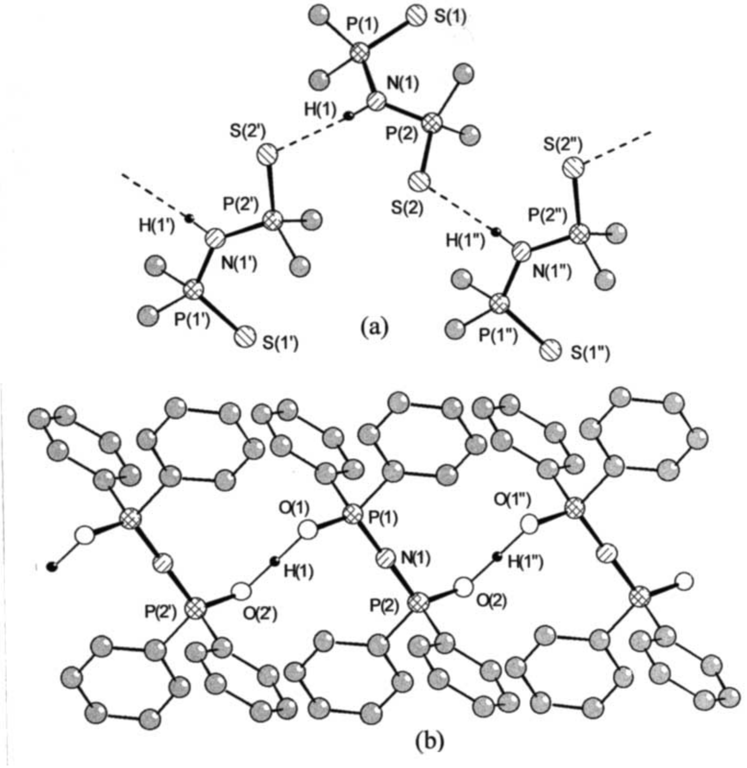

Fig. 6. The polymeric association in the crystal of (a) $(SPMe_2)_2NH$ [70], and (b) $(OPPh_2)_2NH$ [52].

through strong, symmetric and linear intermolecular O···H···O hydrogen bonds (Fig. 6b) [52].

For the imidodiphosphorus acids exhibiting a *syn* conformation of code $(+,\ -)/(+,\ +)$ the association of the molecules into polymeric chains in the solid state are imposed by the opposite orientation of the chalcogen atoms and the acidic proton in the molecular moiety. Therefore, polymeric structures of the type observed for the $(SPMe_2)_2NH$ derivative are usually found in the crystal, e.g. for $(SP^iPr_2)_2NeH$ (Fig. 7a) [73,74]. A different type of polymeric association occurs in the crystal of $[OP(OEt)_2](OPPh_2)NH \cdot 1/2HCl \cdot 1/4H_2O$ [60]. The molecules of *syn* conformation are associated through N–H···Cl···H–N and P=O···H–O–H···O=P hydrogen bonds involving the HCl and water molecules which alternate with molecules of the acid to form chain polymers (Fig. 7b). In contrast, only for $[OP(OC_6H_4CH_3\text{-}2)_2][SP(OC_6H_4CH_3\text{-}2)_2]NH$ [66] do the molecules exhibit a *syn* conformation of type **12** [code $(-,\ -)/(-,\ +)$] and therefore association into dimers is allowed (Fig. 8).

An interesting situation is found with tetraphenyldiselenoimidodiphosphinic acid. When its crystals were grown using a $CHCl_3$–hexane solvent system, the unsolvated species $(SePPh_2)_2NH$ was isolated and was found to be associated into dimeric units (Fig. 4a) [85]. In contrast, when a THF–pentane solvent system was used, crystals of the monomeric species $(SePPh_2)_2NH \cdot THF$ and $(SePPh_2)_2NH \cdot 2THF$ were ob-

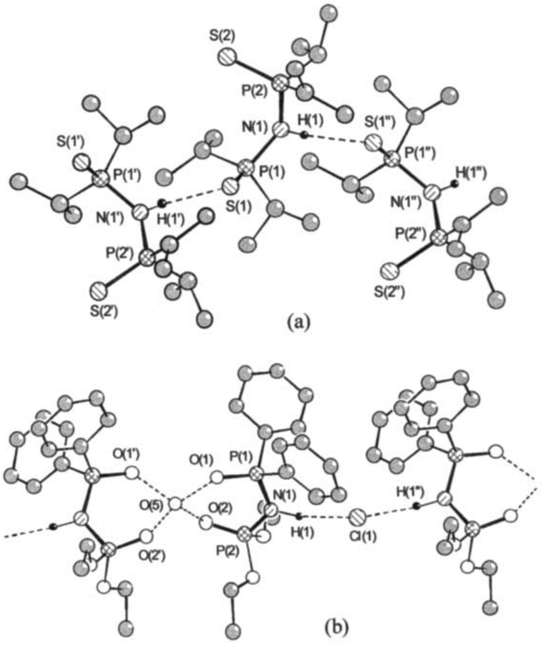

Fig. 7. The polymeric association in the crystal of (a) $(SP^iPr_2)_2NH$ [73], and (b) $[OP(OEt)_2]$-$(OPPh_2)NH \cdot 1/2HCl \cdot 1/4H_2O$ [60].

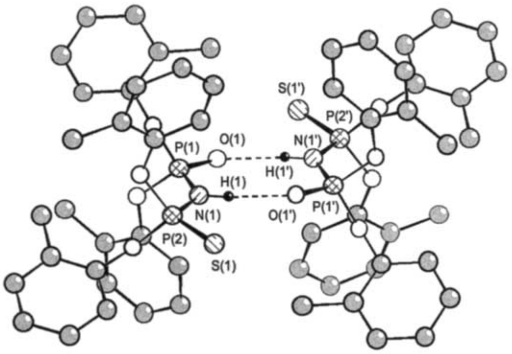

Fig. 8. The dimeric association in the crystal of $[OP(OC_6H_4CH_3\text{-}2)_2][SP(OC_6H_4CH_3\text{-}2)_2]NH$ [66].

tained [87]. In both cases the acid hydrogen of the diseleno acid molecule is linked to a THF molecule through a N–H···O_{THF} hydrogen bond [in the bis(tetrahydrofurane) solvate the second THF molecule is not involved in interactions with the acid molecule). In the three species, the bond distances within the inorganic Se–P–N–P–Se skeleton are similar (Table 9), but the P–N–P angle in the monosolvate is considerably reduced [125.15(14)° versus about 132° in the other two species]. The conformation of the Se–P–N–P–Se fragment is influenced by solvation. In $(SePPh_2)_2NH \cdot 2THF$, as in free $(SePPh_2)_2NH$, it is *anti* (Se–P···P–Se torsion angle 179.2°) (Fig. 9a), but it is *syn* in $(SePPh_2)_2NH \cdot THF$ (Se–P···P–Se torsion angle 81.8°) (Fig. 9b).

It can be concluded from the structural investigations of the imidodiphosphorus acids available so far that changes in the nature of the organic groups and/or the chalcogens bound to phosphorus atoms may have a considerable effect on both the conformation of the inorganic backbone and the degree of association in the solid

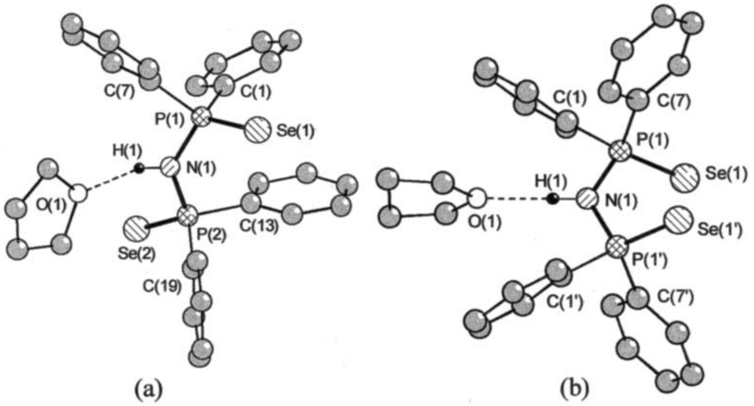

Fig. 9. The molecular structure of (a) $(SePPh_2)_2NH \cdot 2THF$, and (b) $(SePPh_2)_2NH \cdot THF$ [87].

state. Even for isomeric compounds dramatic changes in the structural patterns have been observed, e.g. $[OP(OEt)_2](SPPh_2)NH$ (*anti*/dimer) versus $(OPPh_2)$-$[SP(OEt)_2]NH$ (*syn*/polymer); $(OPPh_2)(SPMe_2)NH$ (*anti*/polymer) versus $(OPMe_2)$-$(SPPh_2)NH$ (*syn*/polymer); $(OPEt_2)[OP(OPh)_2]NH$ (*anti*/dimer) versus $(OPPh_2)$-$[OP(OEt)_2]NH.1/2HCl.1/4H_2O$ (*syn*/polymer).

2.3. Related derivatives

The molecular structures of three derivatives of $(XPPh_2)(YPPh_2)NH$ acids, i.e. $S{=}PPh_2{-}N{=}PPh_2{-}SMe$ [97], $(S{=}PPh_2{-}N{=}PPh_2)_2O$ [99] and $(Se{=}PPh_2{-}N{=}PPh_2)_2O$ [22,56], were established by X-ray diffraction and their molecular parameters are useful for comparative purposes in the investigation of imidodiphosphorus acids and their metal complexes.

The *S*-Me ester $S{=}PPh_2{-}N{=}PPh_2{-}SMe$ was previously prepared by reacting the free acid with diazomethane [13]. It was also isolated as a decomposition product during attempts to prepare $Me_3Sb(V)$ derivatives of tetraphenyldithioimidodiphosphinic acid, by migration of a methyl group from the metal atom to sulfur [97]. The ^{31}P-NMR spectrum of the ester exhibits, as expected, two resonances at δ 42.4 (*P*=S) and 27.5 (*P*–S–Me) ppm [13]. In the crystal, the molecules of $S{=}PPh_2{-}N{=}PPh_2{-}SMe$ display a X–P–N–P–Y skeleton of *syn* conformation (S–P···P–S torsion angle of 75.5°), with the chalcogen atoms placed on opposite sides of the PNP plane (Fig. 10). The phosphorus–sulfur and phosphorus–nitrogen bond distances in the molecular unit are different, consistent with single and double bond character, respectively (Table 11).

The two $(X{=}PPh_2{-}N{=}PPh_2)_2O$ (X = S, Se) derivatives are the *O*-anhydrides of the asymmetric $(OPPh_2)(SPPh_2)NH$ and $(OPPh_2)(SePPh_2)NH$ acids, respectively. The preparative methods for these compounds have not yet been described. Both derivatives were obtained as hydrolysis by-products during attempts to grow crystals of metal complexes, i.e. $[(2\text{-}Me_2NCH_2)C_6H_4]BiCl[(SPPh_2)_2N]$ [99] and $Ph_3Te[(SePPh_2)_2N]$ [56], respectively. The seleno derivative was also obtained when the potassium salt $K[(SePPh_2)_2N]$ was treated with water [22]. Their solid state molecular structures are shown in Fig. 11. The conformation of the whole inorganic $X_2N_2P_4O$ backbone is very similar in the two molecules as is the conformation of

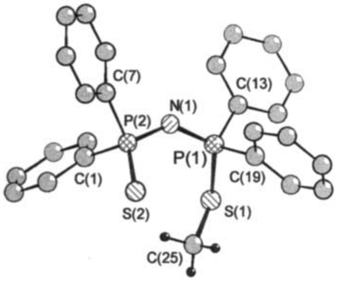

Fig. 10. The molecular structure of $S{=}PPh_2{-}N{=}PPh_2{-}SMe$ [97].

Table 11
X-ray data [bond lengths (Å) and bond angles (°)] for related imidodiphosphinic acid derivatives

Compound	P–S	P–Se	P–O	P–N	P–N–P	P–O–P	Ref.
S=PPh$_2$–N=PPh$_2$–SMe	1.956(3)			1.610(4)	135.8(4)		[97]
	2.069(3)			1.568(4)			
(S=PPh$_2$–N=PPh$_2$)$_2$O	1.962(2)			1.619(4)	135.5(3)	140.4(3)	[99]
			1.626(2)	1.552(4)			
(Se=PPh$_2$–N=PPh$_2$)$_2$O		2.116(1)		1.621(3)	136.7(2)	141.4(2)	[56]
			1.615(3)	1.545(3)			

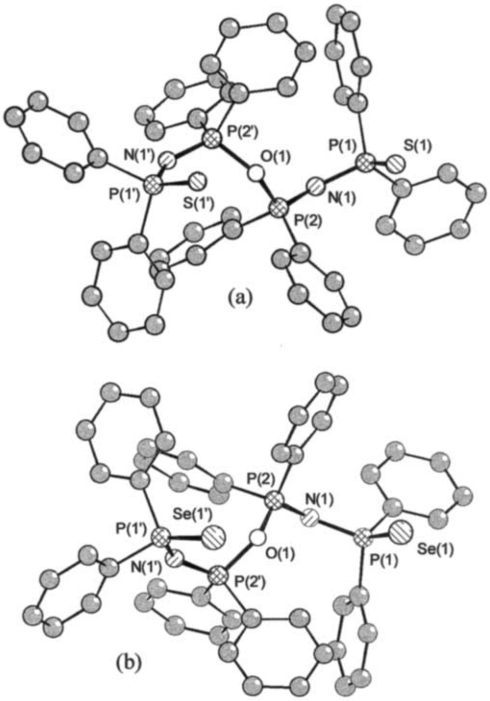

Fig. 11. The molecular structure of (a) S=PPh$_2$–N=PPh$_2$–O–PPh$_2$=N–PPh$_2$=S [99], and (b) Se=PPh$_2$–N=PPh$_2$–O–PPh$_2$=N–PPh$_2$=Se [56].

the X–P–N–P–O fragments (*syn*, S–P···P–O and Se–P···P–O torsion angles of 63.1 and 64.6°, respectively). The phosphorus–chalcogen bond distances are consistent with single (for oxygen) and double (for sulfur and selenium) bond character. The phosphorus–nitrogen bond distances are different and of the same magnitude as in the case of the ester described above (Table 11).

3. Metal complexes containing neutral $(XPR_2)(YPR'_2)NH$ ligands

Both tetraphenylimidodiphosphinic acid and its dithio analog can behave as neutral ligands. They always coordinate to the metal atom through both chalcogen atoms thus resulting in chelate structures (**14**):

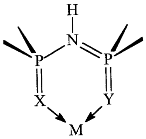

(14)

Generally, the complexes of this type are not very stable and changes in the reaction solvent or the use of reflux temperature results in decomposition.

Tin(IV) halide complexes containing $(OPPh_2)_2NH$ acid as a neutral ligand were described in the earlier works of Schmidpeter and co-workers [14,100]. Three types of such complexes have been reported (Table 12):

- neutral complexes, $SnX_4[(OPPh_2)_2NH]$;
- ionic compounds containing two phosphorus ligand units per molecule of complex, $[SnX_2\{(OPPh_2)_2NH\}_2][ClO_4]_2$;
- ionic compounds containing both neutral and anionic imidodiphosphinic units per molecule of complex, $[SnX_2\{(OPPh_2)_2NH\}\{(OPPh_2)_2N\}_2][ClO_4]$.

All these complexes are easily interconverted by solvolysis, depending on the nature of the solvent used. Thus, treatment of SnX_4 (X = Cl, Br) with $(OPPh_2)_2NH$ leads to $SnX_4[(OPPh_2)_2NH]$ complexes. In boiling water or methanol, or by thermal treatment, the corresponding Sn(IV) complexes containing deprotonated ligand units, $SnX_2[(OPPh_2)_2N]_2$, are formed [14,100]. Reconversion to the neutral complexes can be achieved by treatment with hydrogen halides. In contrast, SnI_4 reacts with $(OPPh_2)_2NH$ to form directly the deprotonated complex, $SnI_2[(OPPh_2)_2N]_2$ [14,100]. Treatment of $SnX_2[(OPPh_2)_2N]_2$ (X = Cl, Br, I) derivatives with perchloric acid yields anionic $[SnX_2\{(OPPh_2)_2NH\}_2][ClO_4]_2$ complexes [14]. Depending on the solvolyzing medium, the removal of $HClO_4$ leads back to $SnX_2[(OPPh_2)_2N]_2$ (in methanol) or to $[SnX_2\{(OPPh_2)_2N\}\{(OPPh_2)_2NH\}][ClO_4]$ complexes (in acetonitrile) [Eq. (14)] [14]:

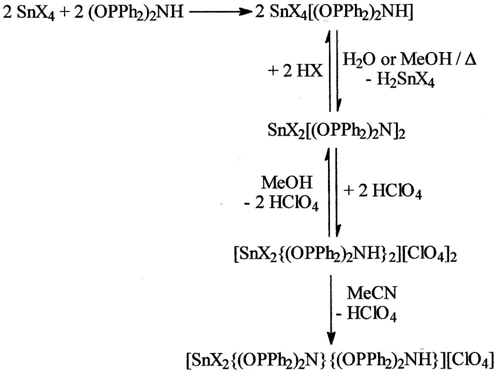

(14)

Table 12
Metal complexes containing imidodiphosphinic acids as neutral ligand

Compound	Synthesis, yield (%)	M.p. (°C)	$\delta(^{31}P)$ (ppm)/solvent	X-ray studies	Spectroscopic studies
$[Al\{(OPEt_2)_2N\}_2\{(OPEt_2)_2NH\}][I_3]$[a]	[42]				
$[Al\{(OPPh_2)_2N\}_2\{(OPPh_2)_2NH\}][I_3]$[a]	83 [42]			[42]	MS [42]
$[Al\{(OPPh_2)_2N\}\{(OPPh_2)_2NH\}_2][H_2PO_4]_2$[a,b]	[42]			[42]	MS [42]
$SnCl_4[(OPPh_2)_2NH]$	95 [100]	286–292			IR, Mössbauer [14]
$SnBr_4[(OPPh_2)_2NH]$	100 [100]	278–280			IR, Mössbauer [14]
$[SnCl_2\{(OPPh_2)_2NH\}_2][ClO_4]_2$	[14]		$45.8/CH_2Cl_2$		IR, ^{31}P [14]
$[SnBr_2\{(OPPh_2)_2NH\}_2][ClO_4]_2$	[14]		$44.5/CH_2Cl_2$		IR, ^{31}P [14]
$[SnI_2\{(OPPh_2)_2NH\}_2][ClO_4]_2$	[14]		$43.3/CH_2Cl_2$		IR, ^{31}P [14]
$[SnX_2\{(OPPh_2)_2NH\}\{(OPPh_2)_2N\}_2][ClO_4]$, X = Cl, Br, I	[14]				

[a] See the comments of the structures in the text.

[b] 1,4-Dioxane adduct.

The infrared spectra were considered to be indicative of the presence of the imidodiphosphinic acid coordinated as a neutral ligand because of the presence of characteristic absorptions for the NH group in the 3100–2600 cm^{-1} region. The presence of the acidic proton on nitrogen is in contrast with the solid state structure of the free acid (see above). However, it should be mentioned here that the molecular structure of $MoO_2Cl_2[(OPPh_2)_2NH]$ was established by X-ray diffraction [101].

The 1:1 $SnX_4/(OPPh_2)_2NH$ complexes can be formulated either as neutral, $SnX_4[(OPPh_2)_2NH]$, or anionic, $[SnX_2\{(OPPh_2)_2NH\}_2][SnX_6]$, octahedral derivatives. The insolubility of these complexes in non-solvolyzing media prevented molecular weight determinations which can distinguish between these two possibilities. The Mössbauer spectra showed only one resonance line with isomeric shifts (IS 0.40 and 0.63 mm s^{-1} for X = Cl and Br, respectively) consistent with the presence of octahedral, neutral complexes, $SnX_4[(OPPh_2)_2NH]$ [14].

For the complexes of the type $[SnX_2\{(OPPh_2)_2NH\}_2][ClO_4]_2$, the IR and ^{31}P-NMR spectra are consistent with the anionic formulation, but cannot distinguish between *cis* or *trans* SnX_2 fragments in the cation [14].

A recent paper [42] reported the synthesis of ionic aluminum complexes formulated as '$[Al\{(OPR_2)_2N\}_3][I_3]$' (R = Et, Ph), which implies an oxidation state +4 for aluminum. The formulation of the cation as $[Al\{(OPR_2)_2N\}_2\{(OPR_2)_2NH\}][I_3]$, with both protonated and deprotonated phosphorus ligands, would be consistent with an Al^{+3} compound and hence be far more probable. For R = Ph the solid state structure was investigated by single-crystal X-ray diffraction. The complex cation contains an aluminum atom coordinated by three chelated phosphorus ligands thus resulting in an octahedral AlO_6 core (Fig. 12). No hydrogen atom was located on a nitrogen atom but a careful analysis of the phosphorus–oxygen bond

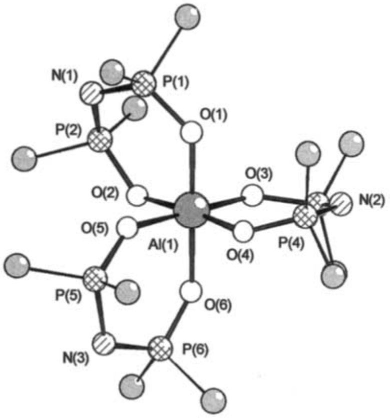

Fig. 12. The structure of the cation in $[Al\{(OPPh_2)_2N\}_2\{(OPPh_2)_2NH\}][I_3]$ [42] [the hydrogen on N(2) atom was not located, and, for clarity, only *ipso* carbons of the phenyl groups are shown].

distances reveals some interesting trends, which support the mixed deprotonated/protonated formulation. Thus, for two ligands, the P–O distances are in the range 1.52(3)–1.56(3) Å, consistent with deprotonated $[(OPPh_2)_2N]^-$ units. For the third ligand the phosphorus–oxygen bond distances are shorter [P(3)–O(3) 1.49(2), P(4)–O(4) 1.48(1) Å], clearly indicating double bond character and thus supporting a protonated unit, $(OPPh_2)_2NH$ [cf. for $Ph_2P(=O)OH$ [102]: P–O 1.526(6), P=O 1.486(6) Å].

A third aluminum complex reported in the same paper was the dioxane adduct of '$[Al\{(OPPh_2)_2NH\}_3][HPO_4]_2$' [42]. Here all phosphorus ligands were included in the complex as protonated units, but again the resulting oxidation state of the metal atom is +4. A more probable formulation, which is consistent with an Al^{+3} derivative, would be $[Al\{(OPPh_2)_2N\}\{(OPPh_2)_2NH\}_2][H_2PO_4]_2$. In the solid state, a similar octahedral structure was found for the complex cation, but again no hydrogen atoms were located on nitrogen atoms. The phosphorus–oxygen bond distances again appear to be consistent with the presence of protonated/deprotonated species [P–O range 1.46(1)–1.49(1) Å for the protonated ligands, and P(5)–O(5) 1.49(1), P(6)–O(6) 1.52(1) Å, for the deprotonated one]. A reinvestigation of the structures of these aluminum complexes is required with data of good enough quality to confirm, with confidence, the presence or absence of hydrogen atoms on nitrogen.

For main group metals only one complex containing a neutral dithioimidodiphosphinic ligand, i.e. $ZnCl_2[(SPPh_2)_2NH]$, has been reported [79]. The complex was prepared under mild conditions from $ZnCl_2$ and the free acid, in $CHCl_3-Et_2O$, and is rather unstable. It is quantitatively converted into the deprotonated species, $Zn[(SPPh_2)_2N]_2$, by boiling for a few minutes in methanol. Its formulation was based on the IR spectrum, i.e. the presence of a strong band at 921 cm^{-1} assigned to the $\nu_{as}(P_2NH)$ stretching vibration.

4. Metal complexes containing deprotonated $[(XPR_2)(YPR'_2)N]^-$ ligands

Metal complexes containing deprotonated imidodiphosphorus acids exhibit some common preparative and spectroscopic patterns:

1. Most of the metal derivatives were prepared by metathesis reactions of metal halides or salts with alkali metal derivatives of imidodiphosphorus acids (when specific methods of synthesis were used, they will be mentioned in the subsequent discussion). Although in many cases the compounds are quite stable to moisture and oxygen, inert atmosphere is recommended to avoid hydrolysis of the metal complexes (the presence of free imidodiphosphorus acids can be easily established by ^{31}P-NMR spectroscopy).
2. The strong infrared absorptions in the 1250–1200 cm^{-1} region, assigned to the $\nu_{as}(P_2N)$ stretching vibration, are indicative of the presence of deprotonated imidodiphosphorus ligands (cf. strong IR absorptions in the 950–900 cm^{-1} region assigned to the $\nu_{as}(P_2NH)$ stretching vibration for the free acids).

3. The loss of the acidic proton is generally reflected in a significant shift to lower field of the ^{31}P-NMR resonances. In many cases, either phosphorus–phosphorus and/or phosphorus–element (carbon, selenium, metal) coupling constants were observed and were used for the assignment of the ^{31}P resonances (when available, the ^{31}P-NMR data were included in the tables listing the compounds known so far).
4. The single-crystal X-ray diffraction data demonstrate that in most cases the phosphorus–chalcogen bonds are lengthened and the phosphorus–nitrogen bonds are shortened upon deprotonation (range values are usually given in the tables). The P–N–P fragment of the ligand is bent in the known complexes. The flexibility of the X–P–N–P–Y skeleton is reflected in the variety of conformations of the six-membered $MXYP_2N$ inorganic rings.
5. When six-membered $MXYP_2N$ inorganic rings are formed, the variety of observed conformations reflects the flexibility of the X–P–N–P–Y skeleton (see tables listing the X-ray data).

In the subsequent discussion of the structure of metal complexes, particular attention will be given to the coordination patterns of the deprotonated imidodiphosphorus ligand and to the resulting coordination geometry at the metal center.

4.1. Group 1: Li, Na, K

The alkali metal salts of imidodiphosphorus acids are of particular interest since they are usually used as starting materials in the synthesis of other metal complexes. In many cases, when solvents with coordination potential were used for recrystallization, the alkali salts were isolated as adducts. The compounds known so far are listed in Table 13, the available ^{31}P-NMR data are given in Table 14, and important molecular dimensions are listed in Table 15.

4.1.1. Lithium

Although lithium salts of imidodiphosphorus acids are intermediates in the synthesis of the free acids [method (v) with $LiBu^n$ as coupling agent], their value for synthetic purposes has not been exploited to date. Only recently have the synthesis and spectroscopic properties of some imidodiphosphinates been reported. Recrystallization from anhydrous THF usually affords isolation of adducts with one or two molecules of solvent. However, neither $Li[(OPMe_2)(SPPh_2)N]$ nor $Li[(OPPh_2)_2N]$ form THF adducts [103]. A 2:3 $Li[(SPPh_2)_2N]$ adduct with 1,4-dioxane was also reported and a structure with a bridging solvent molecule was proposed for this dinuclear compound on the basis of ^{1}H-NMR data [13].

Only the solid state structure of the water adduct $Li[(OPPh_2)(SPMe_2)N]\cdot 2H_2O$, isolated from moist THF, has been established [103]. The crystal contains two, very similar, independent molecules. The monothioimidodiphosphinato ligands act as bimetallic biconnective (bridging) units which involve only the oxygen atom in the coordination [O(1)–Li(1) 1.927(9), O(1)–Li(1′) 1.951(9) Å, in molecule 1]. This leads to dimers which contains a planar Li_2O_2 four-membered ring (Fig. 13). The

Table 13
Group 1 metal salts of imidodiphosphorus acids

Compound	Yield (%)	M.p. (°C)	X-ray diffraction studies	Spectroscopic studies
$Li[(OPPh_2)_2N]$	81 [103]	269		IR, ^{1}H, ^{13}C, ^{31}P [103]
$[Li\{(SPPh_2)_2N\}]_2(1,4\text{-dioxane})_3$	[13]	217–221		IR, ^{1}H [13]
$Li[(SPPh_2)_2N] \cdot 2THF$	78 [13]	155–163		IR [13,103]
	89 [103]	167		^{1}H, ^{13}C, ^{31}P [103]
$Li[(OPMe_2)(SPPh_2)N]$	92 [103]	282–283		IR, ^{1}H, ^{13}C, ^{31}P [103]
$Li[(OPPh_2)(SPMe_2)N] \cdot THF$	79 [103]	256–258		IR, ^{1}H, ^{13}C, ^{31}P [103]
$Li[(OPPh_2)(SPMe_2)N] \cdot 2H_2O$			[103]	
$Li[(OPPh_2)(SPPh_2)N] \cdot THF$	83 [103]	198–200		IR, ^{1}H, ^{13}C, ^{31}P [103]
$Na[(OPPh_2)_2N]$	80 [100]			
$Na[\{OP(OPh)_2\}_2N]$	[64]	176–177	[104]	
$Na[(SPMe_2)_2N] \cdot H_2O$	[18]	103–104^{a}		
$Na[(SPMe_2)_2N] \cdot 2H_2O$	95 [18]	112^{b}		IR [19]
				^{1}H, ^{31}P [18,19]
$Na[(SPPh_2)_2N]$	[71]			IR, Raman [71]
$Na[(SPMe_2)(SPPh_2)N] \cdot MeOH$	71 [18]	187–189		IR, ^{1}H, ^{31}P [18,19]
$Na[(OPMe_2)(SPPh_2)N]$	[88]	138–140		IR, ^{1}H, ^{13}C, ^{31}P [88]
$Na[(OPPh_2)(SPPh_2)N]$	73 [90]	180–182		IR, ^{1}H, ^{13}C, ^{31}P [90]
$Na[(OPPh_2)(SPPh_2)N] \cdot 2THF$			[90]	
$K[(OPMe_2)_2N]$	[18]	253–254		^{1}H [18]
$K[(OPPh_2)_2N]$				^{31}P [105]
$[K(18\text{-crown-}6)][(OPPh_2)_2N] \cdot H_2O$	85 [106]		[106]	IR, ^{31}P [106]
$K[(OPMe_2)(OPPh_2)N]$	87 [57]	264–269		IR, ^{1}H, ^{13}C, ^{31}P [57]
	[18]			
$K[\{OP(OEt)_2\}(OPPh_2)N]$	99 [60]	190		IR, ^{1}H, ^{13}C, ^{31}P [60]
$K[(SPMe_2)_2N]$	96 [70]	235–237	[56]	IR, ^{31}P [19,70]
				^{1}H, ^{13}C [70]
$K[(SPPh_2)_2N]$	82 [13]	363–366	[80]	IR [13,19,79,80,107]
	[80]			Raman [107]
				^{31}P [15,19,80,105]
$[K(18\text{-crown-}6)][(SPPh_2)_2N]$	80 [108]	209–211	[108]	IR [106]
$K[(SPMe_2)(SPPh_2)N]$	90 [109]	251–253		IR, ^{1}H, ^{13}C, ^{31}P [109]
$K[(SePPh_2)_2N]$	95 [86]			IR, MS, ^{31}P [86]
$[K(18\text{-crown-}6)][(SePPh_2)_2N]$	82 [110]	223–224	[110]	IR, ^{1}H, ^{31}P [110]
$K[(OPMe_2)(SPPh_2)N]$	[88]	138–140		IR, ^{1}H, ^{13}C, ^{31}P [88]
$K[(OPPh_2)(SPMe_2)N]$	98 [88]	227–230		IR, ^{1}H, ^{13}C, ^{31}P [88]
$K[(OPPh_2)(SPPh_2)N]$	92 [16]	295–298		IR [16,71,89,91]
	61 [16]			^{1}H [89,91], ^{13}C [91]
	95 [91]	286–288		^{31}P [15,16,89,91]
	94 [89]			
$K[\{OP(OEt)_2\}(SPPh_2)N] \cdot H_2O$	98 [60]	119–122	[60]	IR, ^{1}H, ^{13}C, ^{31}P [60]
$K[(OPPh_2)(SePPh_2)N]$	78 [89]			IR, ^{1}H, ^{31}P [89]
$K[(SPPh_2)(SePPh_2)N]$	97 [93]			IR, ^{1}H, ^{31}P [93]

[a] From THF/H_2O.

[b] From moist CH_3CN/Et_2O.

Table 14
^{31}P-NMR data for Group 1 metal salts of imidodiphosphorus acids

Compound	Solvent	$\delta(^{31}P)$ (ppm), $^{n}J(PX)$ (Hz)			Ref.
$Li[(OPPh_2)_2N]$	$CDCl_3$		19.7s		[103]
$Li[(SPPh_2)_2N] \cdot 2THF$	$CDCl_3$		39.3s		[103]
$Li[(OPMe_2)(SPPh_2)N]$	$CDCl_3$	33.5d (PS), $^2J(PP)$ 7.8, $^1J(PC)$ 105.3		31.6d (PO), $^2J(PP)$ 7.8, $^1J(PC)$ 89.2	[103]
$Li[(OPPh_2)(SPMe_2)N] \cdot THF$	$CDCl_3$	40.8s (PS)		19.1d (PO), $^2J(PP)$ 7.8, $^1J(PC)$ 131.4	[103]
$Li[(OPPh_2)(SPPh_2)N] \cdot THF$	$CDCl_3$	37.3s (PS)		20.6s (PO)	[103]
$Na[(SPMe_2)_2N] \cdot 2H_2O$	CH_3CN		43.8s		[18,19]
$Na[(SPMe_2)(SPPh_2)N] \cdot MeOH$	CH_3OH	43.3s (P–Me)		37.6s (P–Ph)	[18,19]
$Na[(OPMe_2)(SPPh_2)N]$	$CDCl_3$	37.2s (PS), $^1J(PC)$ 105.3		35.8s (PO), $^1J(PC)$ 86.6	[88]
$Na[(OPPh_2)(SPPh_2)N]$	$CDCl_3$/DMSO-d_6	35.8s (PS), $^1J(PC)$ 105.3		15.8s (PO), $^1J(PC)$ 132.1	[90]
$K[(OPPh_2)_2N]$			10.5s		[105]
$[K(18\text{-crown-}6)][(OPPh_2)_2N] \cdot H_2O$			12.2s		[106]
$K[(OPMe_2)(OPPh_2)N]$		28.9d (P–Me), $^2J(PP)$ 7.8, $^1J(PC)$ 89.7		13.7d (P–Ph), $^2J(PP)$ 7.8, $^1J(PC)$ 132.1	[57]
$K[\{OP(OEt)_2\}(OPPh_2)N]$	$CDCl_3$	15.2d (P–Ph), $^2J(PP)$ 21.8		4.4d (P–OEt), $^2J(PP)$ 21.8	[60]
$K[(SPMe_2)_2N]$	CD_3OD		44.0s		[70]
$K[(SPPh_2)_2N]$	DMSO		35.6s		[15]
	MeOH/glycol		35.6s		[19]
			35.8s		[80]
			37.1s		[105]
$K[(SPMe_2)(SPPh_2)N]$	CD_3OD	44.2d (P–Me), $^2J(PP)$ 13.7		38.0d (P–Ph), $^2J(PP)$ 13.7	[109]
$K[(SePPh_2)_2N]$	DMSO-d_6		28.5s, $^1J(PSe)$ 687		[86]
$[K(18\text{-crown-}6)][(SePPh_2)_2N]$	$CDCl_3$		29.2s		[110]
$K[(OPPh_2)(SPMe_2)N]$	$CDCl_3$	47.8s (PS)		21.2s (PO)	[88]
$K[(OPMe_2)(SPPh_2)N]$	$CDCl_3$	35.8s (PS), $^1J(PC)$ 104.9		31.6s (PO), $^1J(PC)$ 88.8	[88]
$K[(OPPh_2)(SPPh_2)N]$	MeOH/glycol	34.7s (PS)		12.4s (PO)	[15,16]
	CD_3OD	37.9s (PS)		16.1 (PO)	[91]
	MeOH/C_6D_6	35.3d (PS), $^2J(PP)$ 3.3		13.9d (PO), $^2J(PP)$ 3.3	[89]
$K[\{OP(OEt)_2\}(SPPh_2)N] \cdot H_2O$	$CDCl_3$	37.3d (PS), $^2J(PP)$ 20.6		5.3d (PO), $^2J(PP)$ 20.6	[60]
$K[(OPPh_2)(SePPh_2)N]$	THF/C_6D_6	23.6d (PSe), $^2J(PP)$ 2.2, $^1J(PSe)$ 664		12.9d (PO), $^2J(PP)$ 2.2	[89]
$K[(SPPh_2)(SePPh_2)N]$	DMSO-d_6	37.6d (PS), $^2J(PP)$ 7		26.7d (PSe), $^2J(PP)$ 7, $^1J(PSe)$ 682	[93]

Table 15
X-ray data [bond lengths (Å) and bond angles (°)] for Group 1 metal salts of imidodiphosphorus acids

Compound		M–X	P–X	P–N	P–N–P	Association degree	Ref.
Li[(OPPh$_2$)(SPMe$_2$)N] · 2H$_2$O	Mol. 1	1.927(9)/1.951(9)[a] (M–O)	1.508(3) (P–O)	1.596(4)	130.9(3)	Dimer	[103]
			2.007(2) (P–S)	1.591(4)			
	Mol. 2	1.938(10)/1.968(10)[a] (M–O)	1.502(3) (P–O)	1.586(4)	134.2(3)	Dimer	
			2.015(2) (P–S)	1.593(5)			
Na[{OP(OPh)$_2$}$_2$N]	Mol. 1	2.26–2.65[b]	1.48	1.56	130.5[c]	Hexamer	[104]
	Mol. 2	2.23–2.34	1.48	1.56	133.7[c]		
	Mol. 3	2.23–2.38[d]	1.48	1.56	132.0[c]		
Na[(OPPh$_2$)(SPPh$_2$)N] · 2THF		2.245(9)/2.396(9)[e] (M–O)	1.494(7) (P–O)	1.577(9)	130.8(6)	Dimer	[90]
		2.975(6) (M–S)	1.979(4) (P–S)	1.606(9)			
K[(SPMe$_2$)$_2$N][f]		3.189(2)–3.365(2)	1.999(2)/1.986(2)	1.605(4)/1.616(4)	131.2(3)	Polymer	[56]
K[(SPPh$_2$)$_2$N][g]		3.203(1)/3.279(1)	1.978(1)	1.592(2)	128.6(2)	Polymer	[80]
K[{OP(OEt)$_2$}(SPPh$_2$)N] · H$_2$O[h]	Mol. 1	2.677(3)/2.745(3) (M–O)	1.473(3) (P–O)	1.567(4)	135.5(3)	Polymer	[60]
		3.274(2) (M–S)	1.990(2) (P–S)	1.577(3)			
	Mol. 2	2.593(3)/2.915(3) (M–O)	1.486(3) (P–O)	1.560(3)	142.2(3)		
		3.309(2) (M–S)	1.966(2) (P–S)	1.595(4)			
[K(18-crown-6)][(OPPh$_2$)$_2$N] · H$_2$O		2.832(5)/2.925(4)[i]	1.503(3)/1.496(4)	1.592(4)/1.585(4)	129.3(3)	Monomer	[106]
[K(18-crown-6)][(SPPh$_2$)$_2$N][j]			1.976(1)	1.599(1)	132.8(2)	Polymer	[108]
[K(18-crown-6)][(SePPh$_2$)$_2$N][k]			2.128(1)	1.608(2)	131.8(4)	Polymer	[110]
[Ph$_3$PNPPh$_3$][(SPPh$_2$)$_2$N]			1.975(2)	1.554(2)	180.0(1)	Monomer	[111]

[a] Li–O$_{water}$ 1.966(10), 1.947(10) Å (molecule 1); 1.962(10), 1.954(10) (molecule 2).

[b] Na(3)–O$_{phenoxy}$ 3.05 Å.

[c] Calculated from published atomic coordinates.

[d] Na(2)–O$_{phenoxy}$ 2.84 Å.

[e] Na(1)–O$_{THF}$ 2.35(1), 2.37(1) Å.

[f] K–N 2.937 Å.

[g] K–C 3.35, 3.51 Å.

[h] K–O$_{water}$ 2.774(3)–2.859(3) Å, K (1)–O(3)$_{ethoxy}$ 3.331(3) and K(2)–O(6)$_{ethoxy}$ 2.888(3) Å, and K(1)–C 3.296(5)–3.418(5) Å.

[i] K–O$_{crown}$ 2.905(5)–3.037(5), K–O$_{water}$ 3.110(5).

[j] K–C 3.30, 3.46.

[k] K–C 3.307(7), 3.470(7).

tetrahedral coordination at the lithium atom is completed by two additional O-water atoms. The sulfur atoms of the monothioimidodiphosphinato groups are not involved in intra- or intermolecular interactions [S(1)···Li(1) 4.237, S(1)···Li(1′) 4.257 Å, respectively, in molecule 1] and are placed on opposite sides of the Li_2O_2 ring. In spite of this fact, in contrast to the free acid, the conformation of the O–P–N–P–S skeleton is *syn* (O–P···P–S torsion angle of ca. 12°) and the two chalcogen atoms are situated on the same side of the P_2N plane of a ligand unit.

4.1.2. Sodium

A dimeric association was also observed in the crystal of the THF adduct $Na[(OPPh_2)(SPPh_2)N]\cdot 2THF$ [90]. In contrast to the lithium adduct described above, the monothioimidodiphosphinato ligands act as bimetallic triconnective (bridging) units. The sulfur atoms are also involved in coordination to the metal, in addition to the oxygen atoms of the phosphorus ligand (Fig. 14). The result is a tricyclic system with a central planar four-membered Na_2O_2 ring and an overall ladder structure. The $NaOSP_2N$ rings are symmetrically folded about the

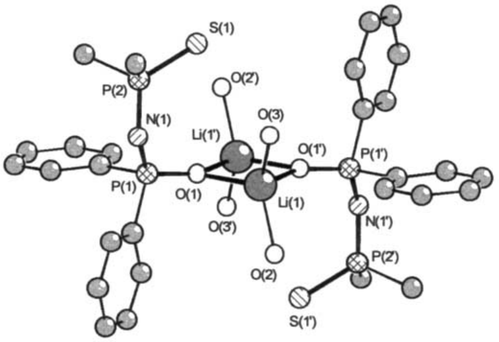

Fig. 13. The dimeric association in the crystal of $Li[(OPPh_2)(SPMe_2)N]\cdot 2H_2O$ (molecule 1) [103].

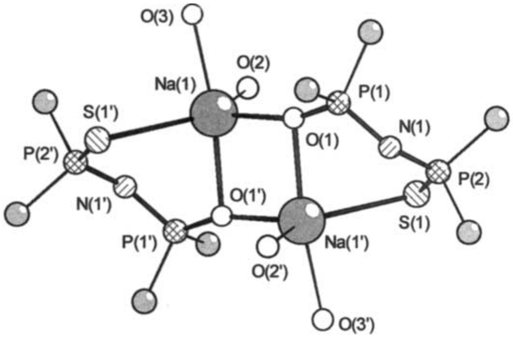

Fig. 14. The dimeric association in the crystal of $Na[(OPPh_2)(SPPh_2)N]\cdot 2THF$ [90] (for clarity, only *ipso* carbons of the phenyl groups, and oxygen atoms of the THF, respectively, are shown).

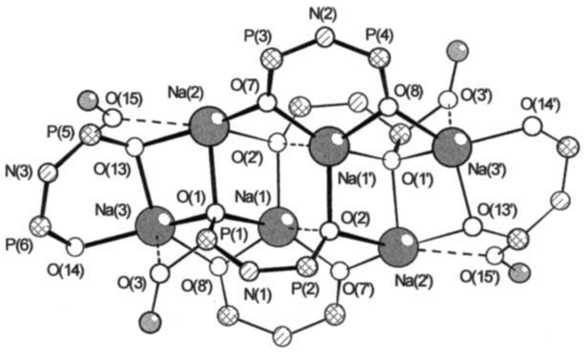

Fig. 15. The inorganic core of the hexameric association in the crystal of Na[{OP(OPh)$_2$}$_2$N] [104] (only for the two phenoxy groups involved in coordination the oxygen and the corresponding *ipso* carbon are shown).

Na(1)···N(1a) and Na(1a)···N(1) axes, respectively, in the opposite side relative to the central ring, with a dihedral angle between best NaOPN and NaSPN planes of 112.3°. The coordination at a sodium atom is completed by the oxygen atoms of two THF molecules, thus leading to a trigonal bipyramidal geometry [O(1′) and O(3) atoms in axial positions, O(1′)–Na(1)–O(3) 171.5(4)°].

The reaction between [OP(OPh)$_2$]$_2$NH and sodium hydride in anhydrous benzene resulted in the unsolvated sodium salt, Na[OP(OPh)$_2$}$_2$N] [104]. In the crystal the three independent molecules are associated into hexameric units. The compound is stable to moisture due to the lipophilic protection of the inorganic Na$_6$O$_{12}$ core (Fig. 15) provided by the phenyl groups.

The coordination pattern of the imidodiphosphato ligands (codified here as N$_1$, N$_2$ and N$_3$ corresponding to the nitrogen atoms) is different (schematic representations are depicted in **15**–**17**). For ligands N$_1$ and N$_3$ an oxygen atom of a phenoxy group is also involved in interactions to sodium atoms. As a consequence, the coordination pattern can be considered as pentametallic hexaconnective (**15**), trimetallic tetraconnective (**16**) and bimetallic tetraconnective (**17**) for N$_1$, N$_2$ and N$_3$ ligands, respectively.

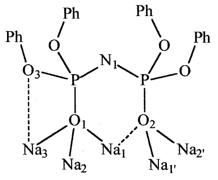

(15)

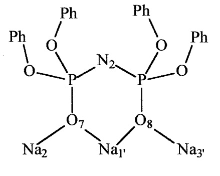

(16)

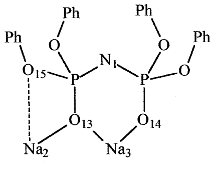

(17)

All sodium atoms are pentacoordinated, the geometry of the NaO$_5$ core varying from distorted trigonal bipyramidal [for Na(1)] to square planar [for Na(2)].

4.1.3. Potassium

Unsolvated $K[(SPMe_2)_2N]$ and $K[(SPPh_2)_2N]$ were obtained after recrystallization of potassium salts from anhydrous methanol. The methyl derivative exhibits a two-dimensional polymeric structure (Fig. 16a) built up as result of an unusual bridging coordination pattern of the phosphorus ligand, i.e. tetrametallic pentaconnective through four K–S interactions (range 3.189–3.365 Å) and one K–N interaction (2.937 Å) (Fig. 16b) [56]. The conformation of the S–P–N–P–S skeleton is *anti* (S–P···P–S torsion angle of ca. 108°). In the fused polycyclic skeleton one can distinguish four-membered planar K_2S_2 and KSPN rings, as well as eight-membered $K_2S_2P_2N_2$, $K_2S_3P_2N$ and K_3S_3PN rings. The coordination geometry of the KS_4N core is distorted trigonal bipyramidal [S(1′) and S(2″) atoms in axial positions, S(1′)–K(1)–S(1″) 158.34(5)°].

In contrast, the phenyl derivative contains a polymeric ladder structure (Fig. 17a), with four-membered planar K_2S_2 and six-membered KS_2P_2N (distorted boat) rings, as a result of the trimetallic tetraconnective pattern of type (**16**) exhibited by the dithio ligand [80]. In addition, one phenyl group of each phosphorus atom in the ligand unit establishes π interactions through one C–C bond with neighboring metal atoms (Fig. 17b) [K···(C–C) bond centroid distance 3.36 Å]. The coordination

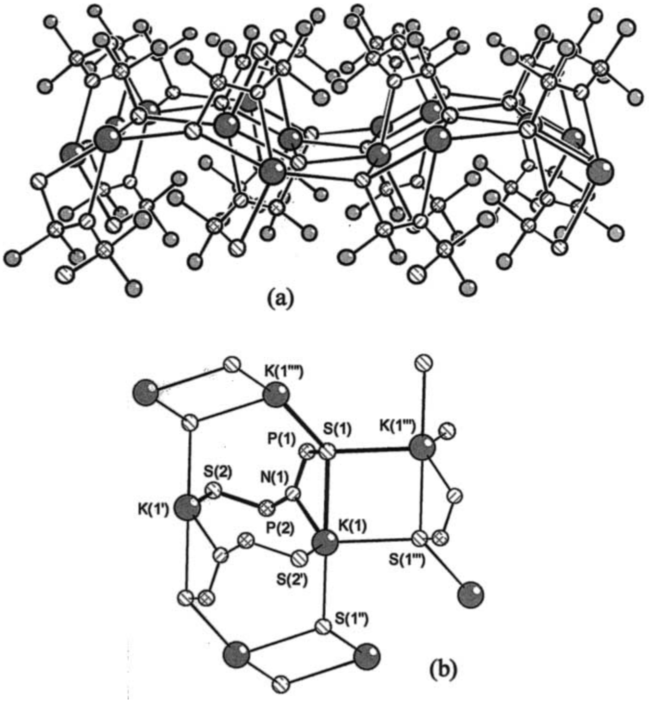

Fig. 16. (a) The layer polymeric association in the crystal of $K[(SPMe_2)_2N]$, and (b) a fragment showing the coordination pattern of the dithio ligand and the coordination geometry around K atoms (carbon atoms not shown) [56].

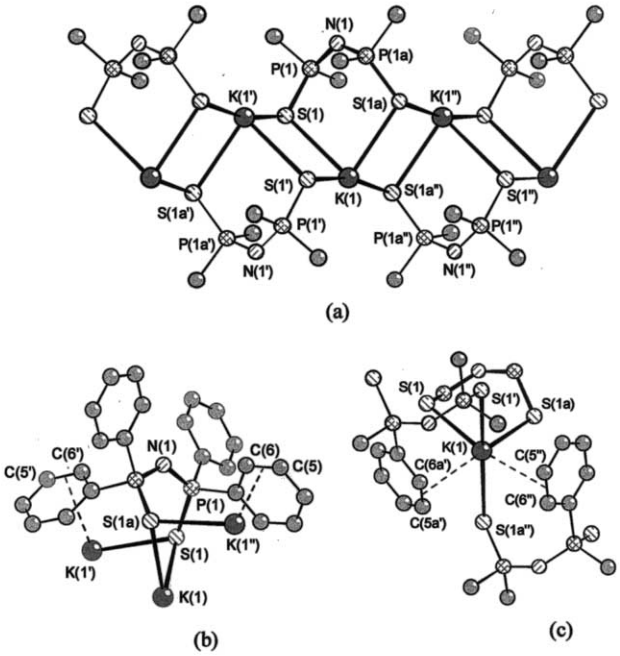

Fig. 17. (a) The ladder polymeric structure in the crystal of $K[(SPPh_2)_2N]$, (b) a fragment showing the coordination pattern of the dithio ligand, and (c) the coordination geometry around K atoms (only *ipso* carbon atoms and the phenyl groups involved in π interactions are shown) [80].

geometry at the potassium atom is thus distorted octahedral, with the K···(C–C) centroid vectors *trans* to the sulfur atoms exhibiting stronger interactions to the metal atom [K(1)–S(1) 3.203(1) Å] and *trans* S–K–S of 169.3(1)° (Fig. 17c).

In the crystal of the water adduct $K[\{OP(OEt)_2\}(SPPh_2)N]\cdot H_2O$ there are two independent molecules which are associated into a complicated polymeric structure [60]. The organophosphorus ligands for both molecules might be each considered as chelated through sulfur and the terminal oxygen atom to a metal center, the conformation of the resulting six-membered $KOSP_2N$ inorganic rings being twisted boat. In addition, one of the phenyl groups belonging to the ligand unit O,S-chelated to a K(2) atom exhibits interactions with the K(1) atom type through three of its carbon atoms [K(1)–C(10) 3.368(5), K(1)–C(11) 3.296(5), K(1)–C(12) 3.418(5) Å]. Two centrosymetrically related K(1)/K(2) dinuclear units are associated to form a tetranuclear core through two K(1)–O_{water}–K(2a) bridges and additional interactions established between the ligand unit O,S-chelating a K(1) atom and the K(2a) atom involving the terminal O(4)–phosphorus atom and an O(6)–Et atom. Moreover, these tetranuclear units are linked together into a polymeric structure through additional K(1)–O interactions involving the K(2)–O,S-chelated ligand unit of a neighboring tetranuclear system (Fig. 18a).

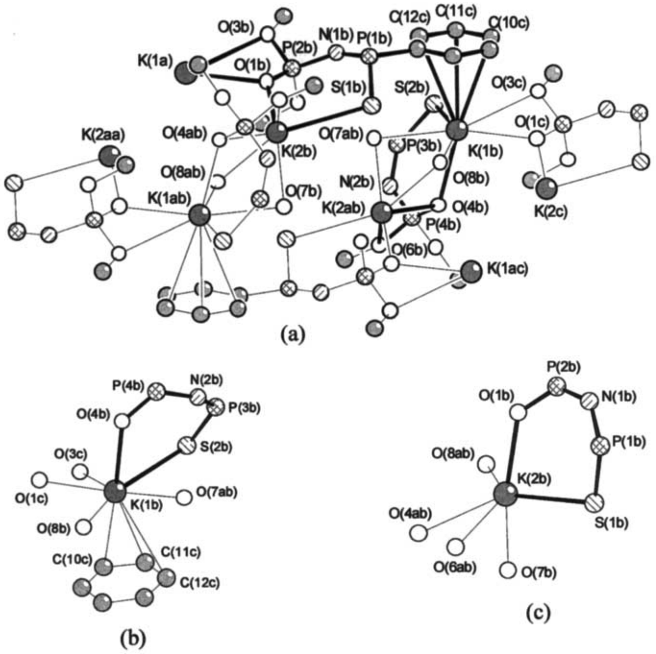

Fig. 18. (a) The polymeric association in the crystal of $K[\{OP(OEt)_2\}(SPPh_2)N] \cdot H_2O$ [only the phenyl group involved in coordination to K(1) atom and the carbon atoms attached to oxygen for the ethoxy group are shown], and coordination geometry around (b) K(1) atom and (c) K(2) atom [60].

The overall coordination patterns established by the monothioimidodiphosphinato ligands in this salt are different. Basically they are bimetallic tetraconnective of type (**17**), but one of them exhibits additional π $K–C_{phenyl}$ interactions.

The potassium ions of the two independent molecules also have differing coordination at the cores. The K(1) atom has the coordination number 9 made up of a S,O-chelating phosphorus ligand, an O,O(Et)-coordinated neighboring phosphorus ligand, two oxygen atoms from water molecules and three carbon atoms of a phenyl group (Fig. 18b). The K(2) atom has the coordination number 6 made up of a S,O-chelating phosphorus ligand, an O,O(Et)-coordinated neighboring phosphorus ligand, and two oxygen atoms from water molecules (Fig. 18c). It should also be noted that the potassium–sulfur bond distances are similar to the longer K–S distances observed for the polymeric $\{K[(SPPh_2)_2N]\}_n$ salt [80], while the K–O bond lengths cover a wider range [2.593(3)–3.331(3) Å].

Attempts to obtain compounds containing free $[(XPR_2)(YPR'_2)N]^-$ anion were made by complexing the K^+ cation by 18-crown-6 ether. In the case of $K[(OPPh_2)_2N]$, a water adduct was isolated, i.e. $[K(18\text{-crown-}6)][(OPPh_2)_2N] \cdot H_2O$ [106]. The lack of water solubility was considered to be indicative of a chelate structure. Indeed, the imidodiphosphinato ligand is monometallic biconnective, with non-equivalent potassium–oxygen interactions, resulting in a twisted boat conformation of the KO_2P_2N ring. The metal is additionally coordinated by all six oxygen atoms of the 18-crown-6 ether molecule [K–O_{crown} range 2.905(5)–3.037(5) Å] and a water molecule [K–O_{water} 3.110(5) Å] (Fig. 19a). As a result, the potassium atom lies in the center of a nine-vertex coordination polyhedron, at 2.30 and 1.05 Å from the two parallel O(1)O(2)O(9) and O_{crown} planes (dihedral angle of 2°).

In contrast, the dithio and diseleno analogs, [K(18-crown-6)][$(XPPh_2)_2N$] (X = S [108], Se [110]), exhibit a different structure. In these cases none of the chalcogen atoms of the ligand unit is involved in coordination to the metal. This behavior does not affect the magnitude of the phosphorus–chalcogen and phosphorus–nitrogen bond distances in comparison with the molecular dimensions found for the salts described above. However, a polymeric association is formed through π

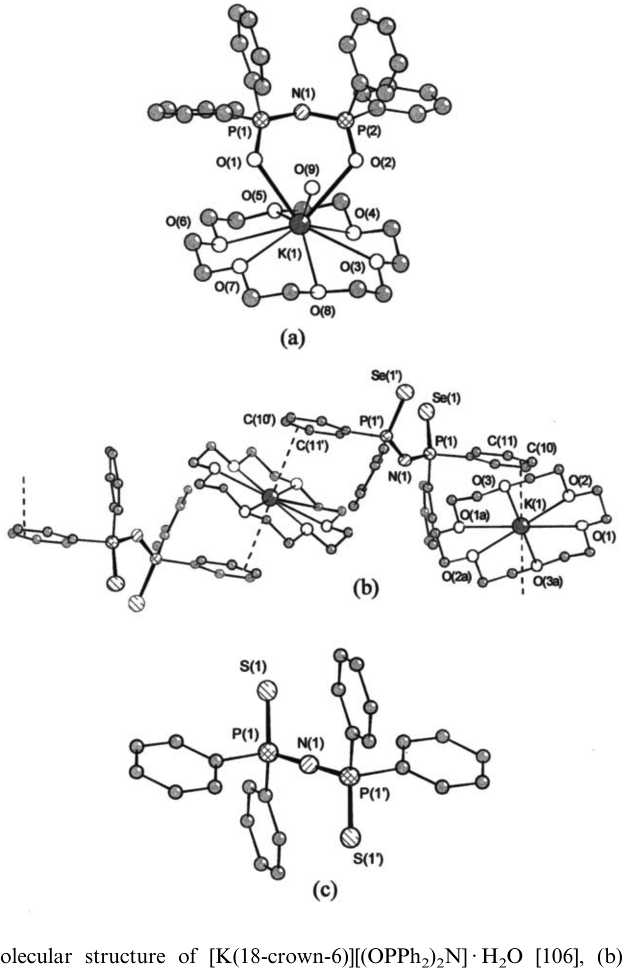

Fig. 19. (a) The molecular structure of [K(18-crown-6)][$(OPPh_2)_2N$]·H_2O [106], (b) the polymeric association in the crystal of [K(18-crown-6)][$(SePPh_2)_2N$] [110], and (c) the structure of the anion in [Ph_3PNPPh_3][$(SPPh_2)_2N$] [111].

interactions established between a C–C bond of one phenyl group of each phosphorus atom in the ligand moiety and metal centers of two complex cations (illustrated for Se derivative in Fig. 19b). Thus, the potassium atom can be considered as 8-coordinated, with the K···(C–C) centroid vectors *trans* on opposite sides of the KO_6 system.

A completely free dithioimidodiphosphinato anion was found in the crystal of the $[Ph_3PNPPh_3][(SPPh_2)_2N]$ salt [111]. Here the anion was found to exhibit a linear P–N–P fragment (Fig. 19c), and the whole S–P–N–P–S system is planar, with an *anti* orientation of the chalcogen atoms. The phosphorus–sulfur distances are intermediate between single P–S and double P=S bonds, but the phosphorus nitrogen distances are clearly shortened in comparison with the bent anion, consistent with an increased double bond character. The differences in bond distances and angles of the bent and linear $[(SPPh_2)_2N]^-$ anions were described in terms of the canonical forms (**18**) (sp^3-hybridized N atom) and (**19**) (sp-hybridized N atom).

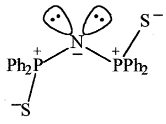

(**18**)

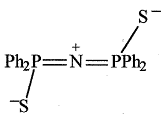

(**19**)

4.2. Group 2: Be, Ca, Ba

The known Group 2 metal compounds containing imidodiphosphorus ligands are listed in Table 16, along with the spectroscopic methods (including ^{31}P-NMR data) used for their characterization. So far only a beryllium and a barium complex have been investigated by single-crystal X-ray diffraction and their important molecular dimensions are included in Table 18, together with those for the Group 12 metal complexes.

4.2.1. Beryllium

Thermal treatment (ca. 100 °C for 12 h) of beryllium acetylacetonate in the presence of an excess of free $(OPPh_2)_2NH$ acid (1:1.7 molar ratio) gave the mixed complex, $Be[(OCMe)_2CH][(OPPh_2)_2N]$, quantitatively [55]. This compound did not disproportionate on further heating. However, the $Be[(OPPh_2)_2N]_2$ complex was isolated when a 1:1 molar mixture of $Be[(OCMe)_2CH][(OPPh_2)_2N]$ and $(OPPh_2)_2NH$ was heated at ca. 170 °C. The thermal treatment of a 1:1 molar mixture of $Be[(OCMe)_2CH][(OPPh_2)_2N]$ and $Ph_2P(O)OH$ failed to result into the mixed-phosphorus ligand species, but the $Be[(OPPh_2)_2N]_2$ complex was isolated in 66% yield [55]. The bis-complex was also obtained either by refluxing $Be[(OCMe)_2CH]_2$ and the free acid in anhydrous benzene (a benzene solvate was isolated) or by reacting $BeCl_2$ with the corresponding potassium salt [55,112]. The formation of a mixed-ligand complex, $Be[OPPh_2(NPPh_2)_3O][(OPPh_2)_2N]$, was also

Table 16
Group 2 metal complexes of imidodiphosphorus acids

Compound	Synthesis, yield (%)	M.p. (°C)	$\delta(^{31}P)$ (ppm)/solvent	X-ray studies	Spectroscopic studies
$Be[(OCMe)_2CH][(OPPh_2)_2N]$	100 [55]	193–193.5	$28.8s/C_6H_6$		IR, ^{31}P [55]
$Be[OPPh_2(NPPh_2)_3O][(OPPh_2)_2N]$	[55]	357–359	$28.8s/C_6H_6$		IR [55]
$Be[(OPPh_2)_2N]_2$ (benzene solvate)	[55,112]	221–222			IR [55]
$Be[(OPPh_2)_2N]_2$	[55,112]	237–238	$27.2s/C_6H_6$ $28.3s/CDCl_3$	[112]	IR [55], MS [112] ^{31}P [55,112]
$Ca[\{OP(OPh)_2\}_2N]_2$	55 [64]	284–285	28.8s/EtOH		^{31}P [64]
$Ba[\{OP(OPh)_2\}_2N]_2$	47 [64]	181–182	28.8s/EtOH		^{31}P [64]
$Ba[(SPPh_2)_2N]_2 \cdot 2THF$	96 [113]				
$Ba[(SPPh_2)_2N]_2 \cdot 2DME$[a]	100 [113]	150[b]	57.6s	[113]	IR, ^{1}H, ^{31}P [113]

[a] DME = 1,2-dimethoxyethane.

[b] Decomposition at 195 °C.

reported [55]. For all these beryllium compounds molecular weight measurements indicated their monomeric nature in benzene solution, while the ^{31}P-NMR data were consistent with equivalent phosphorus atoms in the ligand unit [55].

The monomeric nature of $Be[(OPPh_2)_2N]_2$ in the solid state was confirmed by X-ray diffraction [112]. The beryllium atom is tetrahedrally coordinated by the four oxygen atoms [O–Be–O range 108.1(5)–111.3(6)°], and the six-membered BeO_2P_2N inorganic rings exhibit a slight distortion from planarity towards a boat conformation.

4.2.2. Barium

Only the adduct $Ba[(SPPh_2)_2N]_2 \cdot 2DME$ (DME = 1,2-dimethoxyethane) has been structurally characterized (Fig. 20) [113]. The two dithio ligands also act as monometallic biconnective moieties, but the resulting BaS_4 system is square trapezoidal [S(1)–Ba(1)–S(4) 127°, S(2)–Ba(1)–S(3) 72°, and endocyclic S–Ba(1)–S 80°, as calculated from published atomic coordinates], with a dihedral angle of 7.04° between the BaS_2 planes of the BaS_2P_2N rings. The metal atom is also coordinated by the oxygen atoms of the two ether molecules, positioned above and below the BaS_4 plane. A pseudo-cubic coordination environment is thus obtained with dihedral angles of 5.8° between the planes of the BaO_2 units and nearly perpendicular BaS_2 and BaO_2 planes, respectively.

4.3. Group 12: Zn, Cd, Hg

In view of the filled d shells, the elements belonging to Group 12, as expected, exhibit few of the characteristic properties of transition metals. Because their chemical behavior resembles those of the Group 2 elements, the zinc, cadmium and mercury complexes containing imidodiphosphorus ligands are included in this first part of the review dedicated to main group metals. The known complexes are listed in Table 17, while Table 18 contains important molecular dimensions for metal complexes investigated by single-crystal X-ray diffraction. For zinc and cadmium only inorganic complexes have been reported so far, while for mercury both inorganic and organometallic derivatives are known.

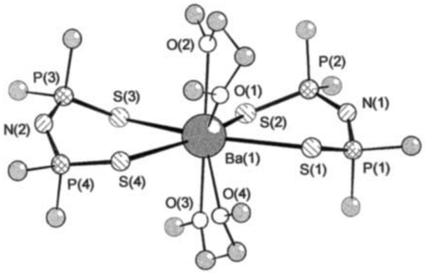

Fig. 20. The molecular structure of $Ba[(SPPh_2)_2N]_2 \cdot 2DME$ [113] (for clarity, only *ipso* carbons of the phenyl groups are shown).

Table 17
Group 12 metal complexes of imidodiphosphorus acids

Compound	Synthesis, yield (%)	M.p. (°C)	$\delta(^{31}P)$ (ppm), $^{n}J(PX)$ (Hz)[a]			X-ray studies	Spectroscopic studies
			*P*O	*P*S	*P*Se		
Inorganic compounds							
$Zn[(SP^{i}Pr_2)_2N]_2$	90 [73]	144		64.4s		[73]	IR, MS, ^{31}P [73]
$Zn[(SP^{n}Bu_2)_2N]_2$	[75]	Oil		52.0s			IR, MS, ^{31}P [75]
$Zn[(SP^{i}Bu_2)_2N]_2$	[75]			49.1s			IR, MS, ^{31}P [75]
$Zn[(SP^{s}Bu_2)_2N]_2$	[75]			62.8s			IR, MS, ^{31}P [75]
$Zn[(SP^{n}Bu_2)(SP^{i}Bu_2)N]_2$	[75]			51.5d (P–^{n}Bu) 49.6d (P–^{i}Bu), $^{2}J(PP)$ 19.8			IR, MS, ^{31}P [75]
$Zn[(SPPh_2)_2N]_2$	[79]						
$Zn[(SP^{n}Bu_2)(SP^{s}Bu_2)N]_2$	[75]			50.4d (P–^{n}Bu) 64.0d (P–^{s}Bu), $^{2}J(PP)$ 26.4			IR, MS, ^{31}P [75]
$Zn[(SP^{i}Bu_2)(SP^{s}Bu_2)N]_2$	[75]			48.7d (P–^{i}Bu) 63.4d (P–^{s}Bu), $^{2}J(PP)$ 26.4			IR, MS, ^{31}P [75]
$Zn[\{SP(OEt)_2\}(SPPh_2)N]_2$	[82]	Oil		46.9d (P–OEt) 36.3d (P–Ph), $^{2}J(PP)$ 26.4			IR, MS, ^{31}P [82]
$Zn[(SeP^{i}Pr_2)_2N]_2$	87 [44]				59.8d, $^{1}J(PSe)$ 539		IR, MS, ^{31}P [44]
$Zn[(SePPh_2)_2N]_2$	49 [114]	303–305			30.3s		IR, MS, ^{31}P [114]
$Zn[(OP^{i}Pr_2)(SP^{i}Pr_2)N]_2$	59 [44]		52.0d, $^{2}J(PP)$ 22.0	60.8d, $^{2}J(PP)$ 22.0			IR, MS, ^{31}P [44]
$Zn[(OPPh_2)\{SP(OEt)_2\}N]_2$	[92]	Oil	21.6d, $^{2}J(PP)$ 24.2	43.4d, $^{2}J(PP)$ 24.2			IR, MS, ^{31}P [92]
$Zn[\{OP(OEt)_2\}(SPPh_2)N]_2$	[92]	Oil	5.4d, $^{2}J(PP)$ 22.0	35.6d, $^{2}J(PP)$ 22.0		[92]	IR, MS, ^{31}P [92]
$Zn[(SP^{i}Pr_2)(SeP^{i}Pr_2)N]_2$	55 [44]			65.7d, $^{2}J(PP)$ 28.2	56.6d, $^{2}J(PP)$ 28.2, $^{1}J(PP)$ 505		IR, MS, ^{31}P [44]
$Cd[(SPMe_2)_2N]_2$	[115]	164		42.4s		[115]	^{1}H, ^{31}P [115]

Table 17 (*Continued*)

Compound	Synthesis, yield (%)	M.p. (°C)	$\delta(^{31}P)$ (ppm), $^{n}J(PX)$ (Hz)[a]			X-ray studies	Spectroscopic studies
			*P*O	*P*S	*P*Se		
$\mathrm{Cd[(SP^{i}Pr_2)_2N]_2}$	86 [73]	161		63.1s		[73]	IR, MS, ^{31}P [73]
$\mathrm{Cd[(SPPh_2)_2N]_2}$	[79]						IR [79]
$\mathrm{Cd[(SeP^{i}Pr_2)_2N]_2}$	74 [44]				56.6s, $^{1}J(PSe)$ 563, $^{2}J(PCd)$ 30.8	[44]	IR, MS, ^{31}P [44]
$\mathrm{Cd[(SePPh_2)_2N]_2}$	85 [114]				31.7s	[114]	IR, MS, ^{31}P [114]
$\mathrm{Cd_2[(OPMe_2)(SPPh_2)N]_2}$	67 [115]	197	25.4s	33.9s		[115]	^{1}H, ^{31}P [115]
$\mathrm{K[Cd_2\{(OPPh_2)_2N\}_5]}$	[115]					[115]	
$\mathrm{Hg[(SPPh_2)_2N]_2}$	[79]						IR [79]
$\mathrm{HgCl[(SPPh_2)_2N]}$	[79]						IR [79]
$\mathrm{Hg[(SePPh_2)_2N]_2}$	41 [114]				30.2s	[114]	IR, ^{31}P [114]
Organometallic compounds							
$\mathrm{PhHg[\{OP(OPh)_2\}_2N]}$	61 [65,116]	98	−8.0s			[116]	^{31}P [65]
$\mathrm{PhHg[(OPMe_2)(SPPh_2)N]}$	65 [115]	137–138	25.8s	36.7s		[115]	MS, ^{1}H, ^{13}C, ^{31}P [115]
$\mathrm{PhHg[(OPPh_2)(SPPh_2)N]}$	71 [115]	116–118	21.1s	28.8s		[115]	^{1}H, ^{13}C, ^{31}P [115]
$\mathrm{Hg_2[\{OP(OPh)_2\}\text{-}\{OP(OPh)(OC_6H_4\text{-}2)\}N]_2}$	23 [65]	187–188	−3.1d/−8.3d, $^{2}J(PP)$ 0.5, $^{2}J(PHg)$ 24.0/26.7			[65]	^{31}P[65]
$\mathrm{Hg_2[(OPEt_2)\text{-}\{OP(OPh)(OC_6H_4\text{-}2)\}N]_2}$	18 [58]	188	56.1d/51.4s (P–Et) −9.3d/−8.7s (P–OPh), $^{2}J(PP)$ 5			[58]	^{1}H, ^{31}P [58]

[a] In $CDCl_3$.

Table 18
X-ray data [bond lengths (Å) and bond angles (°)] for Group 2 and 12 metal complexes of imidodiphosphorus acids

Compound	M–X	P–X	P–N	P–N–P	Association degree	Ref.
Group 2						
$Be[(OPPh_2)_2N]_2$	1.63(1)/1.66(1)	1.521(5)/1.516(5)	1.590(7)/1.592(7)	120.9(4)	Monomer	[112]
$Ba[(SPPh_2)_2N]_2 \cdot 2DME$	3.211(2)–3.270(3)[a]	1.985[b]	1.577[b]	–[c]	Monomer	[113]
Group 12						
Inorganic compounds						
$Zn[(SP^iPr_2)_2N]_2$	2.345(1)	2.032(1)	1.581(2)	140.5(3)	Monomer	[73]
$Zn[\{OP(OEt)_2\}(SPPh_2)N]_2$	1.946(3) (M–O) 2.318(1) (M–S)	1.479(3) (P–O) 2.013(1) (P–S)	1.551(3) 1.579(3)	134.1(2)	Monomer	[92]
$Cd[(SPMe_2)_2N]_2$	2.515(1)/2.536(1)	2.026(1)/2.024(1)	1.586(3)/1.588(3)	131.2(2)	Monomer	[115]
$Cd[(SP^iPr_2)_2N]_2$	2.514(2)–2.531(2)	2.018(2)–2.032(2)	1.573(3)–1.592(3)	141.0(2)/143.2(2)	Monomer	[73]
$Cd[(SeP^iPr_2)_2N]_2$	2.622(2)–2.636(2)	2.168(4)–2.188(4)	1.56(1)–1.60(1)	142.6(7)/144.4(7)	Monomer	[44]
$Cd[(SePPh_2)_2N]_2$	2.617(1)–2.641(1)	2.163(2)–2.173(2)	1.581(4)–1.600(4)	133.7(3)/137.2(3)	Monomer	[114]
$Cd[(OPMe_2)(SPPh_2)N]_2$	2.215(2)/2.257(2) (M–O)[d] 2.523(1)/2.536(1) (M–S)	1.519(2)/1.506(2) (P–O) 2.022(1)/2.022(1) (P–S)	1.601(2)/1.581(3) 1.596(2)/1.576(3)	126.2(1)/135.2(2)	Dimer	[115]

Table 18 (*Continued*)

Compound	M–X	P–X	P–N	P–N–P	Association degree	Ref.
$K[Cd_2\{(OPPh_2)_2N\}_5]$	2.169(5)–2.271(4)	1.500(5)–1.518(5)	1.570(6)–1.593(7)	127.2(4)–134.7(4)	Dinuclear	[115]
$Hg[(SePPh_2)_2N]_2$	2.612(2)–2.657(2)	2.170(4)–2.184(5)	1.56(2)–1.60(1)	135(1)/139(1)	Monomer	[114]
Organometallic compounds						
$PhHg[\{OP(OPh)_2\}_2N]^e$	2.624^f	1.453(7)/1.465(9)	1.629(9)/1.627(9)	125.8(5)	Dimer	[116]
$PhHg[(OPMe_2)(SPPh_2)N]^g$	2.556(4) (M–O)[h]	1.509(4) (P–O)	1.611(4)	131.1(3)	Dimer	[115]
	2.405(1) (M–S)	2.048(2) (P–S)	1.587(4)			
$PhHg[(OPPh_2)(SPPh_2)N]^i$	2.589(4) (M–O)	1.495(5) (P–O)	1.602(6)	134.7(4)	Dimer	[115]
	2.398(2) (M–S)[j]	2.060(2) (P–S)	1.574(5)			
$Hg_2[\{OP(OPh)_2\}\{OP(OPh)(OC_6H_4)\}N]_2^k$		1.470(1)/1.482(11)	1.666(13)/1.570(12)	132.3(8)	Dinuclear	[65]
$Hg_2[(OPEt_2)\{OP(OPh)(OC_6H_4\text{-}2)\}N]_2^l$		$1.463/1.479^f$	$1.625/1.649^f$	134.8^f	Dinuclear	[58]

[a] Ba–O_{DME} 2.724(7)–2.861(8) Å.

[b] Only average P–S and P–N values given in the original publication.

[c] The P–N–P bond angles not given in the original publication.

[d] Transanular Cd–O 2.415(2) Å.

[e] Hg–C 2.038.9(9), Hg–N 2.125(8) Å.

[f] Calculated from published atomic coordinates.

[g] Hg–C 2.076(6) Å.

[h] Transanular Hg–O 2.754 Å.

[i] Hg–C 2.057(7) Å.

[j] Transannular Hg–S 3.312 Å.

[k] Hg–C 2.061(14), Hg–N 2.151(11) Å.

[l] Hg–C 2.065, Hg–N 2.093 Å — calculated from published atomic coordinates.

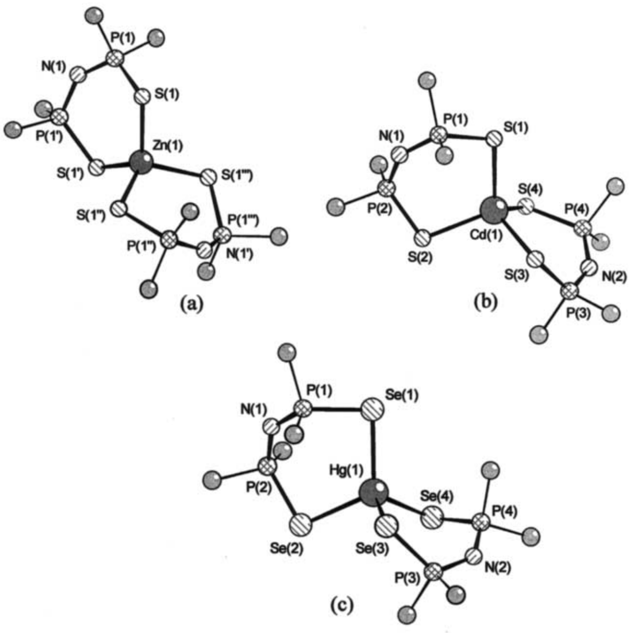

Fig. 21. The molecular structure of (a) $Zn[(SP^{i}Pr_2)_2N]_2$, (b) $Cd[(SP^{i}Pr_2)_2N]_2$ [73], and (c) $Hg[(SePPh_2)_2N]_2$ [114] (for clarity, only carbons bound to phosphorus are shown).

4.3.1. Zinc

A large number of zinc complexes of the type $Zn[(XPR_2)(YPR'_2)N]_2$ have been prepared and investigated by various spectroscopic methods [44,73,75,82,92,114]. In all cases monomeric, distorted tetrahedral complexes containing either ZnX_4 ($X =$ S, Se) or ZnS_2X_2 ($X = O$, Se) were obtained, as a result of the chelating nature of both imidodiphosphorus ligands. For two complexes, i.e. $Zn[(SP^{i}Pr_2)_2N]_2$ (Fig. 21a) [73] and $Zn[\{OP(OEt)_2\}(SPPh_2)N]_2$ [92], the molecular structures were confirmed by X-ray diffraction. The ZnS_2P_2N ring has a pseudo-boat conformation [73], while the $ZnOSP_2N$ ring in the second complex is folded about the Zn···P axis [Zn(1)S(1)P(1)/Zn(1)O(1)P(2)N(1)P(1) dihedral angle of 33°] [92].

4.3.2. Cadmium

Although only a few cadmium complexes have been investigated to date, they exhibit a much broader structural diversity when compared to their zinc analogs.

Thus, monomeric, distorted tetrahedral structures, similar to those established for Zn complexes, were found for derivatives of symmetric phosphorus ligands [44,73,114,115], as exemplified by $Cd[(SP^{i}Pr_2)_2N]_2$ (Fig. 21b). In all these cases the monometallic biconnective pattern of the imidodiphosphinato ligands results in six-membered CdX_2P_2N chelate rings of distorted boat conformation.

In contrast, for the monothioimidodiphosphinato derivative, $Cd[(OPMe_2)$-

$(SPPh_2)N]_2$, a dimeric structure was established in the solid state [115]. One of the phosphorus ligands in the molecular unit is chelated through the chalcogen atoms, while the other bridges two metal atoms. As a consequence a 12-membered $Cd_2O_2S_2P_4N_2$ ring is formed (Fig. 22). The cadmium– and phosphorus–chalcogen bond distances are of the same magnitude for the two types of ligands. In addition, strong transannular Cd–O interactions [2.415(2) Å] are present, thus leading to a tricyclic system with an overall ladder structure containing a planar Cd_2O_2 central ring, similar to that observed in the $Na[(OPPh_2)(SPPh_2)N] \cdot 2THF$ dimer [90]. The bridging ligand can be described as a bimetallic triconnective unit and this coordination pattern results in a P–N–P bond angle almost 10° smaller [126.2(1)°] than in the chelated moiety [135.2(2)°]. The coordination geometry around the metal atoms is distorted trigonal bipyramidal, with the oxygen of the chelated ligand and that of the transannular interaction in the axial positions [O(2)–Cd(1)–O(1) 166.7(1)°].

An unusual and interesting structure was found in the case of the $K[Cd_2\{(OPPh_2)_2N\}_5]$ salt [115]. A dinuclear anion is formed through three bridging imidodiphosphinato ligands, the other two being each chelated to a cadmium atom. The $Cd–O_{chelating}$ bond lengths [range 2.169(5)–2.223(5) Å] are generally shorter than the $Cd–O_{bridging}$ ones [range 2.219(5)–2.271(4) Å]. In contrast with the monothio derivative mentioned above, the P–N–P bond angles of the bridging ligands are not smaller [130.2(4)–134.7(4)°] than those of the chelated moieties [127.2(4)/130.5(4)°]. The resulting coordination geometry around cadmium is distorted square pyramidal, with oxygen atoms of the same bridging ligand [O(3) and O(4) atoms for Cd(1) and Cd(2), respectively] in axial positions. The potassium cation is accommodated co-linear with the cadmium atoms into the $Cd_2(O_2P_2N)_5$ cage, being coordinated by all six oxygen atoms of the bridging ligands [K–O range

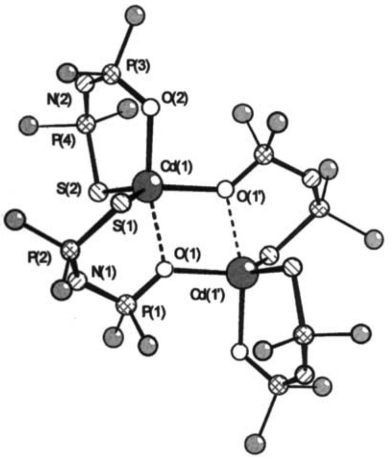

Fig. 22. The dimeric association in the crystal of $Cd[(OPMe_2)(SPPh_2)N]_2$ [115] (the phenyl groups on phosphorus atoms are not shown).

2.365(5)–2.468(5) Å] in a trigonal prismatic arrangement (Fig. 23). Thus, the coordination pattern of the bridging ligands becomes trimetallic tetraconnective. The conformation of the six-membered MO_2P_2N rings is consistent with the high flexibility of such systems: the CdO_2P_2N rings exhibit an almost planar conformation, while two of the KO_2P_2N rings have chair conformations and the third one [including the O(5)/O(6) bridging ligand] is of boat conformation.

4.3.3. Mercury

The $Hg[(SePPh_2)_2N]_2$ derivative is the only inorganic mercury complex whose molecular structure has been investigated by X-ray diffraction [114]. Its crystals contain discrete tetrahedral molecules similar to the zinc and cadmium analogs (Fig. 21c), with distorted boat conformation of the $HgSe_2P_2N$ rings.

An unusual coordination pattern of the imidodiphosphorus ligand was establish in the organometallic $PhHg[\{OP(OPh)_2\}_2N]$ complex prepared from PhHgOH and the free acid [116]. In this case the ligand is attached to the metal atom through its nitrogen atom [Hg(1)–N(1) 2.125(8) Å]. In the crystal, dimeric associations (Fig. 24) are formed by intermolecular mercury–oxygen interactions which involve one

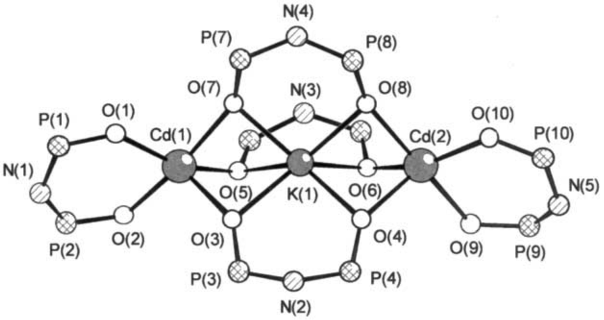

Fig. 23. The inorganic skeleton in the $K[Cd_2\{(OPPh_2)_2N\}_5]$ salt [115].

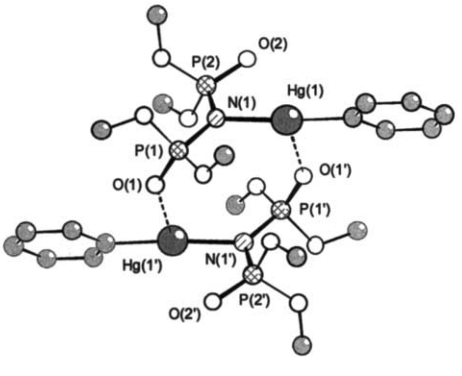

Fig. 24. The dimeric association in the crystal of $PhHg[\{OP(OPh)_2\}_2N]$ [116] (for clarity, only *ipso* carbons of the phenoxy groups are shown).

terminal oxygen atom of a ligand unit [Hg(1)–O(1′) 2.125(8) Å]. Thus, the imidodiphosphorus moiety behaves as an N,O-bimetalic biconnective ligand with an *anti* conformation of its O–P–N–P–O backbone. The coordination at the metal center is T-shaped, with a N–Hg–C angle of 175.0(3)°.

Dimeric associations were also found in the crystals of $PhHg[(OPMe_2)(SPPh_2)N]$ and $PhHg[(OPPh_2)(SPPh_2)N]$ [115], but in these cases the coordination pattern of the monothio ligands is similar to that observed for the bridging ligands in $Cd[(OPPh_2)(SPPh_2)N]_2$ described above, thus leading to 12-membered $Hg_2O_2S_2P_4N_2$ rings. Transannular interactions are also present: for $PhHg[(OPMe_2)(SPPh_2)N]$, these are established by the oxygen atoms (Hg–O 2.754 Å) (Fig. 25a), while for $PhHg[(OPPh_2)(SPPh_2)N]$, the sulfur atoms are involved (Hg–S 3.312 Å) (Fig. 25b). In both cases the tricyclic, overall ladder structure contains a planar Hg_2X_2 central ring. The coordination around the mercury atom in both complexes can be described as distorted pseudo-trigonal bipyramidal, with the *ipso* carbon of the phenyl group and a sulfur atom in the axial positions [C–Hg–S 166.4(2)° and 165.0(2)°, respectively].

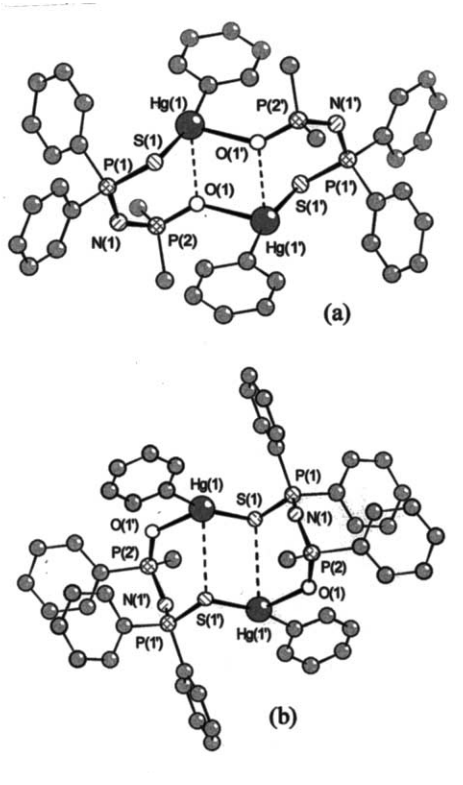

Fig. 25. The dimeric association in the crystal of (a) $PhHg[(OPMe_2)(SPPh_2)N]$, and (b) $PhHg[(OPPh_2)(SPPh_2)N]$ [115] (for clarity, only *ipso* carbons of one of the phenyl groups on P(2) atoms are shown).

The reaction of mercury(II) oxide with $[OP(OPh)_2]_2NH$ or $(OPEt_2\}[OP(OPh)_2]$-NH resulted in *ortho*-mercuration of a phenoxy group and isolation of the dinuclear compounds, $Hg_2[(OPR_2)\{OP(OPh)(OC_6H_4\text{-}2)\}N]_2$ (R = Et [58], OPh [65]). The second covalence at the mercury atom is achieved through a Hg–N bond which involves the nitrogen of a neighboring mercurated imidodiphosphoric ligand, thus resulting in the formation of a 12-membered $Hg_2C_4O_2P_2N_2$ ring with almost linear N–Hg–C fragments {174.9 and 176.9°, respectively). In addition, there appear to be weak Hg···O interactions which involve one terminal oxygen atom (2.837 Å) for R = OPh (Fig. 26a), or both terminal oxygens of the O–P–N–P–O fragment (2.813 and 2.890 Å) for R = Et (Fig. 26b).

4.4. Group 13: B, Al, Ga, In, Tl

Inorganic complexes of imidodiphosphorus ligands have been described for B, Al, Ga and In, but organometallic derivatives are known only for Al, Ga and Tl (Table 19). The solid state structures of most of the compounds have been investigated by single-crystal X-ray diffraction and in all cases discrete monomers were found (Table 20).

4.4.1. Boron

Only one ionic complex of boron has been reported, i.e. $[B\{(OPPh_2)_2N\}_2][I_3]$ [42]. Two crystalline modifications (monoclinic and triclinic) were isolated both of which contain similar cations and anions. The $[B\{(OPPh_2)_2N\}_2]^{1+}$ cation exhibits a tetrahedral BO_4 core as a result of the monometallic biconnective pattern of the imidodiphosphinato ligands (Fig. 27a). The conformation of the inorganic BO_2P_2N rings is distorted boat.

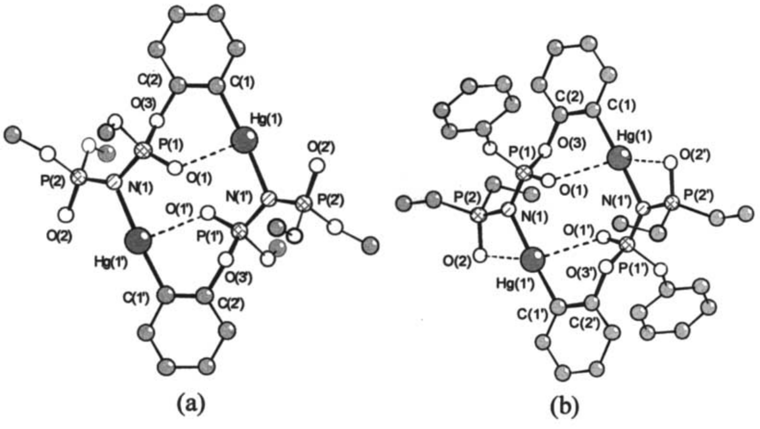

Fig. 26. The structure of dinuclear complexes (a) $Hg_2[\{OP(OPh)_2\}\{OP(OPh)(OC_6H_4\text{-}2)\}N]_2$ [65] (for clarity, only *ipso* carbons of phenoxy groups are shown), and (b) $Hg_2[(OPEt_2)\{OP(OPh)(OC_6H_4\text{-}2)\}N]_2$ [58].

Table 19
Group 13 metal complexes of imidodiphosphorus acids

Compound	Synthesis, yield (%)	M.p. (°C)	$\delta(^{31}P)$ (ppm), $^nJ(PX)$ (Hz)[a]			X-ray studies	Spectroscopic studies
			*P*O	*P*S	*P*Se		
Inorganic compounds							
$[B\{(OPEt_2)_2N\}_2][I_3]$	72 [42]						MS [42]
$[B\{(OPPh_2)_2N\}_2][I_3]$	82 [42]					[42]	MS [42]
$Ga[(OPPh_2)_2N]_3 \cdot CH_2Cl_2$	83 [117]	> 300	25.4s			[117]	IR, MS, ^{31}P [117]
$In[(OPPh_2)_2N]_3$	55 [118]		25.4s			[117]	IR, ^{31}P [118], MS [117]
$In[(SPPh_2)_2N]_3$	75 [118]			34.9s		[118]	IR, ^{31}P [118]
$In[(SePPh_2)_2N]_3$	76 [119]				28.5s	[119]	IR, MS, ^{31}P [119]
$In[(OPPh_2)(SPPh_2)N]_3$	61 [120]	> 320	23.3s	33.6s		[120]	IR, MS, ^{31}P [120]
$InCl[(SP^iPr_2)_2N]_2$	78 [121]			64.7s		[121]	IR, MS, ^{31}P [121]
$InCl[(SeP^iPr_2)_2N]_2$	77 [121]			61.1s		[121]	IR, MS, ^{31}P [121]
$InCl[(SePPh_2)_2N]_2 \cdot CH_2Cl_2$	75 [121]				31.6s, $^1J(PSe)$ 537	[121]	IR, MS, ^{31}P [121]
$InCl[(SPPh_2)(SePPh_2)N]_2$	77 [120]	198		40.5s	28.4s, $^1J(PSe)$ 738	[120]	IR, MS, ^{31}P [120]
Organometallic compounds							
$Me_2Al[(SePPh_2)_2N]$	75 [122]	133–135			54.1m, $^1J(PSe)$ 804		IR, ^1H, ^{31}P, ^{27}Al [122]
$Et_2Al[(SePPh_2)_2N]$	80 [122]	130–133			54.0m, $^1J(PSe)$ 802		IR, ^1H, ^{31}P, ^{27}Al [122]
$^iBu_2Al[(SePPh_2)_2N]$	79 [122]	133–135			54.0m, $^1J(PSe)$ 804		IR, ^1H, ^{31}P, ^{27}Al [122]
$Et_2Ga[(SePPh_2)_2N]$	75 [122]	135–137			29.5m, $^1J(PSe)$ 534	[122]	IR, ^1H, ^{31}P, ^{77}Se [122]
$Ph_2Tl[(SPPh_2)_2N]$	94 [123]			34.6s		[123]	IR, ^{31}P [123]

[a] In $CDCl_3$.

Table 20
X-ray data [bond lengths (Å) and bond angles (°)] for Group 13 metal complexes of imidodiphosphorus acids

Compound		M–X	P–X	P–N	P–N–P	Association degree	Ref.
Inorganic compounds							
$[B\{(OPPh_2)_2N\}_2][I_3]$	(1)[a]	1.44(2)–1.47(2)	1.55(1)–1.57(1)	1.57(2)/1.61(2)	120(1)/120(1)	Monomer	[42]
$[B\{(OPPh_2)_2N\}_2][I_3]$	(2)[b]	1.45(2)–1.48(2)	1.54(1)–1.59(1)	1.56(2)/1.60(2)	119(1)/122(1)	Monomer	[42]
$Ga[(OPPh_2)_2N]_3 \cdot CH_2Cl_2$		1.954(5)–1.996(5)	1.505(6)–1.519(6)	1.576(6)–1.608(7)	122.5(5)–124.3(4)	Monomer	[117]
$In[(OPPh_2)_2N]_3 \cdot C_6H_6$		2.115(3)–2.144(3)	1.509(3)–1.520(3)	1.577(4)–1.595(4)	126.2(2)–127.4(2)	Monomer	[117]
$In[(SPPh_2)_2N]_3$		2.57(1)–2.68(1)	1.99(1)–2.09(2)	1.577(4)–1.595(4)	134–143[c]	Monomer	[118]
$In[(SePPh_2)_2N]_3$		2.708(3)–2.807(3)	2.162(5)–2.187(5)	1.578(16)–1.601(19)	130.5(11)–134.5(9)	Monomer	[119]
$In[(OPPh_2)(SPPh_2)N]_3 \cdot 0.75C_6H_6$		2.121(4)–2.144(4) (M–O)	1.505(5)–1.533(5) (P–S)	1.587(5)–1.594(6)	128.8(3)–133.6(4)	Monomer	[120]
		2.591(1)–2.611(1) (M–S)	2.009(3)–2.021(2) (P–S)	1.566(6)–1.582(5)			
$InCl[(SP^{i}Pr_2)_2N]_2$[d]		2.527(1)/2.616(1)	–[e]	–[e]	138.0(2)	Monomer	[121]
$InCl[(SeP^{i}Pr_2)_2N]_2$[f]		2.645(3)/2.720(3)	–[e]	–[e]	139.4(2)	Monomer	[121]
$InCl[(SePPh_2)_2N]_2 \cdot CH_2Cl_2$[g]		2.595(4)/2.750(4)[h]	–[e]	–[e]	128.8(2)	Monomer	[121]
$InCl[(SPPh_2)(SePPh_2)N]_2$[i]		2.642(3)/2.693(3) (M–S)	2.048(4)/2.088(4) (P–S)	1.597(9)/1.591(10)	127.7(6)/130.9(6)	Monomer	[120]
		2.583(2)/2.570(2) (M–Se)	2.184(4)/2.160(4) (P–Se)	1.603(10)–1.582(10)			
Organometallic compounds							
$Et_2Ga[(SePPh_2)_2N]$[j]		2.514(1)/2.535(1)	2.168(2)/2.173(2)	1.594(5)/1.591(5)	129.8(3)		[122]
$Ph_2Tl[(SPPh_2)_2N]$[k]	Mol. 1	2.736(3)/2.788(2)	2.013(3)/2.021(2)	1.600(6)/1.590(6)	131.8(5)		[123]
	Mol. 2	2.740(2)/2.766(2)	2.010(2)/2.025(3)	1.596(6)/1.575(5)	130.7(4)		

[a] Monoclinic form.

[b] Triclinic form.

[c] Calculated from published atomic coordinates.

[d] In–Cl 2.410(2) Å.

[e] Not given in the original paper.

[f] In–Cl 2.428(1) Å.

[g] In–Cl 2.440(1) Å.

[h] Average values.

[i] In–Cl 2.422(3) Å.

[j] Ga–C 1.977(7), 1.998(7) Å.

[k] Tl(1)–C 2.175(6), 2.099(8) Å and Tl(2)–C 2.145(7), 2.204(8) Å.

4.4.2. Aluminum

Some inorganic aluminum complexes which apparently contain both protonated and deprotonated imidodiphosphinic ligands have already been mentioned in Section 3 (Table 12).

Only organometallic derivatives of tetraphenyldiselenoimidodiphosphinic acid containing two alkyl groups attached to aluminum, $R_2Al[(SePPh_2)_2N]$ (R = Me, Et, ^{i}Bu), have been reported so far [122]. They were prepared by alkane elimination during reaction of R_3Al and $[(SePPh_2)_2NH]$, in toluene at room temperature. Attempts to use 1:2 and 1:3 molar ratios of Me_3Al and $[(SePPh_2)_2NH]$ resulted only in isolation of the 1:1 product. The ^{31}P-NMR chemical shifts and phosphorus–selenium coupling constants for $R_2Al[(SePPh_2)_2N]$ derivatives (Table 19) are very similar to those of the free ligand and this behavior was considered to be indicative of weak Al–Se bonds. Although the solid state structure of $R_2Al[(SePPh_2)_2N]$ has not been investigated by X-ray diffraction, ^{27}Al-NMR data suggests that it is monomeric with tetrahedral coordination of aluminum and hence similar to the structure of the diethylgallium(III) analog described below.

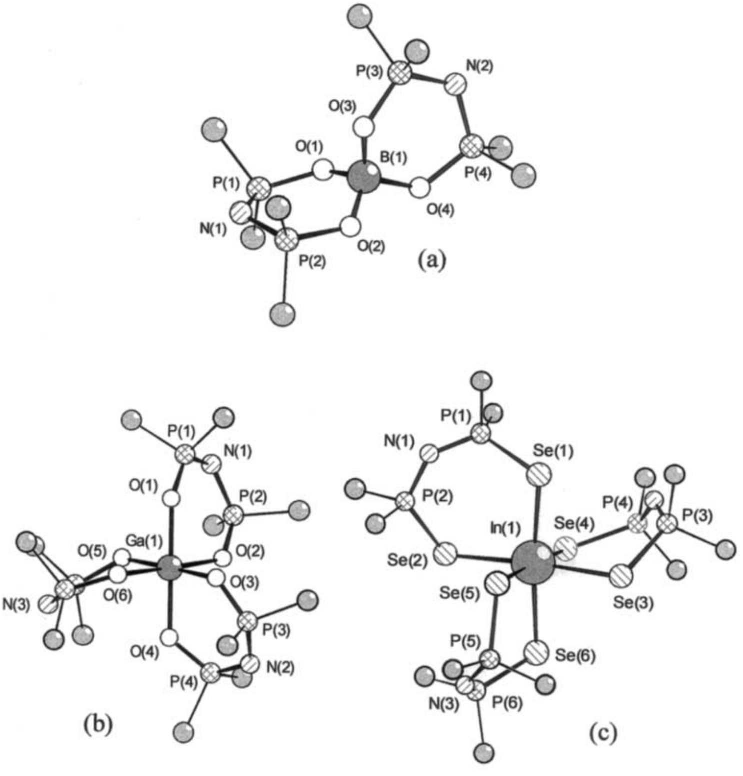

Fig. 27. The structure of (a) the cation in $[B\{(OPPh_2)_2N\}_2][I_3]$ (triclinic form) [42], (b) $Ga[(OPPh_2)_2N]_3$ [117], and (c) $In[(SePPh_2)_2N]_3$ [119] (for clarity, only *ipso* carbons of the phenyl groups are shown).

4.4.3. Gallium

The syntheses and molecular structures of only two gallium(III) compounds have been reported. The inorganic derivative, $Ga[(OPPh_2)_2N]_3$, is monomeric with the metal atom coordinated by the oxygen atoms of three chelated ligands, thus resulting in a slightly distorted octahedral GaO_6 core [*cis*-O–Ga–O 87.4(2)–92.7(2)°] (Fig. 27b) [117]. The ligands exhibit an approximately symmetrical monometallic biconnective pattern [Ga–O 1.954(5)–1.996(5) Å], forming six-membered GaO_2P_2N rings of boat conformation.

The structure of the organometallic derivative, $Et_2Ga[(SePPh_2)_2N]$, has a chelating diseleno ligand, resulting in a $GaSe_2P_2N$ metallacycle of distorted boat conformation [122]. The metal atom has a distorted tetrahedral GaC_2Se_2 environment, the largest deviation from the ideal value of 109.5° being for the C–Ga–C bond angle [125.5(4)°].

4.4.4. Indium

A broader variety of inorganic indium complexes containing imidodiphosphinic ligands have been studied, including compounds of the type $In[(XPPh_2)(YPPh_2)N]_3$ and $InCl[(XPR_2)(YPR'_2)N]_2$, but no organoindium derivatives are known.

The crystals of the tris-derivatives, $In[(XPR_2)(YPR'_2)N]_3$, contain discrete molecules which exhibit an octahedral structure (exemplified in Fig. 27c for $In[(SePPh_2)_2N]_3$), similar to the gallium(III) compound described above. For the complexes containing symmetric ligands, $In[(XPPh_2)_2N]_3$ ($X = O$ [117], S [118], Se [119]), the distortion of the InX_6 core is increased in the order $O > S > Se$, as reflected by the range of *cis*-X–In–X bond angles: 87.6(1)–92.8(1), 82.0(3)–98.4(5) and 76.9(1)–100.6(1)°, respectively. The mixed-chalcogen ligand-containing complex, $In[(OPPh_2)(SPPh_2)N]_3$ [120], displays a *fac* arrangement of the oxygen and sulfur atoms, respectively, in the distorted InO_3S_3 core [*trans*-O–In–S 174.6(1)–178.3(1)°]. In all these compounds the chelate rings exhibit boat conformations with varying degrees of distortion.

The molecular structures of several chloroindium(III) derivatives, $InCl[(XPR_2)(YPR'_2)N]_2$, have also been reported (Table 20) [120,121]. In all cases the compounds are monomeric and no intermolecular interactions were noted. Regardless of the nature of the ligands (symmetric or asymmetric) or the organic groups (^{i}Pr or Ph) attached to phosphorus atoms, a distorted trigonal bipyramidal environment is achieved around the metal atom as a result of the monometallic biconnective pattern of the imidodiphosphinato units. The chlorine atom always occupies an equatorial position. For complexes of dithio- or diselenoimidodiphosphinic acids, $InCl[(XPR_2)_2N]_2$, the $In–X_{axial}$ bond distances are longer than the $In–X_{equatorial}$ ones. In the case of the complex containing mixed-chalcogen ligand units, $InCl[(SPPh_2)(SePPh_2)N]_2$, the axial positions are occupied by the sulfur atoms. The deviation from 180° of the angle between axial indium–chalcogen bonds is larger for the aromatic derivatives [$InCl[(SePPh_2)_2N]_2$: Se–In–Se 166.42(2)° [121]; $InCl[(SPPh_2)(SePPh_2)N]_2$: S–In–S 168.53(8) [120], respectively] than for the aliphatic complexes [$InCl[(SeP^iPr_2)_2N]_2$: Se–In–Se 176.69(2)°; $InCl[(SP^iPr_2)_2N]_2$: S–In–S 179.83(5)° [121], respectively]. In all these chloroindium(III) derivatives the six-membered chelate rings exhibit a distorted boat conformation.

4.4.5. Thallium

Only one organometallic derivative of Tl(III), $Ph_2Tl[(SPPh_2)_2N]$, has been reported so far [123]. The crystals contain two independent, very similar, molecules. The dithio ligand is essentially a symmetrical chelate through its chalcogen atoms (Fig. 28). Due to the large C–Tl(1)–C angle [151.0(3)° for molecule 1 and 148.1(4)° for molecule 2] the resulting TlC_2S_2 core is described as intermediate between tetrahedral and pseudo-trigonal bipyramidal. As found for the other Group 13 metal complexes described above, the TlS_2P_2N ring displays a distorted boat conformation.

4.5. Group 14: Si, Ge, Sn, Pb

For Group 14 elements the known compounds containing imidodiphosphorus ligands are listed in Table 21, along with the spectroscopic methods (including ^{31}P-NMR data) used for their characterization. For the heavier elements (tin and lead) inorganic complexes in both oxidation states +2 and +4 have been described as well as organometal(IV) derivatives. The solid state structures of many of the Sn and Pb compounds have been investigated by single-crystal X-ray diffraction (Table 22).

4.5.1. Silicon

In earlier work, Schmidpeter and Stoll reported that when silicon(IV) tetrahalides, SiX_4 (X = Cl, Br), were treated with $(OPPh_2)_2NH$ in methylene chloride, substitution of three halide atoms was always achieved, regardless of the molar ratio or the reaction conditions used, and ionic compounds, $[Si\{(OPPh_2)_2N\}_3]X$, were isolated [17]. The remaining halide atom was readily exchanged for nitrate on reaction with $AgNO_3$ and derivatives containing other complex anions were also reported. A tricyclic structure containing an octahedral SiO_6 core was suggested for the $[Si\{(OPPh_2)_2N\}_3]^+$ cation on the basis of ^{31}P-NMR data.

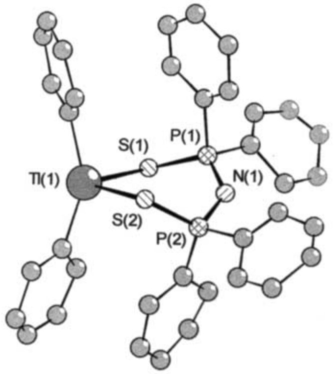

Fig. 28. The molecular structure of $Ph_2Tl[(SPPh_2)_2N]$ (molecule 1) [123].

Table 21
Group 14 metal complexes of imidodiphosphorus acids

Compound	Synthesis, yield (%)	M.p. (°C)	$\delta(^{31}P)$ (ppm), $^{n}J(PX)$ (Hz)[a]			X-ray studies	Spectroscopic studies
			*P*O	*P*S	*P*Se		
Inorganic compounds							
$[Si\{(OPPh_2)_2N\}_3]Cl$	100 [17]	250	29.4s				^{31}P [17]
$[Si\{(OPPh_2)_2N\}_3]Br$	100 [17]						
$[Si\{(OPPh_2)_2N\}_3][Br_3]$	[17]	360					
$[Si\{(OPPh_2)_2N\}_3][SbCl_6]$	[17]	355					
$[Si\{(OPPh_2)_2N\}_3][CuCl_3]$	[17]	305					
$[Si\{(OPPh_2)_2N\}_3][NO_3]$	[17]	250					
$[Ge\{(OPPh_2)_2N\}_3]Cl$	100 [17]	264	31.3s				^{31}P [17]
$[Ge\{(OPPh_2)_2N\}_3][SbCl_6]$	[17]	315					
$[Ge\{(OPPh_2)_2N\}_3][NO_3]$	[17]	320					
$Sn[(OPPh_2)_2N]_2$	80 [100] [14]	223–224 215–217	17.9s (broad)			[100]	^{31}P [14,100]
$Sn[(SePPh_2)_2N]_2$	85 [124]				31.7s	[114,124]	IR, MS, ^{1}H, ^{31}P, ^{77}Se, ^{119}Sn [124]
$SnCl_2[(OPPh_2)_2N]_2$	[14,100][b] 80 [14,100][d] 70 [14,100][e]	325–327	29.3d (*cis*-Ph_2PO)[c] 30.3d (*trans*-Ph_2PO), $^{2}J(PP)$ 4				^{31}P [14,100], ^{119}Sn [100]
$SnBr_2[(OPPh_2)_2N]_2$	90 [100][b] 50 [14,100][d] 85 [14,100][e] 70 [14,100][f]	283–285	28.1d (*cis*-Ph_2PO)[c] 29.3d (*trans*-Ph_2PO), $^{2}J(PP)$ 3.7				^{31}P [14,100], ^{119}Sn [100]
$SnI_2[(OPPh_2)_2N]_2$	95 [14,100][b]	258–260	26.5d (*cis*-Ph_2PO)[c], $^{2}J(PP)$ 3.1 28.2dd (*trans*-Ph_2PO), $^{2}J(PP)$ 3.1, $^{4}J(PP)$ 0.3			[100]	^{31}P [14,100], ^{13}C, ^{119}Sn [100]

Table 21 (*Continued*)

Compound	Synthesis, yield (%)	M.p. (°C)	δ(^{31}P) (ppm), ^{n}J(PX) (Hz)^{a}			X-ray studies	Spectroscopic studies
			*P*O	*P*S	*P*Se		
[Sn{(OPPh$_2$)$_2$N}$_3$]Cl	[17]	178	35.7s				^{31}P [17]
[Sn{(OPPh$_2$)$_2$N}$_3$]I	[17]	380					
[Sn{(OPPh$_2$)$_2$N}$_3$][Br$_3$]	[17]	284					
[Sn{(OPPh$_2$)$_2$N}$_3$][ICl$_2$]	[17]	279					
[Sn{(OPPh$_2$)$_2$N}$_3$][I$_3$]	[17,42]	365					
[Sn{(OPPh$_2$)$_2$N}$_3$][I$_8$]	[17]	370					
[Sn{(OPPh$_2$)$_2$N}$_3$][SbCl$_6$]	[17]	270					
[Sn{(OPPh$_2$)$_2$N}$_3$][CuCl$_3$]	[17]	322					
[Sn{(OPPh$_2$)$_2$N}$_3$][HgI$_3$]	[17]	360					
[Sn{(OPPh$_2$)$_2$N}$_3$][NO$_3$]	[17]	332					
[Sn{(OPPh$_2$)$_2$N}$_3$][ClO$_4$]	[17,42]	400				[42]	
[Sn{(OPPh$_2$)$_2$N}$_3$][MnO$_4$]	[17]						
[Sn{(OPPh$_2$)$_2$N}$_3$]OH	[17]	188					
Pb[(OPPh$_2$)$_2$N]$_2$	76 [105]	228–232	17.0				IR, ^{1}H [105], ^{31}P [50,105]
Pb[(SPPh$_2$)$_2$N]$_2$	89 [125]	242–243		36.3s			
	[105]	239–241		38.2s		[125]	IR, ^{31}P [105,125]
Pb[(SPPh$_2$)$_2$N]$_2$ · (1,10-Phen)	86 [105]	193–196		35.3s			IR, ^{1}H, ^{31}P [105]
Pb[(SePPh$_2$)$_2$N]$_2$	81 [114]	204–206			30.2s	[114]	IR, MS, ^{31}P [114]
Pb[(OPPh$_2$)(SPPh$_2$)N]$_2$ · C$_6$H$_6$	82 [126]	204–206	20.8s	33.9s		[126]	IR, ^{31}P [126]
Organometallic compounds							
^{n}BuSnCl$_2$[(OPPh$_2$)(SPPh$_2$)N]	68 [56]	143	29.4s	33.1s		[56]	IR, ^{1}H, ^{13}C, ^{31}P [56]
Me$_2$Sn[(OPPh$_2$)$_2$N]$_2$	93 [127]	240–241	19.9s				IR, ^{1}H, ^{13}C, ^{31}P [127]
^{n}Bu$_2$Sn[(OPPh$_2$)$_2$N]$_2$	92 [127]	208–210	19.0s			[127]	IR, ^{1}H, ^{13}C, ^{31}P [127]
Bz$_2$Sn[(OPPh$_2$)$_2$N]$_2$	87 [127]	142–143	21.1s				IR, ^{1}H, ^{13}C, ^{31}P [127]
Ph$_2$Sn[(OPPh$_2$)$_2$N]$_2$	88 [127]	264–265	22.7s				IR, ^{1}H, ^{13}C, ^{31}P [127]
Me$_2$Sn[(OPMe$_2$)(OPPh$_2$)N]$_2$	75 [57]	232–234	18.8s (PhP) 37.2s (MeP)			[57]	IR, ^{1}H, ^{13}C, ^{31}P, ^{119}Sn [57]
^{n}Bu$_2$Sn[(OPMe$_2$)(OPPh$_2$)N]$_2$	82 [57]	197–199	18.1s (PhP) 36.6s (MeP)			[57]	IR, ^{1}H, ^{13}C, ^{31}P, ^{119}Sn [57]
Bz$_2$Sn[(OPMe$_2$)(OPPh$_2$)N]$_2$	55 [57]	269–271	17.8s (PhP) 38.5s (MeP)				IR, ^{1}H, ^{13}C, ^{31}P, ^{119}Sn [57]

Table 21 (*Continued*)

Compound	Synthesis, yield (%)	M.p. (°C)	$\delta(^{31}P)$ (ppm), $^{n}J(PX)$ (Hz)[a]			X-ray studies	Spectroscopic studies
			*P*O	*P*S	*P*Se		
$Ph_2Sn[(OPMe_2)(OPPh_2)N]_2$	84 [57]	235–237	20.90s (PhP), $^{2}J(PSn)$ 55.9 21.74s (PhP), $^{2}J(PSn)$ 52.3 39.51s (MeP) 39.63s (MeP)			[57]	IR, ^{1}H, ^{13}C, ^{31}P [57]
$Me_2Sn[(SPPh_2)_2N]_2$	61 [128,129]	265–266				[129]	IR, Mössbauer [128,129]
$^{n}Bu_2Sn[(SPPh_2)_2N]_2$	44 [128]	255–257					IR, Mössbauer [128]
$^{n}Bu_2Sn[(SePPh_2)_2N]_2$	86 [130]	205–206			28.3s	[130]	IR, MS, ^{31}P, ^{77}Se, ^{119}Sn [130]
$Ph_2SnCl[(SePPh_2)_2N] \cdot H_2O$	86 [130]	197–198			31.9s, $^{1}J(PSe)$ 512	[130]	IR, MS, ^{31}P, ^{119}Sn [130]
$Me_2Sn[(OPPh_2)(SPPh_2)N]_2$	76 [91]	251	20.0s	35.0s		[91]	IR, ^{1}H, ^{13}C, ^{31}P [91]
$^{n}Bu_2Sn[(OPPh_2)(SPPh_2)N]_2$	69 [91]	206–208	19.5s	35.4s			IR, ^{1}H, ^{13}C, ^{31}P, ^{119}Sn [91]
$Bz_2Sn[(OPPh_2)(SPPh_2)N]_2 \cdot C_6H_5CH_3$	73 [91]	198–200	19.5s	34.1s			IR, ^{1}H, ^{13}C, ^{31}P, ^{119}Sn [91]
$Ph_2Sn[(OPPh_2)(SPPh_2)N]_2$	29 [91]	257–259	20.3s	33.2s		[91]	IR, ^{31}P [91]
$Me_3Sn[(OPMe_2)(OPPh_2)N]$	77 [57]	139–42	8.2s (PhP), $^{1}J(PC)$ 134.7 24.3s (MeP)				IR, ^{1}H, ^{13}C, ^{31}P [57]
$Me_3Sn[(SPPh_2)_2N]$	66 [128,129]	135		36s		[131]	IR [128,129], ^{1}H, ^{13}C, ^{31}P, Mössbauer [128]
$Bz_3Sn[(SPPh_2)_2N]$	40 [128]	113–115		35.9s			IR, ^{1}H, ^{13}C, ^{31}P, Mössbauer [128]
$Ph_3Sn[(SPPh_2)_2N]$	46 [128]	172–175		37.6s			IR, ^{1}H, ^{13}C, ^{31}P, Mössbauer [128]
$Me_3Sn[(OPPh_2)(SPPh_2)N]$	84 [91]	58–60	10.3s	39.7s			IR, ^{1}H, ^{13}C, ^{31}P, ^{119}Sn [91]
$Ph_3Sn[(OPPh_2)(SPPh_2)N]$	86 [91]	115–125	20.5s	38.7s			IR, ^{1}H, ^{13}C, ^{31}P [91]
$Me_2Pb[(OPPh_2)_2N]_2$	[132]					[132]	
$Ph_2Pb[(OPPh_2)_2N]_2$	88 [132]	228–229	19.7s			[133]	IR, ^{1}H, ^{13}C, ^{31}P [132]
$Ph_2Pb[(OPPh_2)(SPPh_2)N]_2$	89 [132]	190	21.8s	31.8s			IR, ^{1}H, ^{13}C, ^{31}P [132]
$Me_3Pb[(OPPh_2)_2N]$	95 [132]	147–149	13.8s,br				IR, ^{1}H, ^{13}C, ^{31}P [132]
$Ph_3Pb[(OPPh_2)(SPPh_2)N]$	82 [132]	114–116	14.3s	31.8s			IR, ^{1}H, ^{13}C, ^{31}P [132]

[a] In $CDCl_3$.

[b] Method (i).

[c] In CH_2Cl_2.

[d] Method (ii).

[e] Method (iii).

[f] Method (iv).

Table 22
X-ray data [bond lengths (Å) and bond angles (°)] for Group 14 metal complexes of imidodiphosphorus acids

Compound		M–X	P–X	P–N	P–N–P	Association degree	Ref.
Inorganic compounds							
$Sn[(OPPh_2)_2N]_2$		2.128(2)/2.134(2)[a]	1.529(2)/1.528(3)	1.580(3)/1.582(3)	125.4(2)/128.0(2)	Monomer	[100]
		2.382(3)/2.317(2)[b]	1.513(2)/1.515(3)	1.596(3)/1.591(4)			
$Sn[(SePPh_2)_2N]_2$	SP[c] Mol. 1	2.643(3)/2.662(2)	2.173(6)/2.177(6)	1.564(17)/1.597(20)	136.2(13)	Monomer	[114,124]
	Mol. 2	2.634(3)/2.681(3)	2.170(7)/2.170(6)	1.623(20)/1.531(17)	138.7(12)		
	P[c]	2.803(3)[a]/2.943(2)[b]	2.188(5)/2.161(5)	1.623(15)/1.582(15)	129.3(10)		
$[Sn\{(OPPh_2)_2N\}_3][ClO_4]$[d]		2.012(5)–2.027(5)	1.541(6)–1.549(6)	1.569(7)–1.581(7)	125.3(4)–129.9(5)	Monomer	[42]
$SnI_2[(OPPh_2)_2N]_2$		2.069(4)–2.082(3)	1.536(4)–1.545(4)	1.572(5)–1.597(5)	123.2(3)/129.5(3)	Monomer	[100]
$Pb[(SPPh_2)_2N]_2$[e]		2.695(4)/2.943(4)	2.015(5)/1.993(5)	1.58(1)/1.62(1)	128.4(6)	Polymer	[125]
$Pb[(SePPh_2)_2N]_2$		2.874(3)/2.997(2)	2.186(6)/2.151(6)	1.596(15)/1.594(15)	130.1(10)	Monomer	[114]
$Pb[(OPPh_2)(SPPh_2)N]_2 \cdot C_6H_6$[f]		2.283(7)/2.284(7) (M–O)	1.510(7)/1.519(7) (P–O)	1.564(9)/1.588(8)	134.2(6)/130.5(6)	Dimer	[126]
		2.890(3)/3.037(3) (M–S)[g]	1.996(4)/2.000(4) (P–S)	1.622(9)/1.574(4)			
Organometallic compounds							
$^nBuSnCl_2[(OPPh_2)(SPPh_2)N]$[h]		2.16(1) (M–O)	1.52(2) (P–O)	1.61(2)	127(1)	Monomer	[56]
		2.482(7) (M–S)	2.07(1) (P–S)	1.56(2)			
$^nBu_2Sn[(OPPh_2)_2N]_2$		2.202(5)/2.204(5)	1.527(6)/1.520(6)	1.573(6)/1.598(6)	130.4(4)	Monomer	[127]
$Me_2Sn[(OPMe_2)(OPPh_2)N]_2$		2.212(2)	1.511(3) (P–Me)	1.592(3)	124.4(2)	Monomer	[57]
		2.222(2)	1.510(2) (P–Ph)	1.597(3)			
$^nBu_2Sn[(OPMe_2)(OPPh_2)N]_2$		2.215(4)	1.507(4) (P–Me)	1.581(5)	129.9(3)	Monomer	[57]
		2.217(4)	1.520(4) (P–Ph)	1.576(5)			
$Ph_2Sn[(OPMe_2)(OPPh_2)N]_2$		2.18(1)	1.52(1) (P–Me)	1.55(1)	136(1)	Monomer	[57]
		2.18(1)	1.50(1) (P–Ph)	1.57(1)			

Table 22 (*Continued*)

Compound		M–X	P–X	P–N	P–N–P	Association degree	Ref.
$Me_2Sn[(SPPh_2)_2N]_2$		2.733(2)/2.737(2)	2.009(3)/2.019(3)	1.582(7)/1.582(6)	136.0(4)	Monomer	[129]
$^{n}Bu_2Sn[(SePPh_2)_2N]_2$		2.843(1)/2.847(1)	2.167(2)/2.165(2)	1.595(6)/1.596(6)	134.3(5)	Monomer	[130]
$Ph_2SnCl[(SePPh_2)_2N] \cdot H_2O$[i]		2.603(1)[a]/2.868(1)[b]	2.214(2)/2.170(2)	1.582(7)/1.611(7)	126.2(4)	Monomer	[130]
$Me_2Sn[(OPPh_2)(SPPh_2)N]_2$		2.199(2) (M–O)	1.524(2) (P–O)	1.599(3)	132.0(2)	Monomer	[91]
		2.758(1) (M–S)	2.023(1) (P–S)	1.578(3)			
$Ph_2Sn[(OPPh_2)(SPPh_2)N]_2$		2.189(5) (M–O)	1.530(5) (P–O)	1.593(7)	134.1(4)	Monomer	[91]
		2.680(4) (M–S)	2.018(3) (P–S)	1.581(7)			
$Me_3Sn[(SPPh_2)_2N] \cdot C_6H_6$		2.517(4)[j]	2.048(3)/1.972(3)	1.572(5)/1.605(5)	133.4(2)	Polymer	[131]
$Me_2Pb[(OPPh_2)_2N]_2$	Mol. 1	2.342(5)–2.462(5)	1.505(6)–1.519(6)	1.583(6)–1.598(7)	130.8(5)/130.8(5)	Monomer	[132]
	Mol. 2	2.363(6)–2.432(5)	1.502(6)–1.516(6)	1.580(7)–1.600(7)	127.3(5)/135.3(5)		
$Ph_2Pb[(OPPh_2)_2N]_2$		2.347(3)–2.376(3)	1.515(3)–1.520(3)	1.584(4)–1.589(4)	127.7(2)/135.4(3)	Monomer	[133]

[a] Equatorial Sn–O bond distances.

[b] Axial Sn–O bond distances.

[c] SP = square planar, P = pyramidal.

[d] Triclinic form.

[e] Intramolecular Pb(1)–C 3.31(1)–3.70(2) Å.

[f] Intermolecular Pb(1)–C 3.424–3.579 Å — calculated from published atomic coordinates.

[g] Intermolecular Pb(1)···S(1′) 3.386(3) Å.

[h] Sn(1)–Cl(1) 2.335(9), Sn(1)–Cl(2) 2.449(8) Å.

[i] Sn–Cl 2.519(3) Å.

[j] Intermolecular Sn(1)···S(2′) 3.627 Å.

4.5.2. Germanium

Similar reactions using $GeCl_4$ resulted in the formation of the tris-substituted product, $[Ge\{(OPPh_2)_2N\}_3]Cl$, when carried out in boiling tetrachloroethane, but no reaction was noted at room temperature [17]. The remaining chloride can be substituted by complex anions (e.g. $[SbCl_6]^-$ or $[CuCl_2]^-$), but, as for silicon derivatives, reports of spectroscopic data are scarce.

4.5.3. Tin

Only two Sn(II) complexes have been described so far. The $Sn[(OPPh_2)_2N]_2$ compound is soluble in polar organic solvents as well as in benzene and is monomeric in solution [14]. Since its ^{31}P-NMR spectrum exhibited only one broad resonance both at room temperature and $-80°C$, a fast exchange between axial and equatorial oxygen atoms of a pseudo-trigonal bipyramidal SnO_4 core was assumed [100]. A single-crystal X-ray investigation shows that the monomeric nature of this complex is preserved in the solid state [100]; a bis-chelate structure with a distorted pseudo-trigonal bipyramidal geometry around the metal atom

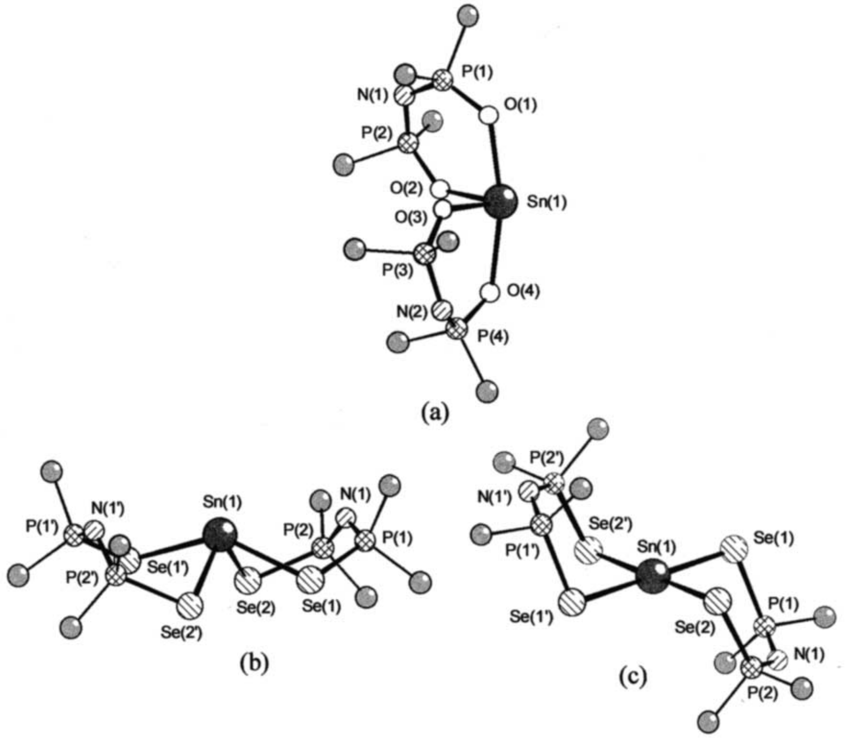

Fig. 29. The molecular structure of (a) $Sn[(OPPh_2)_2N]_2$ [100], (b) $Sn[(SePPh_2)_2N]_2$ (pyramidal), and (c) $Sn[(SePPh_2)_2N]_2$ (square planar, molecule 1) [114,124] (for clarity, only *ipso* carbons of the phenyl groups are shown).

being formed (Fig. 29a). The equatorial positions are occupied by one oxygen atom from each imidodiphosphinato moiety [O(2)–Sn(1)–O(3) 88.2(1)°] and the lone pair of electrons of the tin atom. The equatorial Sn–O bond distances are shorter than the axial (Table 22), which are bent away from the equatorial position occupied by the lone pair [O(1)–Sn(1)–O(4) 164.6(1)°]. The SnO_2P_2N chelate rings display a distorted boat conformation.

During attempts to grow X-ray quality crystals of the selenium analog, $Sn[(SePPh_2)_2N]_2$, both yellow triclinic prisms and red tetragonal octahedra were isolated [114,124]. Their analysis revealed interesting structural patterns. Thus, the few red crystals which were separated, consist of discrete molecules whose geometry was described as intermediate between a distorted square-planar pyramid, with the tin atom placed in the apex, and a very distorted pseudo-trigonal bipyramid [Se(1)–Sn(1)–Se(1′) 143.6(1)°, Se(2)–Sn(1)–Se(2′) 112.7(1)°], respectively (Fig. 29b). The axial Sn–Se bond distances are again longer [2.943(2) Å] than the equatorial ones [2.803(2) Å]. The $SnSe_2P_2N$ chelate rings are of boat conformation, with the metal and nitrogen atoms in the apices.

In contrast, the yellow crystals of the same compound contain two independent molecules which display an unusual square-planar $SnSe_4$ core, with *trans* Se–Sn–Se bond angles of 180.0(0)° (Fig. 29c). The Sn–Se bond distances are now quite similar and a three-center four-electron type bonding was considered for the linear Se–Sn–Se system [124]. The six-membered $SnSe_2P_2N$ rings display a more unusual distorted chair conformation. On the basis of theoretical studies it was suggested that the stabilization of the square-planar isomer of $Sn[(SePPh_2)_2N]_2$ might be due to intermolecular interactions between selenium and hydrogen atoms belonging to phenyl rings from a neighboring molecule [114]. π–π Interactions between interlocked phenyl rings may also account for a stabilized planar tin(II) structure as indicated by further theoretical calculations [134].

A relatively large number of inorganic Sn(IV) compounds containing two or three deprotonated $[(OPPh_2)_2N]^-$ moieties are known. In contrast to the tetrahalides of the lighter elements, SnX_4 (X = Cl, Br) react directly with $(OPPh_2)_2NH$ to give the $SnX_4[(OPPh_2)_2NH]_2$ adducts (see Section 3), which are subsequently decomposed to $SnX_2[(OPPh_2)_2N]_2$ complexes under the action of weak bases [14]. The di-substituted complexes could also be isolated using other methods, including the oxidation of the Sn(II) derivative by halogens [Eq. (15)] [14,100]:

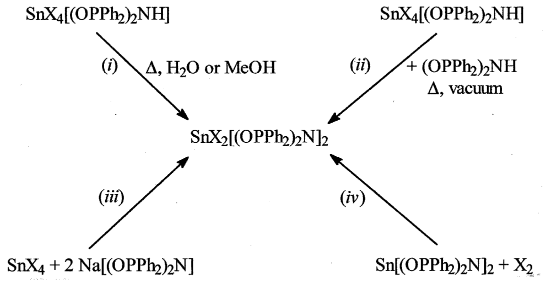

(15)

A *cis* arrangement of the halogen atoms in $SnX_2[(OPPh_2)_2N]_2$ was suggested on the basis of their dipole moments in dioxane solutions [14]. Many years later a detailed multinuclear NMR study confirmed the presence of the *cis* isomer in solution, regardless the nature of the halogen atoms [100]. The ^{31}P- and ^{119}Sn-NMR spectra are also consistent with two types of $OPPh_2$ units, i.e. *cis* and *trans* to the halogen atoms. The solid state structure of $SnI_2[(OPPh_2)_2N]_2$ is consistent with a *cis* arrangement of the iodine atoms [I(1)–Sn(1)–I(2) 93.69(2)°] (Fig. 30a) [100]. Both phosphorus ligands act as symmetric monometallic biconnective moieties, leading to a distorted octahedral SnI_2O_4 core [O(2)–Sn(1)–O(4) 171.5(1)°, *trans* I–Sn(1)–O 172.9(1), 177.2(1)°]. No significant length differences are observed for Sn–O bonds *cis* and *trans* to halogen atoms. The inorganic SnO_2P_2N chelate rings are of distorted boat conformation, similar to that observed for the Sn(II) derivative described above.

The preparation of a number of ionic compounds of type $[Sn\{(OPPh_2)_2N\}_3]X$ was reported in a short paper of Schmidpeter (Table 21), without further spectroscopic characterization [17]. As indicated above, $[Sn\{(OPPh_2)_2N\}_3]X$ (X = Cl, Br) cannot be obtained directly from SnX_4 and $(OPPh_2)_2NH$; only disubstituted derivatives, $SnX_2[(OPPh_2)_2N]_2$, being isolated. However, the substitution of the third chloride leading to $[Sn\{(OPPh_2)_2N\}_3]Cl$ was achieved by using the sodium salt of the imidodiphosphinic acid [17]. The $SnCl_2[(OPPh_2)_2N]_2$ derivative can also be converted to other tris-substituted derivatives, either by treatment with $AgNO_3$ (with a molar ratio of 1:2, $[Sn\{(OPPh_2)_2N\}_3][NO_3]$ was isolated as a result of disproportionation) or by thermal treatment in the presence of $NaOCH_3$ or some other electrophilic reagents (I_2, MeI, HgI_2) [17]. The replacement of the remaining halide atom in $[Sn\{(OPPh_2)_2N\}_3]Cl$ by oxo anions or complex halogen anions was also achieved [17]. The iodo analog, $[Sn\{(OPPh_2)_2N\}_3]I$, exhibited greater resistance to substitution, and only treatment with excess of anhydrous perchloric acid

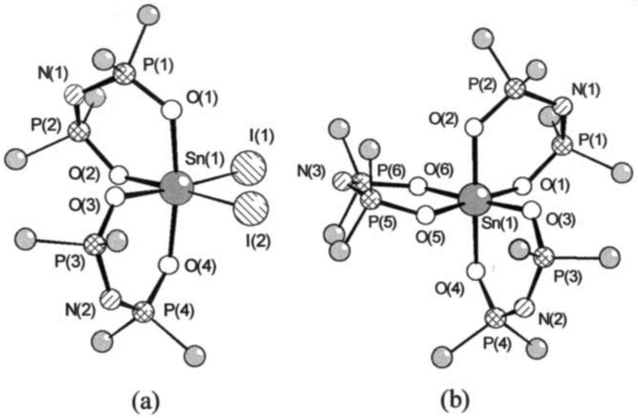

Fig. 30. The structure of (a) $SnI_2[(OPPh_2)_2N]_2$ [100], and (b) the cation in $[Sn\{(OPPh_2)_2N\}_3][ClO_4]$ (triclinic modification) [42] (for clarity, only *ipso* carbons of the phenyl groups are shown).

resulted in isolation of the corresponding perchlorate derivative. Treatment of the iodo derivative with molecular iodine afforded the isolation of both triiodide and octaiodide complexes [17].

The molecular structure of a tris-substituted complex, $[Sn\{(OPPh_2)_2N\}_3][ClO_4]$, was reported some 20 years later [42]. The complex, prepared from the corresponding triiodide and $HClO_4$, was isolated in two crystalline modifications (triclinic and hexagonal). The triclinic modification contains discrete $[Sn\{(OPPh_2)_2N\}_3]^-$ anions, in which the tin atom is symmetrically chelated by three ligand moieties through their oxygen atoms in a slightly distorted octahedral arrangement [*trans* O–Sn(1)–O range 177.8(2)–178.9(2)°] (Fig. 30b). All three six-membered SnO_2P_2N rings display boat conformations, with varying degrees of distortion.

Organotin(IV) derivatives are by far the most investigated among organometallic compounds of main group elements containing imidodiphosphorus ligands. Complexes containing one, two or three organic groups on tin have been reported and many of them investigated by X-ray diffraction.

The mixed-ligand complex, $^nBuSnCl_2[(OPPh_2)(SPPh_2)N]$, is the only example of a monoorganotin(IV) derivative characterized so far [56]. The compound displays a monomeric structure, with distorted trigonal bipyramidal geometry around the tin atom (Fig. 31a). The monothio ligand is coordinated through both chalcogen atoms and the resulting $SnOSP_2N$ ring exhibits a distorted boat conformation, with S(1) and P(1) atoms in the apices. One of the chlorine atoms is in an axial position *trans* to the oxygen atom of the phosphorus ligand [Cl(2)–Sn(1)–O(1) 171.7(5)°], while the second chlorine, the sulfur and the C(1) atom of the butyl group are in equatorial positions [the sum of equatorial angles at Sn(1) is 359.9°]. The two tin–chlorine interatomic distances are different, with the axial Sn(1)–Cl(2) bond significantly longer than the equatorial Sn(1)–Cl(1) bond.

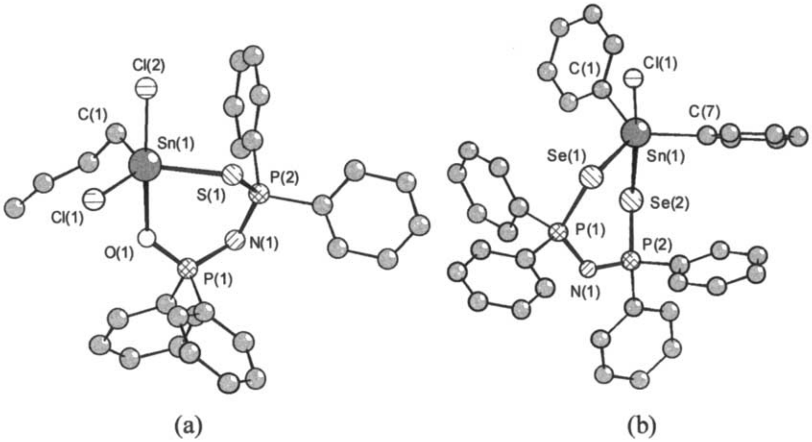

Fig. 31. The molecular structure of (a) $^nBuSnCl_2[(OPPh_2)(SPPh_2)N]_2$ [56], and (b) $Ph_2SnCl[(SePPh_2)_2N]$ [130].

A mixed-ligand complex containing two organic groups on the tin atom, $Ph_2SnCl[(SePPh_2)_2N]$, has also been reported [130]. The compound is again monomeric and the coordination geometry around the tin atom is distorted trigonal bipyramidal [diaxial Cl(1)–Sn(1)–Se(2) angle 174.0(1)°] (Fig. 31b). The phosphorus ligand is coordinated asymmetrically through both selenium atoms; the axial Sn(1)–Se(2) bond [2.868(1) Å] being considerably longer than the equatorial Sn(1)–Se(1) bond [2.603(1) Å]. The conformation of the $SnSe_2P_2N$ chelate ring is distorted boat, with Se(1) and P(1) atoms in the apices; thus being similar to that observed for the $SnOSP_2N$ ring in the monothio derivative above. The presence of only one ^{31}P-NMR resonance in solution suggests that in solution, at room temperature, fluxional behavior results in equivalent phosphorus environments.

A large number of disubstituted diorganotin(IV) derivatives, $R''_2Sn[(XPR_2)(YPR'_2)N]_2$, containing both symmetric, $[(XPPh_2)_2N]^-$ (X = O [127], S [128,129], Se [130]), and asymmetric ligands, $[(OPMe_2)(OPPh_2)N]^-$ [57] or $[(OPPh_2)(SPPh_2)N]^-$ [91], have been prepared and structurally investigated in solution and the solid state. Regardless of the nature of the imidodiphosphorus moieties and of the organic groups attached to tin, all complexes investigated by X-ray diffraction exhibit some common solid state structural patterns, exemplified for some compounds in Fig. 32:

- the crystals contain discrete molecular units, separated by normal van der Waals distances;
- the two ligand moieties are monometallic biconnective, thus resulting in a *spiro*-bicyclic structure, with the tin atom as spiro atom;
- the coordination around tin is distorted octahedral, with C–Sn–C, X–Sn–X (*trans*) and Y–Sn–Y (*trans*) angles of 180°, and a planar equatorial SnX_2Y_2 system;
- for complexes containing asymmetric ligands, $R''_2Sn[(OPPh_2)(YPR'_2)N]_2$, of the two possible isomers (**20**) (YPR'_2 *trans* YPR'_2) and (**21**) (YPR'_2 *trans* $OPPh_2$) only isomer (**20**) is observed.

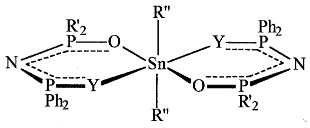

(20)

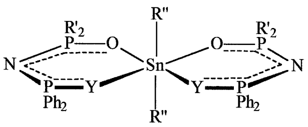

(21)

It should be noted here that, with very few exceptions, for complexes of type $R_2Sn(XY_2E)_2$ (E = COR′, CNR'_2, $P(OR')_2$, PR'_2, AsR'_2) the 1,1-dichalcogeno ligands are asymmetric monometallic biconnective. This results in a strongly distorted octahedral (or skew-trapezoidal bipyramidal) geometry around tin, with an angular SnC_2 system, short *cis* Sn–X covalent bonds, and long Sn···Y intramolecular interactions. The molecular structures of $Me_2Sn(S_2PEt_2)_2$ [135], $Me_2Sn(OSPEt_2)_2$ [136] and $Ph_2Sn(O_2CMe)_2$ [137] are typical examples. A similar structure was also

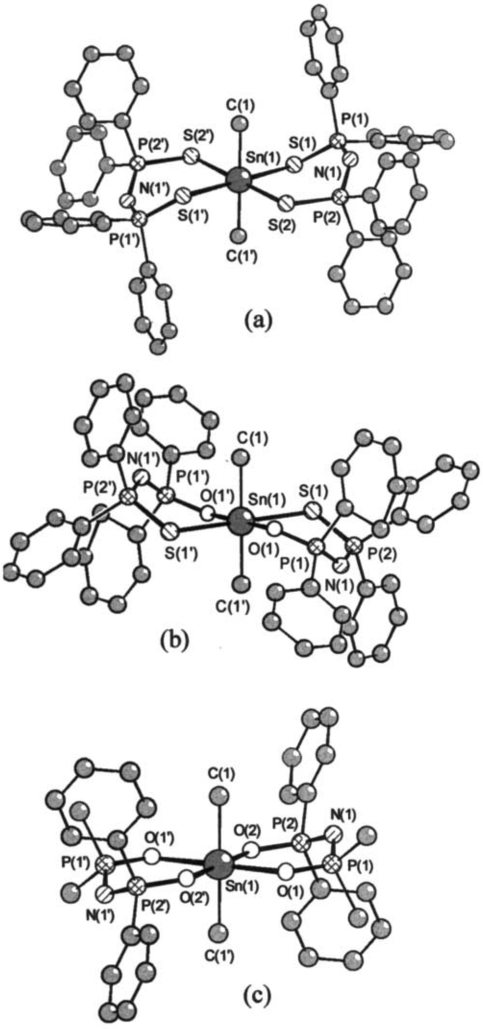

Fig. 32. The molecular structure of (a) $Me_2Sn[(SPPh_2)_2N]_2$ [129], (b) $Me_2Sn[(OPPh_2)(SPPh_2)N]_2$ [91], and (c) $Me_2Sn[(OPMe_2)(OPPh_2)N]_2$ [57].

established for the related diorganotin(IV) derivatives of monothio-β-diketones, $Me_2Sn[(OCR)(SCR)CH]_2$ (R = Me, Ph) [138].

The conformation of the six-membered $SnXYP_2N$ inorganic rings in these $R''_2Sn[(XPR_2)(YPR'_2)N]_2$ derivatives covers a wide range from distorted boat to distorted chair. Both the ligand bite and the flexibility of the XPNPY ligand skeleton might account for the differences noted in the angles at tin and chalcogen atoms, respectively.

The NMR data for $R''_2Sn[(XPR_2)(YPR'_2)N]_2$ complexes suggest that structural changes occur during the transition from the solid state to solution. The C–Sn–C angles were calculated for the dimethyl- and dibutyltin(IV) derivatives based on the observed $^2J(^{119}SnC^1H)$ and $^1J(^{119}Sn^{13}C)$ coupling constants. A SnC_2 arrangement close to linearity was found for $R''_2Sn[(OPPh_2)_2N]_2$ (ca. 175°) [127] and $R''_2Sn[(OPMe_2)(OPPh_2)N]_2$ (ca. 180°) [57], but angular SnC_2 fragments were established for $R''_2Sn[(OPPh_2)(SPPh_2)N]_2$ (ca. 150–160°) [91].

Multinuclear NMR data for freshly prepared samples are consistent with the formation of triorganotin(IV) derivatives, $R''_3Sn[(XPR_2)(YPR'_2)N]$ [57,91,128,129], when R''_3SnCl and the alkali salt of the appropriate imidodiphosphinic acid are mixed together in organic solvents.

For $Me_3Sn[(SPPh_2)_2N]$ [128] and $Me_3Sn[(OPPh_2)(SPPh_2)N]$ [91], the ^{119}Sn-NMR data (δ 117.8 and 146.2 ppm, respectively) are indicative of a tetracoordinated triorganotin derivative. The values of the $^2J(^{119}SnC^1H)$ and $^1J(^{119}Sn^{13}C)$ coupling constants fall in the region for four-coordinate tin resulting in estimated C–Sn–C angles of 113 and 109°, respectively. The ^{31}P-NMR spectra suggest that coordination of the monothioimidodiphosphinato ligand is through the oxygen atom in $Me_3Sn[(OPPh_2)(SPPh_2)N]$ [91], while fluxional behavior, fast intramolecular exchange of the sulfur atom involved in coordination to tin, can be considered for the dithio derivative, where only a broad ^{31}P resonance at 36 ppm is observed [128].

In contrast, for $Me_3Sn[(OPMe_2)(OPPh_2)N]$, the calculated C–SnC angle (ca. 120°) is consistent with a planar SnC_3 moiety, thus suggesting a five-coordinated metal atom and bridging imidodiphosphinato groups in solution [57].

For most of the $R''_3Sn[(XPR_2)(YPR'_2)N]$ complexes, attempts to grow X-ray quality crystals afforded only the isolation of the diorganotin(IV) derivatives due to a redistribution process [Eq. (16)]:

$$2R''_3Sn[(XPR_2)(YPR'_2)N] \rightarrow R''_2Sn[(XPR_2)(YPR'_2)N]_2 + SnR''_4 \qquad (16)$$

The $Ph_3Sn[(OPMe_2)(OPPh_2)N]$ derivative could not even be isolated as a pure compound from the mixture obtained by reacting the potassium salt of the phosphorus ligand with Ph_3SnCl, in toluene, and time-dependent ^{31}P-NMR spectra are consistent with the fast conversion of the Ph_3Sn(IV) complex into the Ph_2Sn(IV) compound [57].

Only for (tetraphenyldithioimidodiphosphinato)trimethyltin(IV) could the molecular structure be established by X-ray diffraction [131]. The crystal consists of $Me_3Sn[–S–PPh_2=N–PPh_2=S]$ units linked into a one-dimensional polymer by weak secondary Sn···S intermolecular interactions [Sn(1)–S(1) 2.517(4), Sn(1)···S(2′) 3.627 Å]. The coordination pattern of the dithioimidodiphosphinato ligand can thus be considered to be asymmetric bimetallic biconnective (also supported by the differences observed in the lengths of phosphorus–sulfur and phosphorus–nitrogen bond distances) (Fig. 33), generating a supramolecular structure which acts as a host for benzene molecules aligned along the *b*-axis of the crystal. The coordination geometry about tin is distorted trigonal bipyramidal *trans*-SnS_2C_3, with two sulfur atoms in axial positions [Sn(1)–Sn(1)···S(2′) 174.2(4)°] and methyl groups in equatorial sites. The Me_3Sn moiety is flattened but not coplanar [C–Sn–C range 114.6(4)–

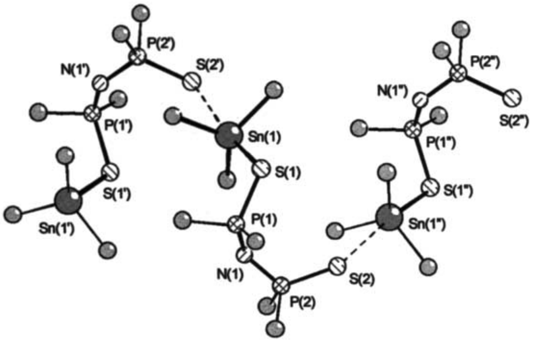

Fig. 33. The polymeric association in the crystal of $Me_3Sn[(SPPh_2)_2N]$ [131].

117.7(3)°], with tin lying 0.40 Å above the C_3 plane towards the covalently bonded S(1) atom.

4.5.4. Lead

Much fewer investigations have been carried out on lead complexes than on their tin analogs, but both inorganic lead(II) and organolead(IV) derivatives have been described and interesting structural patterns established.

Thus, for $Pb[(XPR_2)(YPR'_2)N]_2$, different solid state structures were found. The crystals of $Pb[(SePPh_2)_2N]_2$ contain discrete molecules with an overall structure (Fig. 34a) similar to that of the tin(II) analog (red isomer) [114]; the ligands being asymmetric monometallic biconnective leading to very distorted pseudo-trigonal bipyramidal arrangement around the metal atom [Se(1)–Pb(1)–Se(1′) 141.8(1)°, Se(2)–Pb(1)–Se(2′) 113.0(1)°], with the axial Pb–Se bond [2.997(2) Å] longer than the equatorial ones [2.874(3) Å]. No further intra- or intermolecular interactions at the lead atom were observed.

In contrast, the crystal of the dithio analog contains monomeric $Pb[(SPPh_2)_2N]_2$ molecules in which the coordination to lead is supplemented by two additional π-Pb–phenyl intramolecular interactions [$Pb(1)–C_{1,2,6}$ 3.31(1)–3.70(2) Å] (Fig. 34b) [125]. If these interactions are considered, the coordination geometry around the metal atom can be described as distorted octahedral. The axial Pb–S bonds are now nearly colinear [S(2)–Pb(1)–S(2′) 176.4(1)°] and ca. 0.35 Å longer than the equatorial Pb–S bonds [S(1)–Pb(1)–S(1′) 86.4(1)°] which are *trans* to the vectors of the π-Pb–phenyl interactions. The asymmetric coordination of the dithio ligand is also reflected in small differences in the length of the phosphorus–sulfur and phosphorus–nitrogen bonds within the chelate rings. In both these lead(II) derivatives, the conformation of the PbS_2P_2N and $PbSe_2P_2N$ rings is distorted boat, but with S(1) and P(2) atoms, and Pb(1) and N(1) atoms in the apices, respectively.

The molecules of the monothio derivative, $Pb[(OPPh_2)(SPPh_2)N]_2$ are associated in the solid state to form discrete dimers (Fig. 34c) [126]. The coordination patterns of the two ligand moieties in the molecular unit are different. One of them is chelated to the lead atom (monometallic biconnective), while the other is bimetallic

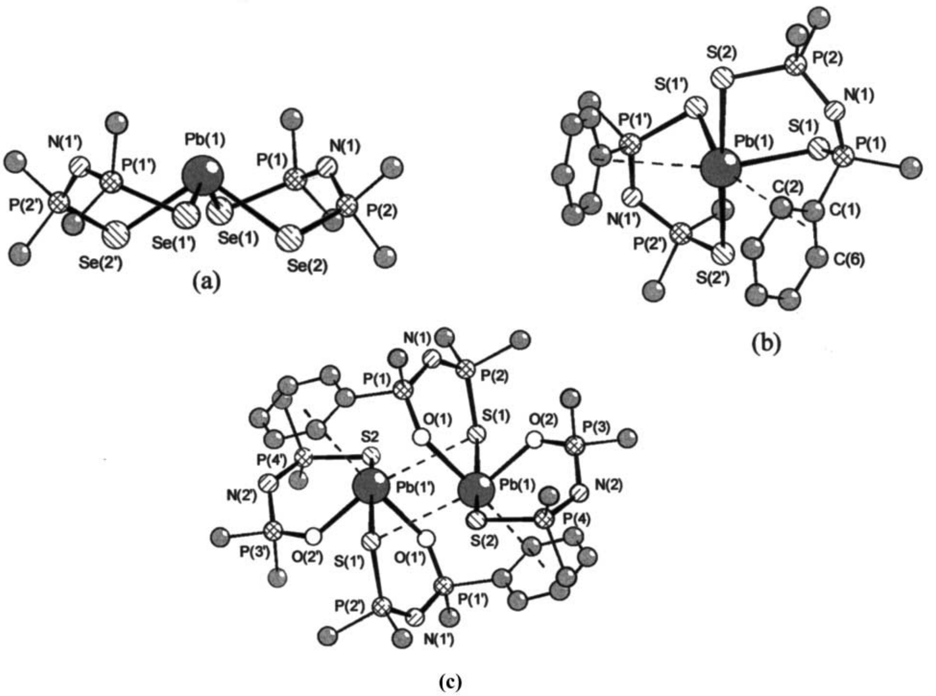

Fig. 34. The structure of (a) $Pb[(SePPh_2)_2N]_2$ [114], (b) $Pb[(SPPh_2)_2N]_2$ [125], and (c) the dimeric association in the crystal of $Pb[(OPPh_2)(SPPh_2)N]_2$ [126] (for clarity, only *ipso* carbons and the whole phenyl groups involved in interaction to lead, respectively, are shown).

triconnective, its sulfur atom being involved in an intermolecular interaction with the lead atom of the neighboring molecule [Pb(1)···Sn(1′) 3.386(3) Å]. In addition, an intermolecular π-Pb–phenyl interaction is also established [Pb(1)–$C_{1,2,6}$ 3.424–3.579 Å] by the second ligand, whose vector is *trans* to the oxygen atom of the chelating ligand. Thus, again a distorted octahedral coordination can be considered around the metal center, with sulfur atoms in axial positions [S(1)–Pb(1)–S(2) 165.1(1)°]. The two covalent Pb–S distances in the molecular unit are different, with that corresponding to the sulfur atom involved in the bridging system considerably longer than the other. The $PbOSP_2N$ rings are both of distorted boat conformation, but the chelating one has the Pb(1) and N(2) atoms in the apices, while the other has S(1) and P(1) atoms in the apices. The angles within the six-membered rings are also considerably different, e.g. Pb–O–P 130.0(4) and 141.4(0)°, O–Pb–S 87.8(2) and 82.3(2)°, respectively.

Both diorgano- and triorganolead(IV) complexes were prepared by reacting $R_{4-n}PbCl_n$ with the alkaline salt of the appropriate imidodiphosphinato ligand [132,133] and the magnitudes of the ^{207}Pb-proton and ^{207}Pb-carbon coupling constants are indicative of the presence of two and three organic groups, respectively, attached to the metal atom. However, crystals suitable for X-ray diffraction could only be grown for $R_2Pb[(OPPh_2)_2N]_2$ (R = Me, Ph) and, as for the triorganotin(IV) derivatives, attempts to grow crystals of $Me_3Pb[(OPPh_2)_2N]$ resulted in isolation of $Me_2Pb[(OPPh_2)_2N]_2$. In this case the decomposition process involves the migration of a methyl group from the metal atom to the ligand; evidence for the formation of the O-methyl ester being obtained by means of NMR spectroscopy [132,133].

The crystals of $R_2Pb[(OPPh_2)_2N]_2$ (R = Me [132], Ph [133]) contain discrete molecules whose structures are similar to the tin analogs. The imidodiphosphinato ligands act as monometallic biconnective units, leading to a spiro-bicyclic system, with lead as the spiro atom in a distorted octahedral environment and some distinctive features worth mentioning. In the dimethylead(IV) derivative, which has two independent molecules in the unit cell, the ligands are coordinated asymmetrically through the oxygen atoms and this is more clearly seen in one of the molecules (molecule 1, Fig. 35a) [132]. The Pb–O bond lengths differ in the equatorial PbO_4 system with *cis* short, Pb(1)–O(1) and Pb(1)–O(3) [2.342(5), 2.352(6) Å], and *cis* long bonds, Pb(1)–O(2) and Pb(1)–O(4) [2.420(6), 2.462(5) Å]. Moreover, the corresponding exocyclic angles at the lead atom differ, with the angle O(1)–Pb(1)–O(3) [88.5(2)°] considerably smaller than O(2)–Pb(1)–O(4) [100.7(2)°]. As a consequence, the *trans* O–Pb(1)–O angles deviate significantly from the ideal value [172.6(2), 174.2(2)°]. The PbC_2 fragment is similar [173.4(3)°] with the axial Pb–C bonds inclined towards the open O–Pb–O angle between the longer Pb–O

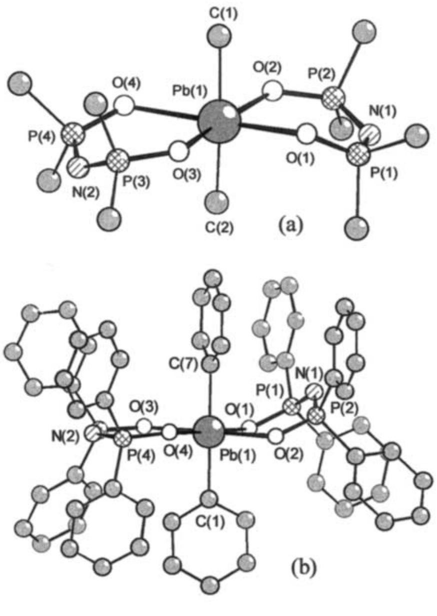

Fig. 35. The molecular structure of (a) $Me_2Pb[(OPPh_2)_2N]_2$ (molecule 1) [132] (for clarity, only *ipso* carbons of the phenyl groups attached to phosphorus atoms are shown), and (b) $Ph_2Pb[(OPPh_2)_2N]_2$ [133].

bonds. In the second molecule of $Me_2Pb[(OPPh_2)_2N]_2$, the differences in the Pb–O bond lengths are less pronounced as is the distortion of the octahedral PbC_2O_4 core [*trans* C–Pb–C and O–Pb–O range 176.5(2)–178.7(4)°]. This is also the case for $Ph_2Pb[(OPPh_2)_2N]_2$ [*trans* C–Pb–C and O–Pb–O range 177.7(1)–178.9(2)°] [133]. The differences in the conformation of the two *six-membered* PbO_2P_2N rings in the molecular units can be described as (a) distorted boat, with Pb/N and O/P atoms in the apices for the two $Me_2Pb[(OPPh_2)_2N]_2$ molecules, but (b) distorted boat (Pb/N atoms in apices) and distorted chair close to planarity for the $Ph_2Pb[(OPPh_2)_2N]_2$ molecule (Fig. 35b).

4.6. Group 15: Sb, Bi

Both inorganic and organometallic complexes have been described for antimony and bismuth in oxidation state III, but only organometallic derivatives of antimony in oxidation state V are known (Table 23). The solid state structures of most of the compounds have been investigated by single-crystal X-ray diffraction and their important molecular dimensions are included in Table 24.

4.6.1. Antimony

Only two inorganic Sb(III) compounds containing imidodiphosphinato ligands have been described. The crystals of the tris-substituted complex contain discrete $Sb[(SePPh_2)_2N]_3$ molecules [119]. The ligands are chelated asymmetrically to the metal center. The coordination geometry around antimony is distorted octahedral (Fig. 36a), with *fac* short $Sb(1)–Se_{1,3,5}$ [2.742(2)–2.863(1) Å] and long $Sb(1)–Se_{2,4,6}$ bonds [2.890(1)–3.042(2) Å], respectively, and *trans* Se–Sb(1)–Se bond angles close to 180° [170.7(1)–178.9(1)°]. This coordination polyhedron of the $SbSe_6$ core suggests a stereochemically inactive lone pair of electrons. The conformation of the inorganic $SbSe_2P_2N$ rings is distorted boat, but two rings have Se and P atoms in the apices [Se(2)/P(1) and Se(6)/P(5)], while the third has the metal and N(2) atoms.

The reaction of antimony powder with molecular iodine activated by free $(SPPh_2)_2NH$ acid, afforded the isolation of an unexpected dinuclear product, whose structure was established by X-ray diffraction [139]. The two metal atoms are bridged by a sulfide and two iodide anions (Fig. 36b). Each antimony atom is further coordinated, almost symmetrically, by the sulfur atoms of a dithioimidodiphosphinato ligand. The resulting SbI_2S_3 core is distorted square pyramidal, with the bridging sulfur atom in the apical position and the iodine atoms *trans* to the sulfur atoms of the dithio ligand in the basal plane [167.46(5), 168.99(5)°]. The overall coordination geometry can also be described as pseudo-octahedral if a stereochemically active lone pair is considered to be *trans* to the apical sulfur atom. The SbS_2P_2N ring displays a boat conformation with the metal and nitrogen atoms in the apices.

Both organo-antimony(III) and antimony(V) complexes are known. The mixed-ligand complexes, $PhSbCl[(XPR_2)(YPR'_2)N]$, were found to disproportionate to $PhSb[(XPR_2)(YPR'_2)N]_2$ and $PhSbCl_2$ [142]. The crystals of $PhSb[(SPPh_2)_2N]_2$ contain discrete molecules. The ligands are coordinated asymmetrically through both

Table 23
Group 15 metal complexes of imidodiphosphorus acids

Compound	Yield (%)	M.p. (°C)	$\delta(^{31}P)$ (ppm), ^nJ(PX) (Hz)[a]			X-ray studies	Spectroscopic studies
			*P*O	*P*S	*P*Se		
Inorganic compounds							
$Sb[(SePPh_2)_2N]_3$	66 [119]				29.4s	[119]	IR, MS, ^{31}P [119]
$(\mu\text{-}S)(\mu\text{-}I)_2[Sb(SPPh_2)_2N]_2$	45 [139]	260–263		33.0s/34.4s[b]		[139]	IR, ^{31}P [139]
$Bi[(OPPh_2)_2N]_3$	[50]	270	17.3s			[117]	MS [117], ^{31}P [50]
$Bi[(OPPh_2)_2N]_3] \cdot C_6H_6$	[50]	271–273					
$Bi[(SPMe_2)_2N]_3$	47 [140]	185–190					^1H [140]
$Bi[(SPPh_2)_2N]_3$	57 [50]	235–236		34.9s		[141]	^{31}P [50]
$Bi[(SePPh_2)_2N]_3$	73 [119]				27.2s	[119]	IR, MS, ^{31}P [119]
Organometallic compounds							
$PhSbCl[(SPPh_2)_2N]$	90 [142]	92		37.3s,br			IR, ^1H, ^{31}P [142]
$PhSb[(SPPh_2)_2N]_2$	77 [142]			37.6s		[142]	IR, ^{31}P [142]
$PhSbCl[(OPPh_2)(SPPh_2)N]$	86 [142]	160–162	27.6s	33.4s			IR, ^1H, ^{31}P [142]
$PhSb[(OPPh_2)(SPPh_2)N]_2$	78 [97]	158–160	23.2s,br	35.5s,br		[97]	IR, ^{31}P [97]
$Ph_2SbCl_2[(OPPh_2)_2N]$	63 [143]	257	25.5s			[143]	IR, MS, ^1H, ^{13}C, ^{31}P [143]
$Ph_2SbCl_2[(OPPh_2)(SPPh_2)N] \cdot 0.5C_6H_5CH_3$	63 [143]	254–255	26.5d, ^2J(PP) 2.3	32.1d, ^2J(PP) 2.3		[143]	IR, MS, ^1H, ^{13}C, ^{31}P [143]
$Ph_2SbCl_2[(OPMe_2)(OPPh_2)N]$	77 [143]	236–237	26.5d (P–Ph), ^2J(PP) 3.9 46.0s,br (P–Me)				IR, MS, ^1H, ^{13}C, ^{31}P [143]
$Me_3SbCl[(OPPh_2)_2N]$	77 [97]	135–137	14.6s[c] 13.2s, 21.4s[d]				IR, ^1H, ^{13}C, ^{31}P [97]
$Me_3Sb[(OPPh_2)_2N]_2$	73 [142]	178–180	21.1s 14.5s				IR, ^{31}P [142]
$Me_3SbCl[(OPPh_2)(SPPh_2)N]$	100 [97]	112	16.02s, 16.08s[c,d], ^1J(PC) 144.7	40.12s, 40.37s[c,d], ^1J(PC) 109.2			IR, ^1H, ^{13}C, ^{31}P [97]
$Me_3Sb[(OPPh_2)(SPPh_2)N]_2$	94 [142]	153–154	16.8s, ^1J(PC) 139.9	40.1s, ^1J(PC) 107.6		[142]	IR, ^1H, ^{13}C, ^{31}P [97,142]
$[2\text{-}(Me_2NCH_2)C_6H_4]\text{-}BiCl[(SPPh_2)_2N]$	84 [99]	196–197		37.9s		[99]	IR, ^1H, ^{13}C, ^{31}P [99]
$[2\text{-}(Me_2NCH_2)C_6H_4]\text{-}BiCl[(SePPh_2)_2N]$	85 [99]	190				[99]	IR, ^1H, ^{13}C [99]

[a] In $CDCl_3$.

[b] ^{31}P CP-MAS NMR data.

[c] Isomer I (**22**).

[d] Isomer II (**23**).

Table 24
X-ray data [bond lengths (Å) and bond angles (°)] for Group 15 metal complexes of imidodiphosphorus acids

Compound	M–X	P–X	P–N	P–N–P	Association degree	Ref.
Inorganic compounds						
$Sb[(SePPh_2)_2N]_3$	2.742(2)–3.042(2)	2.144(3)–2.202(3)	1.570(12)/1.611(12)	131.7(7)–133.6(7)	Monomer	[119]
$(\mu\text{-}S)(\mu\text{-}I)_2[Sb(SPPh_2)_2N]_2$[a]	2.562(2)/2.599(2)	2.035(3)/2.023(3)	1.575(6)/1.589(5)	136.4[b]	Dinuclear	[139]
$Bi[(OPPh_2)_2N]_3$	2.256(7)–2.404(8)	1.509(8)–1.539(9)	1.568(12)–1.593(9)	128.9(7)–133.0(7)	Monomer	[117]
$Bi[(SPPh_2)_2N]_3 \cdot (CH_3)_2CO$	2.728(3)–2.986(3)	1.994(4)–2.025(3)	1.586(7)–1.602(7)	132.9(5)–136.5(5)	Monomer	[141]
$Bi[(SePPh_2)_2N]_3$	2.835(3)–3.047(3)	2.154(5)–2.193(5)	1.557(18)–1.613(18)	132.6(10)–134.8(9)	Monomer	[119]
Organometallic compounds						
$PhSb[(SPPh_2)_2N]_2$	2.666(1)–2810(1)	2.011(1)–2.030(1)	1.587(3)–1.596(3)	134.3(2)/135.6(2)	Monomer	[142]
$PhSb[(OPPh_2)(SPPh_2)N]_2$	2.169(5)/2.329(5) (M–O)	1.532(5)/1.515(5) (P–O)	1.572(6)/1.606(6)	134.6(4)	Monomer	[97]
	2.902(2)/2.661(2) (M–S)	2.004(3)/2.036(3) (P–S)	1.597(6)/1.577(6)	131.5(4)		
$Ph_2SbCl_2[(OPPh_2)_2N]$[c]	2.112(3)/2.129(3)	1.539(3)/1.546(3)	1.582(4)/1.592(4)	125.8(2)	Monomer	[143]
$Ph_2SbCl_2[(OPPh_2)(SPPh_2)N] \cdot 0.5C_6H_5CH_3$[d]	2.113(3)	1.543(4)	1.582(4)	132.3(3)	Monomer	[143]
	2.614(2)	2.037(2)	1.587(4)			
$Me_3Sb[(OPPh_2)(SPPh_2)N]_2$	2.090(5)/2.109(5)	1.544(6)/1.556(5) (P–O)	1.571(7)/1.564(6)	134.1(5)/132.6(4)	Monomer	[142]
		1.962(3)/1.972(3) (P–S)	1.601(7)/1.618(6)			
$[2\text{-}(Me_2NCH_2)C_6H_4]BiCl[(SPPh_2)_2N]$[e]	2.825(2)/2.847(2)	2.010(3)/2.020(3)	1.604(6)/1.590(6)	131.1(4)	Dimer	[99]
$[2\text{-}(Me_2NCH_2)C_6H_4]BiCl[(SePPh_2)_2N]$[f]	2.890(1)/3.018(1)	2.176(2)/2.159(2)	1.578(6)/1.605(7)	130.7(4)	Dimer	[99]

[a] Sb(1)–S(1)$_{\text{bridging}}$ 2.425(2), Sb(1)–I(1) 3.216(1), Sb(1)–I(1′) 3.157(1) Å.

[b] Calculated from published atomic coordinates.

[c] Sb(1)–Cl 2.420(1), 2.452(1) Å.

[d] Sb(1)–Cl 2.422(2), 2.428(2) Å.

[e] Bi(1)–Cl(1) 2.669(2), Bi(1)–N(2) 2.553(6) Å.

[f] Bi(1)–Cl(1) 2.647(2), Bi(1)–N(2) 2.575(7) Å.

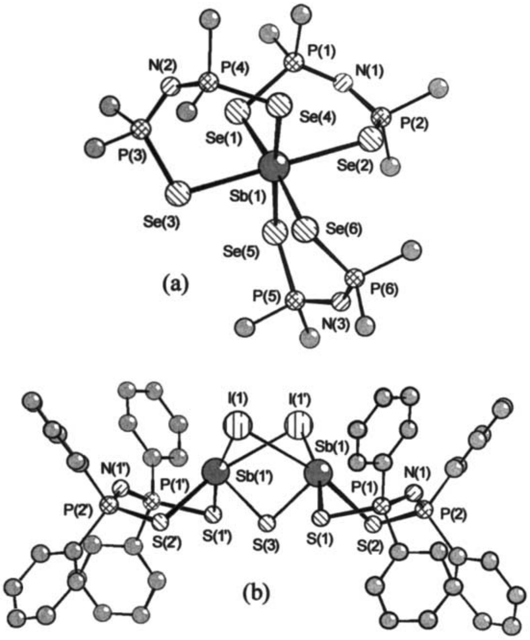

Fig. 36. The structure of (a) $Sb[(SePPh_2)_2N]_3$ [119] (for clarity, only *ipso* carbons of the phenyl groups attached to phosphorus atoms are shown), and (b) $(\mu\text{-}S)(\mu\text{-}I)_2[Sb(SPPh_2)_2N]_2$ [139].

sulfur atoms, with a *cis* arrangement of the short Sb(1)–S [2.666(1), 2.690(1) Å, S(2)–Sb(1)–S(3) 80.73(3)°] and long Sb(1)–S bonds [2.778(1), 2.810(1) Å, S(1)–Sb(1)–S(4) 93.76(4)°], respectively (Fig. 37a) [142]. The coordination geometry around the metal atom is distorted square pyramidal, with the SbS_4 system forming the basal plane [*trans* S–Sb(1)–S 169.55(3), 170.17(3)°; S–Sb(1)–C range 83.8(1)–96.2(1)°]. The lone pair of antimony can be considered to be stereochemically active occupying a position *trans* to the *ipso* carbon of the phenyl group attached to the metal. The conformation is distorted boat in both of the inorganic SbS_2P_2N rings but with different atom types in the apices; the metal and N(1) atoms in one and P(3) and S(4) atoms in the other.

The crystals of the asymmetric ligand complex, $PhSb[(OPPh_2)(SPPh_2)N]_2$, also contain monomeric units with a similar overall structure as the dithio analog (Fig. 37b) [97]. A spiro-bicyclic system is formed as a result of the monometallic biconnective pattern of the monothio ligand, with *trans* O(1)–Sb(1)–O(2) [169.1(2)°] and S(1)–Sb(1)–S(2) [172.5(1)°] fragments. Surprisingly, the two ligands are primary coordinated through different chalcogen atoms as suggested by the Sb(1)–O versus Sb(1)–S bond lengths for a $SbOSP_2N$ ring [Sb(1)–O(1) 2.169(5), Sb(1)–S(1) 2.902(2), and Sb(1)–O(2) 2.329(5), Sb(1)–S(2) 2.661(2) Å, respectively]. Again, different atom types occupy the apex positions of the distorted boat $SbOSP_2N$ rings [Sb(1)/N(2) and P(1)/S(1) atoms, respectively].

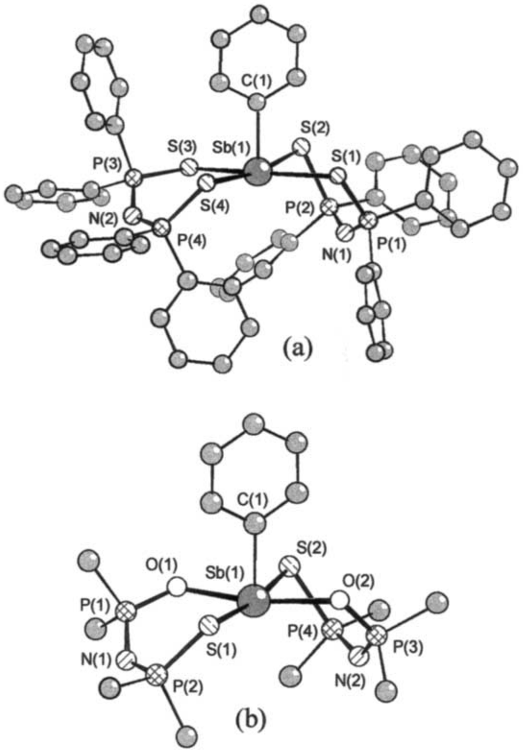

Fig. 37. The molecular structure of (a) $PhSb[(SPPh_2)_2N]_2$ [142], and (b) $PhSb[(OPPh_2)(SPPh_2)N]_2$ [97] (for clarity, only *ipso* carbons of the phenyl groups attached to phosphorus atoms are shown).

Several $Ph_2SbCl_2[(XPR_2)(YPR'_2)N]$ complexes were prepared and NMR data are consistent with the presence in solution of only one isomer with a similar structure to that found in the solid state [143]. The structures of $Ph_2SbCl_2[(OPPh_2)_2N]$ and $Ph_2SbCl_2[(OPPh_2)(SPPh_2)N]$ (Fig. 38a) are similar, regardless of the nature of the imidodiphosphinato ligand [143]. In both cases the crystals contain discrete molecular units, separated by normal van der Waals distances, and the coordination geometry around the metal atom is slightly distorted octahedral, with the phenyl groups in axial positions [C(1)–Sb(1)–C(7) 173.5(2) and 176.8(2)°, respectively] and pairs of chlorine and chalcogen atoms, each in *cis* positions. The $SbCl_2OX$ ($X = O$, S) system is almost planar and the Sb(1)–C bonds are bent towards the O(1)···X side of the equatorial plane. The inorganic $SbOXP_2N$ rings display a similar twisted boat conformation [Sb(1)/N(1) atoms in apices]. The main difference between the molecular structures of these two complexes is the relative orientation of the phenyl groups attached to antimony. In the dioxo derivative the dihedral angle between the phenyl ring planes is 29.2°, while in the monothio complex the phenyl rings are almost perpendicular (85.7°).

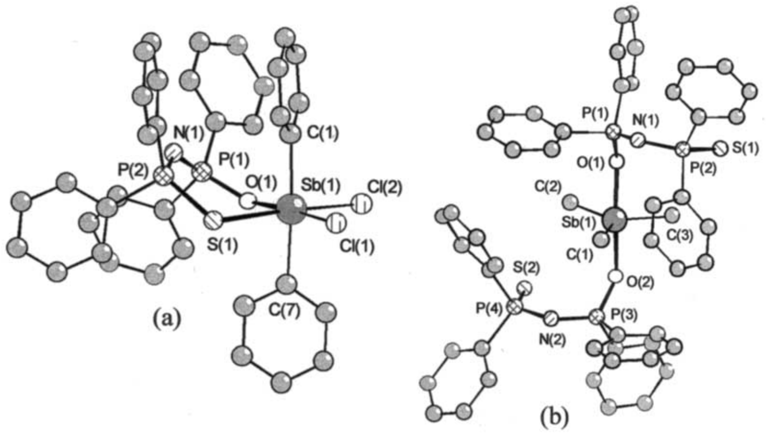

Fig. 38. The molecular structure of (a) $Ph_2SbCl_2[(OPPh_2)(SPPh_2)N]$ [143], and (b) $Me_3Sb[(OPPh_2)(SPPh_2)N]_2$ [142].

The reaction of Me_3SbCl_2 with $K[(SPPh_2)_2N]$ (1:1 molar ratio) resulted in an unstable product, $Me_3SbCl[(SPPh_2)_2N]$, which decomposed to the ester, $MeS–PPh_2=N–PPh_2=S$, as a consequence of migration of a methyl group from the organometallic center to the ligand and the reduction of the antimony from + 5 to + 3 [97]. However, derivatives of the type $Me_3SbCl[(OPPh_2)(XPPh_2)N]$ (X = O, S) were isolated as stable compounds. The presence of two isomers, **22** and **23**, in solution, was established on the basis of multinuclear NMR data [97].

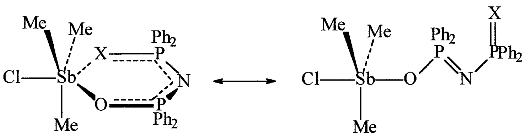

(**22**) - isomer I

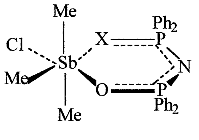

(**23**) - isomer II

The molecular structure of $Me_3Sb[(OPPh_2)(SPPh_2)N]_2$ was also established by X-ray diffraction (Fig. 38b) and this compound is one of the very few known examples that contain true monodentate (monometallic monoconnective) imidodiphosphinato ligands [142]. Here the monothio groups are connected to the metal atom only through the oxygen atoms [Sb(1)–O(1) 2.090(5), Sb(1)–O(2)

2.109(5) Å]. Although the sulfur atoms are not involved in intramolecular interactions with antimony, the O–P–N–P–S skeletons exhibit a *syn* conformation (note that in the free acid it is *anti*) probably as a result of packing forces in the crystal. The resulting coordination geometry is trigonal bipyramidal, with a planar SbC_3 moiety and the oxygen atoms in axial positions [C–Sb(1)–C range 119.6(4)–120.5(4)°, O(1)–Sb(1)–O(2) 173.4(2)°].

4.6.2. Bismuth

The crystals of the tris-derivatives, $Bi[(XPPh_2)_2N]_3$ (X = O [117], S [141], Se[119]), contain discrete molecules with very similar octahedral structures (exemplified in Fig. 39a for $Bi[(OPPh_2)_2N]_3$), that are similar to the indium(III) or antimony(III) compounds described above. The asymmetric nature of the chelating ligands seems to be less marked in the $Bi[(OPPh_2)_2N]_3$ complex than in the thio or seleno analogs, as reflected in the bismuth chalcogen bond distances. However, in all three cases a *fac* arrangement of short Bi(1)–X and long Bi(1)–X bonds, respectively, is obvious. The *trans* X–Bi(1)–X bond angles are close to 180°, thus being consistent with a stereochemically inactive lone pair. There are differences in the conformations of the BiX_2P_2N rings so that for $Bi[(XPPh_2)_2N]_3$ (X = O, S) all of the chelate rings in a molecular unit have distorted boat conformations with the metal and nitrogen atom in the apices, while for the seleno analog the conformations of the chelate rings follow the differences noted above for the antimony derivative.

Few organobismuth(III) derivatives have been described so far and all of them contain an *ortho*-Me_2NCH_2-substituted phenyl group attached to bismuth [99]. The disubstituted derivatives, $[2\text{-}(Me_2NCH_2)C_6H_4]Bi[(XPPh_2)(YPPh_2)N]_2$ (X, Y = O, S, Se), are quite sensitive to moisture and attempts to grow crystals of $[2\text{-}(Me_2NCH_2)C_6H_4]Bi[(SPPh_2)_2N]_2$ resulted in the isolation of the hydrolysis product $S{=}PPh_2–N{=}PPh_2–O–PPh_2{=}N–PPh_2{=}S$, whose molecular structure was described in

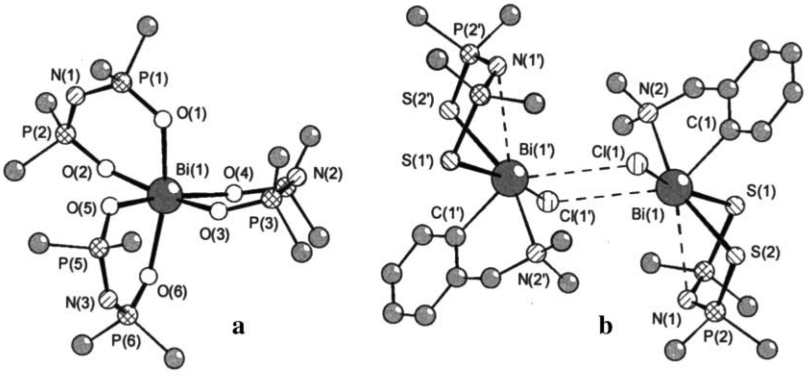

Fig. 39. The structure of (a) $Bi[(OPPh_2)_2N]_3$ [117], and (b) dimeric association in the crystal of $[2\text{-}(Me_2NCH_2)C_6H_4]BiCl[(SPPh_2)_2N]$ [99] (for clarity, only *ipso* carbons of the phenyl groups attached to phosphorus atoms are shown).

Section 2.3. In contrast, the chloro derivatives, [2-(Me_2NCH_2)C_6H_4]BiCl-[($XPPh_2$)($YPPh_2$)N], are stable and can be handled in air. The NMR data at room temperature suggest fluxional behavior in solution.

The solid state molecular structures of [2-(Me_2NCH_2)C_6H_4]BiCl[$(XPPh_2)_2N$] (X = S, Se) are similar [99]. The nitrogen atom of the pendant Me_2NCH_2 arm exhibits a strong intramolecular Bi(1)–N(2) coordination [2.553(6) Å for X = S; 2.575(7) Å for X = Se]. In both compounds the imidodiphosphinato ligand is chelated to the metal atom through both chalcogen atoms, which are *trans* to the chlorine and nitrogen of the pendant arm [X(1)–Bi(1)–Cl(1) 166.6(1), 165.6(1)°, and X(2)–Bi(1)–N(2) 159.6(1), 164.8(2)°, for X = S and Se, respectively). However, the coordination pattern is symmetric for the dithio derivative [Bi(1)–S 2.825(2), 2.847(2) Å], while for the diseleno complex it is clearly asymmetric [Bi(1)–Se 2.890(1), 3.018(1) Å]; the longer Bi–Se bond being *trans* to the chlorine atom. The $BiCNClX_2$ core in the molecular unit is square pyramidal, with the metal atom displaced from the basal plane towards the apical carbon atom. Weak intermolecular Bi···Cl interactions [Bi(1)···Cl(1′) 3.526, 3.572 Å, for X = S and Se, respectively] result in loosely connected dimers in the crystal (Fig. 39b), and the twisted boat conformation of the BiX_2P_2N chelate ring brings the N(1) atom into the proximity of the metal atom, thus allowing a second weak intramolecular Bi(1)···N(1) interaction [3.346, 3.368 Å, for X = S and Se, respectively].

4.7. Group 16: Se, Te

Inorganic complexes of imidodiphosphorus ligands are known for both selenium and tellurium, but only organotellurium derivatives have been described. The compounds are listed in Table 25, along with the spectroscopic methods (including ^{31}P-NMR data) used for their characterization. The solid state structure of several derivatives have been investigated by single-crystal X-ray diffraction and their important molecular dimensions are included in Table 26.

4.7.1. Selenium

The reaction of Se(II) dithiophosphates, $Se[S_2P(OR)_2]_2$, with a salt of the appropriate imidodiphosphinic acid, afforded the isolation of $Se[(XPPh_2)_2N]_2$ (X = S [144], Se [145]), and for both of compounds the solid state molecular structure has been established. The dithio derivative contains distinctly asymmetric chelating ligands, with *cis* short, covalent Se–$S_{1,3}$ bonds [2.264(1), 2.270(1) Å], and weak, intramolecular Se···$S_{2,4}$ interactions [2.948(1), 3.054(1) Å]. A trapezoidal arrangement, close to planarity, of the SeS_4 core is achieved [S(1)–Se(1)–S(3) 98.06(5), S(2)···Se(1)···S(4) 94.99(4)°], and the SeS_2P_2N rings are strongly folded about the S···S axis on the opposite side relative to the planar SeS_4 system [Se(1)–S–P 89.75(5)–99.16(5)°] (Fig. 40a). The two independent molecules of $Se[(SePPh_2)_2N]_2$ present in the asymmetric unit have similar overall structures, but the planar Se(Se_4) core has essentially square planar geometry [exocyclic Se(1)–Se(3)–Se(2′) 91.7, endocyclic Se(1)–Se(3)–Se(2) 88.3°, for molecule 1) (Fig. 40b). The ligands are coordinated symmetrically [Se(3)–Se_{ligand} range 2.643(1)–2.678(1) Å] to form a spiro

Table 25
Group 16 metal complexes of imidodiphosphorus acids

Compound	Synthesis, yield (%)	M.p. (°C)	$\delta(^{31}P)$ (ppm), $^{n}J(PX)$ (Hz)[a]			X-ray studies	Spectroscopic studies
			*P*O	*P*S	*P*Se		
Inorganic compounds							
$Se[(SPPh_2)_2N]_2$	90 [144]	190–192				[144]	IR [144]
$Se[(SePPh_2)_2N]_2$	62 [145]	210			34.3s	[145]	IR, MS, ^{31}P [145]
$Te[(SP^{i}Pr_2)_2N]_2$	96 [146]			58.7s		[146]	IR, MS, ^{31}P [146]
$Te[(SPCy_2)_2N]_2$	67 [146]			51.9s		[146]	IR, MS, ^{31}P [146]
$Te[(SPPh_2)_2N]_2$	75 [147]	257				[147]	IR [147]
$Te[(SPEt_2)(SPPh_2)N]_2$	65 [146]			53.3s/53.7s (P–Et) 32.7s/33.9s (P–Ph)			IR, MS, ^{31}P [146]
$Te[(SP^{i}Pr_2)(SPPh_2)N]_2$	49 [146]			64.3d/63.7d (P–^{i}Pr), $^{2}J(PP)$ 22.5 32.7d/31.8d (P–Ph), $^{2}J(PP)$ 22.5		[146]	IR, MS, ^{31}P [146]
$Te[(SPEt_2)\{SP(OPh)_2\}N]_2$	41 [146]			55.1s (P–Et) 43.7s (PhO–P)		[146]	IR, MS, ^{31}P [146]
$Te[\{SP(OEt)_2\}\{SP(OPh)_2\}N]_2$	72 [146]			65.0s (EtO–P) 43.0s (PhO–P)			IR, MS, ^{31}P [146]
$Te[(SeP^{i}Pr_2)_2N]_2$	62 [146]				58.7s, $^{1}J(PSe)$ 528	[146]	IR, MS, ^{31}P [146]
$Te[(SePPh_2)_2N]_2$	74 [148]	275			24.4s[b], $^{1}J(PSe)$ 586	[148]	^{31}P [148]
$(\mu\text{-}Cl)_2[Te(SPPh_2)_2N]_2$	61 [149]	140–142		27.6s[c]		[149]	^{31}P [149]
Organometallic compounds							
$PhTe[(SPPh_2)_2N]$	47 [150]					[150]	IR [150]
$(4\text{-}MeOC_6H_4)Te[(SPPh_2)_2N]$	19 [148]	167		34.9s[b]		[148]	^{31}P [148]
$[2\text{-}(Me_2NCH_2)C_6H_4]\text{-}Te[(SPPh_2)_2N]$	30 [151]	140		41.9s (P=S) 31.7s (P–S)		[151]	^{1}H, ^{31}P [151]
$(4\text{-}MeOC_6H_4)\text{-}TeCl_2[(SP^{i}Pr_2)_2N]$	73 [146]			62.0s		[146]	IR, MS, ^{31}P [146]

Table 25 (*Continued*)

Compound	Synthesis, yield (%)	M.p. (°C)	$\delta(^{31}P)$ (ppm), $^{n}J(PX)$ (Hz)[a]			X-ray studies	Spectroscopic studies
			*P*O	*P*S	*P*Se		
(4-$MeOC_6H_4$)-$TeCl_2[(SP^iPr_2)(SPPh_2)N]$	32 [146]			69.2d (P–^{i}Pr), $^2J(PP)$ 24.9 34.5d (P–Ph), $^2J(PP)$ 24.9		[146]	IR, MS, ^{31}P [146]
$Me_2Te[(SPPh_2)_2N]_2$	84 [152]	152		35.8s		[152]	^1H, ^{13}C, ^{31}P, ^{127}Te [152]
$Me_2TeCl[(SPPh_2)_2N]$	87 [152]	106		43.2s		[152]	^1H, ^{13}C, ^{31}P, ^{127}Te [152]
$Me_2TeBr[(SPPh_2)_2N]$	[152]	–[d]		43.3s			^1H, ^{13}C, ^{31}P, ^{127}Te [152]
$Me_2TeI[(SPPh_2)_2N]$	86 [152]	105		33.6s		[152]	^1H, ^{13}C, ^{31}P, ^{127}Te [152]
$Me_2Te[(OPPh_2)(SPPh_2)N]_2$	[152]	–[d]	21.3s	39.7s			^1H, ^{13}C, ^{31}P, ^{127}Te [152]
$Me_2TeCl[(OPPh_2)(SPPh_2)N]$	86 [152]	130	21.8s	39.8s		[152]	^1H, ^{13}C, ^{31}P, ^{127}Te [152]
$Me_2TeBr[(OPPh_2)(SPPh_2)N]$	[152]	–[d]	20.3s	39.7s			^1H, ^{13}C, ^{31}P, ^{127}Te [152]
$Me_2TeI[(OPPh_2)(SPPh_2)N]$	[152]	–[d]					^1H, ^{13}C, ^{127}Te [152]
$Ph_3Te[(OPPh_2)_2N]$	83 [153]	168–170	10.1s, $^1J(PC)$ 131.2			[153]	IR, ^1H, ^{13}C, ^{31}P [153]
$Ph_3Te[(OPMe_2)(OPPh_2)_2N]$	[153][e]		29.4s (P–Me) 12.4s (P–Ph), $^1J(PC)$ 128.4				^1H, ^{13}C, ^{31}P [153]
$Ph_3Te[(SPMe_2)_2N]$	[153][e]			39.4s			^1H, ^{13}C, ^{31}P [153]
$Ph_3Te[(SPMe_2)(SPPh_2)_2N]$	[153][e]			40.7s (P–Me) 35.5s (P–Ph)			^1H, ^{13}C, ^{31}P [153]
$Ph_3Te[(OPMe_2)(SPPh_2)_2N]$	[153][e]		36.2s,br	40.9s,br			^1H, ^{13}C, ^{31}P [153]
$Ph_3Te[(OPPh_2)(SPMe_2)_2N]$	[153][e]		9.9s, $^1J(PC)$ 129.5	35.9s,br			^1H, ^{13}C, ^{31}P [153]
$Ph_3Te[(OPPh_2)(SPPh_2)_2N]$	82 [153]	128–130	12.6s, $^1J(PC)$ 134.0	34.5s,br		[153]	IR, ^1H, ^{13}C, ^{31}P [153]
$Ph_3Te[(SPPh_2)_2N]$	86 [154]	195–196		36.9s		[154]	IR, MS, ^1H, ^{13}C, ^{31}P [154]

[a] In $CDCl_3$ or $CHCl_3$.

[b] In $CH_2Cl_2/CDCl_3$.

[c] In CH_2Cl_2.

[d] Viscous product.

[e] NMR tube synthesis.

Table 26
X-ray data [bond lengths (Å) and bond angles (°)] for Group 15 metal complexes of imidodiphosphorus acids

Compound		M–X	P–X	P–N	P–N–P	Association degree	Ref.
Inorganic compounds							
Se[(SPPh$_2$)$_2$N]$_2$		2.264(1)–3.054(1)	1.996(2)–2.074(2)	1.554(3)/1.598(3)	139.1(2)–141.0(2)	Monomer	[144]
Se[(SePPh$_2$)$_2$N]$_2$	Mol. 1	2.646(1)/2.678(1)	–[a]	–[a]	139.5(5)	Monomer	[145]
	Mol. 2	2.643(1)/2.663(1)	–[a]	–[a]	136.4(5)		
Te[(SP^{i}Pr$_2$)$_2$N]$_2$		2.673(1)/2.698(1)	2.035(1)/2.036(1)	1.583(2)/1.584(2)	142.9(1)	Monomer	[146]
Te[SPCy$_2$)$_2$N]$_2$ · 1.5CHCl$_3$		2.682(1)/2.697(1)	2.045(2)/2.046(2)	1.594(4)/1.584(4)	145.3(3)	Monomer	[146]
Te[(SPPh$_2$)$_2$N]$_2$	Mol. 1	2.675(2)/2.699(3)	2.023(3)/2.023(3)	1.597(7)/1.574(7)	139.5(4)	Monomer	[147]
	Mol. 2	2.673(2)/2.691(2)	2.025(3)/2.018(3)	1.590(6)/1.597(7)	137.0(4)		
Te[(SP^{i}Pr$_2$)(SPPh$_2$)N]$_2$		2.678(2) 2.684(2)	2.022(2) (S–P$_{Ph}$) 2.032(2) (S–P$_{Pr}$)	1.589(5) 1.593(5)	138.8	Monomer	[146]
Te[(SPEt$_2$){SP(OPh)$_2$}N]$_2$		2.527(1)/2.91 2.513(1)/2.90	2.046(2)/1.962(2)[b] 2.053(2)/1.968(2)[b]	1.580(3)/1.558(3) 1.567(3)/1.576(3)	142.2(2) –[a]	Monomer	[146]
Te[(SP^{i}Pr$_2$)$_2$N]$_2$		2.794(1)/2.815(1)	2.189(1)/2.194(1)	1.588(3)/1.579(3)	145.1(2)	Monomer	[146]
Te[(SePPh$_2$)$_2$N]$_2$	Mol. 1	2.775(1)/2.806(1)	2.171(1)/2.177(1)	1.596(4)/1.589(4)	137.2(2)	Monomer	[148]
	Mol. 2	2.789(1)/2.815(1)	2.172(1)/2.187(1)	1.584(4)/1.583(4)	140.8(2)		
(μ-Cl)$_2$[Te(SPPh$_2$)$_2$N]$_2$[c]		2.498(1)/2.505(1)	2.055(1)/2.059(1)	1.588(2)/1.594(3)	132.6(3)	Dimer	[149]
Organometallic compounds							
PhTe[(SPPh$_2$)$_2$N]		2.557(3) 2.843(3)[d]	2.044(4) 1.996(4)	1.580(7) 1.589(7)	135.1(5)	Dimer	[150]
(4-MeOC$_6$H$_4$)Te[(SPPh$_2$)$_2$N] · 3CH$_2$Cl$_2$		2.551(3) 2.873(3)[d]	2.041(3) 2.006(4)	1.557(8) 1.624(9)	132.1(6)	Dimer	[148]

Table 26 (*Continued*)

Compound	M–X	P–X	P–N	P–N–P	Association degree	Ref.
$[2\text{-}Me_2NCH_2)C_6H_4]Te[(SPPh_2)_2N]$[e]	2.550(1)	2.057(1)/1.945(1)	1.557(3)/1.612(3)	137.8(2)	Monomer	[151]
$(4\text{-}MeOC_6H_4)TeCl_2[(SP^iPr_2)_2N]$[f]	2.559(1)/2.623(1)	2.061(1)/2.041(2)	1.580(3)/1.580(3)	144.3(2)	Monomer	[146]
$(4\text{-}MeOC_6H_4)TeCl_2[(SP^iPr_2)(SPPh_2)N]$[g]	2.603(3)	2.015(4) $(S–P_{Ph})$	1.599(9)	139.0(6)	Monomer	[146]
	2.669(3)	2.029(4) $(S–P_{Pr})$	1.558(9)			
$Me_2Te[(SPPh_2)_2N]_2$	2.655(6)/3.345(8)	2.039(9)/1.96(1)	1.58(2)/1.61(2)	129(1)	Monomer	[152]
	2.631(7)/3.527(6)	2.05(1)/1.964(8)	1.54(2)/1.63(2)	133(1)		
$Me_2TeCl[(SPPh_2)_2N]$[h]	2.607(2)/3.367(2)	2.047(2)/1.964(2)	1.571(4)/1.599(4)	139.1(3)	Monomer	[152]
$Me_2TeI[(SPPh_2)_2N]$[i]	2.633(8)/3.361(8)	2.05(1)/1.97(1)	1.56(2)/1.62(2)	138(1)	Monomer	[152]
$Me_2TeCl[(OPPh_2)(SPPh_2)_2N]$[j]	2.14(2) (M–O)	1.56(1) (P–O)	1.56(2)	129(1)	Monomer	[152]
	3.413(7) (M–S)	1.973(8) (P–S)	1.64(2)			
$Ph_3Te[(OPPh_2)_2N]$	2.654(6)/2.928(6)	1.504(6)/1.496(6)	1.583(7)/1.572(7)	137.9(5)	Monomer	[153]
$Ph_3Te[(SPPh_2)_2N]$	3.264/3.451	1.983(4)/1.974(5)	1.594(9)/1.580(9)	137.6(6)	Monomer	[154]
$Ph_3Te[(OPPh_2)(SPPh_2)_2N]$	2.77(1) (M–O)	1.53(1) (P–O)	1.594(7)	139.5(5)	Monomer	[153]
	3.282(4) (M–S)	1.967(5) (P–S)	1.562(7)			

[a] Not given in the original paper.

[b] See the text.

[c] $Te–Cl_{bridging}$ 2.906(1), 2.923(1) Å.

[d] Bridging Te–S bond.

[e] Te(1)–N(2) 2.430(3) Å.

[f] Te–Cl 2.550(1), 2.529(1) Å.

[g] Te–Cl 2.505(3), 2.510(3) Å.

[h] Te(1)–Cl(1) 2.526(2) Å.

[i] Te(1)–I(1) 2.900(3) Å.

[j] Te(1)–Cl(1) 2.464(8) Å.

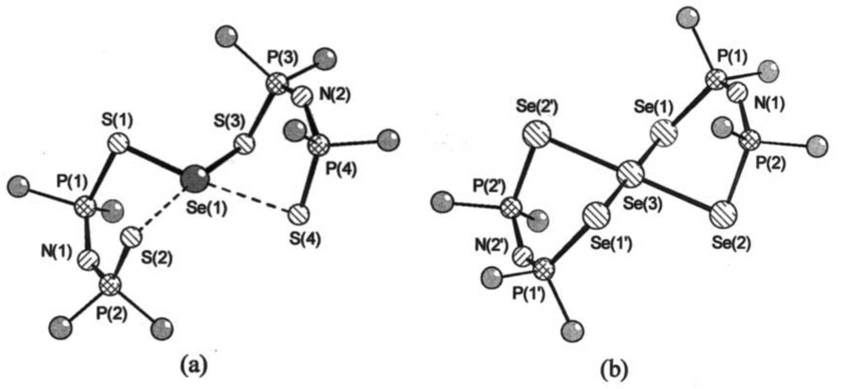

Fig. 40. The molecular structure of (a) Se[(SPPh$_2$)$_2$N]$_2$ [144], and (b) Se[(SePPh$_2$)$_2$N]$_2$ (molecule 1) [145] (for clarity, only *ipso* carbons of the phenyl groups attached to phosphorus atoms are shown).

complex, and the distorted boat Se(Se$_2$P$_2$N) chelate rings display a similar arrangement with respect to the planar SeS$_4$ core [Se(1)–Se–P 88.7(1)–97.1(1)°].

4.7.2. Tellurium

Apart from tin complexes, tellurium derivatives of imidodiphosphinato ligands are the most extensively investigated among main group elements.

Several inorganic tellurium(II) compounds containing either symmetric or asymmetric ligands, Te[(XPR$_2$)(XPR$'_2$)N]$_2$ (X = S, Se) (Table 25), have been described. When asymmetric ligands are present, *trans* and/or *cis* isomers are possible for square planar coordination of the tellurium atom, but only for the derivative Te[(SP^{i}Pr$_2$)(SPPh$_2$)N]$_2$, does the ^{31}P-NMR spectrum exhibit two sets of doublet resonances, indicating that both isomers are present in solution [146].

The solid state molecular structure of most of the Te[(XPR$_2$)(XPR$'_2$)N]$_2$ complexes have been investigated by X-ray diffraction and monomers exhibiting two coordination patterns established. With one exception, Te[(SPEt$_2$){SP(OPh)$_2$}N]$_2$, the overall molecular structure for the tellurium(II) complexes resembles the structure of the Se[(SePPh$_2$)$_2$N]$_2$ analog described above. Usually the TeX$_2$P$_2$N rings exhibits a pseudo-chair conformation, but for the two independent molecules found in the crystals of Te[(SePPh$_2$)$_2$N]$_2$ [148] both boat and chair forms are found for the corresponding heterocyclic rings. The square planar coordination geometry is achieved around the tellurium atom due to symmetrically coordinated imidodiphosphinato ligands, regardless of the nature of the chalcogen atoms or the organic groups attached to the phosphorus atoms. One of the two independent molecules found in the crystal of Te[(SPPh$_2$)$_2$N]$_2$ [147] is shown in Fig. 41 as a typical structure. It should be noted that for Te[(SP^{i}Pr$_2$)(SPPh$_2$)N]$_2$, the *trans* isomer was found in the solid state, where sulfur atoms belonging to the same type of SP^{i}Pr$_2$ and SPPh$_2$ groups occupy opposite corners of the square planar TeS$_4$ core [146].

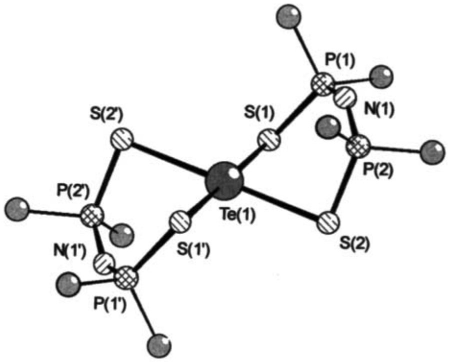

Fig. 41. The molecular structure of $Te[(SPPh_2)_2N]_2$ (molecule 1) [147] (for clarity, only *ipso* carbons of the phenyl groups attached to phosphorus atoms are shown).

In contrast, $Te[(SPEt_2)\{SP(OPh)_2\}N]_2$ [146] displays a molecular structure similar to $Se[(SPPh_2)_2N]_2$ [144]. A trapezoidal geometry of the TeS_4 core is achieved due to the clearly asymmetric monometallic biconnective pattern of the dithio ligands, i.e. *cis* short, covalent Te–S bonds [2.527(1), 2.513(1) Å] through chalcogen atoms belonging to the $SPEt_2$ groups, and weak, intramolecular Te···S interactions [2.91, 2.90 Å] established by the sulfur atoms of the $SP(OPh)_2$ units. The asymmetric coordination is also clearly reflected in the lengths of the phosphorus–sulfur and phosphorus–nitrogen bonds in a ligand unit.

The reaction of $TeCl_4$ with $(SPPh_2)_2NH$ in a 1:1 molar ratio resulted in the isolation of a mixed-ligand tellurium(II) complex, $(\mu\text{-Cl})_2[Te(SPPh_2)_2N]_2$, for which a dinuclear, centrosymmetric structure with symmetrically bridging chlorine atoms [$Te–Cl_{bridging}$ 2.906(1), 2.923(1) Å] was established by X-ray diffraction [149]. The dithio ligand is isobidentate [Te–S 2.498(1), 2.505(1) Å] and thus a slightly distorted square planar coordination geometry is achieved around tellurium [*trans* S–Te–Cl 173.11(3), 174.69(3)°]. The TeS_2P_2N rings are again of distorted chair conformation.

Both organo-tellurium(II) and tellurium(IV) derivatives of imidodiphosphinato ligands are known. The aryltellurium(II) derivatives, $RTe[(SPPh_2)_2N]$, were prepared either by reacting PhTe(ethylenthiourea)Cl with $NH_4[(SPPh_2)_2N]$ [150], or from $(4\text{-MeOC}_6H_4)TeCl_3$ and $K[(SPPh_2)_2N]$ (1:3 molar ratio), following a disproportionation process [148]. For both compounds the crystals contain centrosymetric dimeric associations built through asymmetric bridging dithio ligands, thus resulting in a 12-membered ring, as shown for the phenyltellurium derivative in Fig. 42a. The tellurium atom exhibits T-shaped coordination geometry with a 3c-4e S–Te–S system [S(1)–Te(1)–S(2′) 174.28(9)° for $R = Ph$, 174.20(8)° for $R = 4\text{-MeOC}_6H_4$]. A weak Te(1)···Te(1′) interaction [3.775(1) and 3.761(1) Å for $R = Ph$ and 4-$MeOC_6H_4$, respectively] *trans* to the Te–C bond is also found. If this bonding across the 12-membered ring is considered, the coordination around the tellurium atom becomes distorted square planar. Although the two phosphorus atom in the

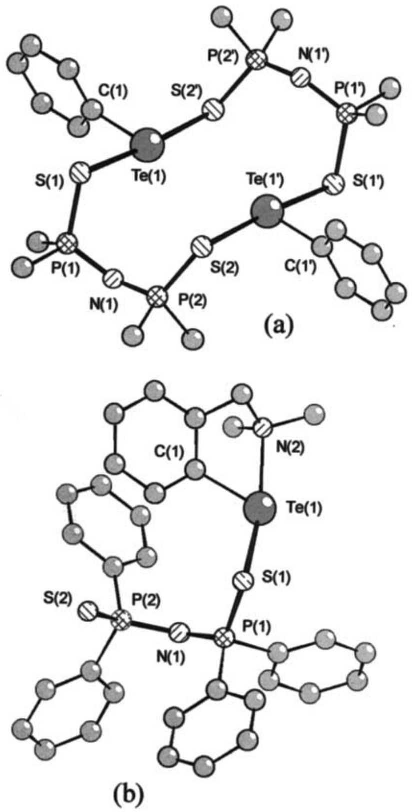

Fig. 42. (a) The dimeric association in the crystal of PhTe[$(SPPh_2)_2N$] [150] (for clarity, only *ipso* carbons of the phenyl groups attached to phosphorus atoms are shown), and (b) the molecular structure of [2-(Me_2NCH_2)C_6H_4]Te[$(SPPh_2)_2N$] [151].

ligand unit are not equivalent in the solid state, the ^{31}P-NMR spectrum of the 4-methoxyphenyltellurium(II) derivative exhibits only one singlet resonance, thus suggesting a fluxional process in solution [148].

The tetraphenyldithioimidodiphosphinato ligand is well known for its ability to act as a bidentate (chelating or bridging) moiety, i.e. both sulfur atoms being involved in coordination to a metal center. However, crystals of [2-(Me_2NCH_2)C_6H_4]Te[$(SPPh_2)_2N$] consist of monomeric molecules which also exhibit T-shaped geometry around the tellurium atom as a result of the strong intramolecular N–Te interaction which involves the nitrogen atom of the pendant CH_2NMe_2 arm [N(1)–Te(1) 2.430(3) Å, N(1)–Te(1)–S(1) 166.11(7)°] (Fig. 42b) [151]. The dithio ligand moiety is monodentate (monometallic monoconnective); only the S(1) atom being connected to tellurium [Te(1)–S(1) 2.5504(11) Å]. The second sulfur atom is not involved in either intramolecular [non-bonding Te(1)···S(2) 5.502 Å] or intermolecular interactions with a tellurium atom. The unusual behavior of the dithioimidodiphosphinato ligand in this complex is also reflected in different phosphorus–sulfur and phosphorus–nitrogen distances within the highly flexible SPNPS skeleton, which correspond to single [P(1)–S(1) 2.0568(13), P(2)–N(2) 1.612(3) Å] and double [P(2)–S(2) 1.9449(14), P(1)–N(2) 1.557(3) Å] bonds, respectively. A multinuclear NMR study provides evidence for the preservation of the monomeric structure of $[2\text{-}(Me_2NCH_2)C_6H_4]Te[(SPPh_2)_2N]$ in solution, i.e. monodentate dithio ligand and intramolecular N–Te coordination.

Organotellurium(IV) derivatives of imidodiphosphinato ligands, containing one, two or three organic groups attached to tellurium, have been described. When $(4\text{-}MeOC_6H_4)TeCl_3$ and $K[(SP^iPr_2)(SPR_2)N]$ (1:1 molar ratio) are mixed in methanol no disproportionation occurs and the mixed-ligand aryltellurium(IV) complexes, $(4\text{-}MeOC_6H_4)TeCl_2[(SP^iPr_2)(SPR_2)N]$ ($R = {}^iPr$, Ph) [146], are isolated as crystalline products. The ^{31}P-NMR data indicate the presence in solution of monomeric species with equivalent phosphorus atoms. The monomeric nature is also preserved in the solid state and the crystals contain monomers resulting in square pyramidal coordination around tellurium with the carbon in the apical position and a nearly perfect square planar $TeCl_2S_2$ system. Alternatively, the structure can be described as pseudo-octahedral, if the lone pair of electrons is considered to be *trans* to the carbon atom. The TeS_2P_2N rings are folded about the S···S axis with an almost planar S_2P_2N system [dihedral angle 108–109°].

The preparation and spectroscopic characterization of a variety of dimethyltellurium(IV) compounds of the type $Me_2Te[(XPPh_2)(SPPh_2)N]_2$ and $Me_2Te(Hal)[(XPPh_2)(SPPh_2)N]$ (X = O, S; Hal = Cl, Br, I) has been reported [152]. For some complexes full characterization, including single-crystal X-ray diffraction, was achieved, while the formation of the others was confirmed by multinuclear NMR spectroscopy. The compounds are monomeric in the solid state and the immediate environment about Te is that of a sawhorse structure in which the lone pair is apparently stereochemically active and occupying an equatorial position in a distorted pseudo-trigonal bipyramid.

In $Me_2Te[(SPPh_2)_2N]_2$ the axial positions are occupied by the sulfur atoms of the dithioimidophosphinato groups [S(1)–Te(1)–S(3) 169.6(2)°]. However, the apparently non-bonded S(2) and S(4) atoms are both oriented toward the tellurium center at Te···S distances of 3.345(8) and 3.572(6) Å, consistent with an asymmetric monometallic biconnective pattern of the dithio ligand. The orientation of the two dithio ligands thus results in a distorted octahedral environment about Te(1), in which the S(2) and S(4) atoms are essentially *trans* to carbon atoms of the methyl groups [C(1)···Te(1)···S(2) 166.7(7)°, C(2)–Te(1)···S(4) 164.9(7)°] (Fig. 43a). This behavior suggests an essentially inactive lone pair, or one with a high percentage of s-character [152].

The molecules of the two halodimethyltellurium(IV) derivatives, $Me_2TeCl[(SPPh_2)_2N]$ and $Me_2TeI[(SPPh_2)_2N]$ (Fig. 43b), contain the halogen atoms in one of the axial positions of the immediate pseudo-trigonal bipyramidal environment about tellurium [X(1)–Te(1)–S(1) 172.2(1) and 172.7(2)°, for X = Cl and I, respectively] [152]. The Te(1)–S(1) distances in these two halo complexes are apparently similar to those in the bis-substituted compound, which suggests that the halogen atoms exert minimal *trans* influence on the sulfur atoms in $(SPPh_2)_2N$. In the

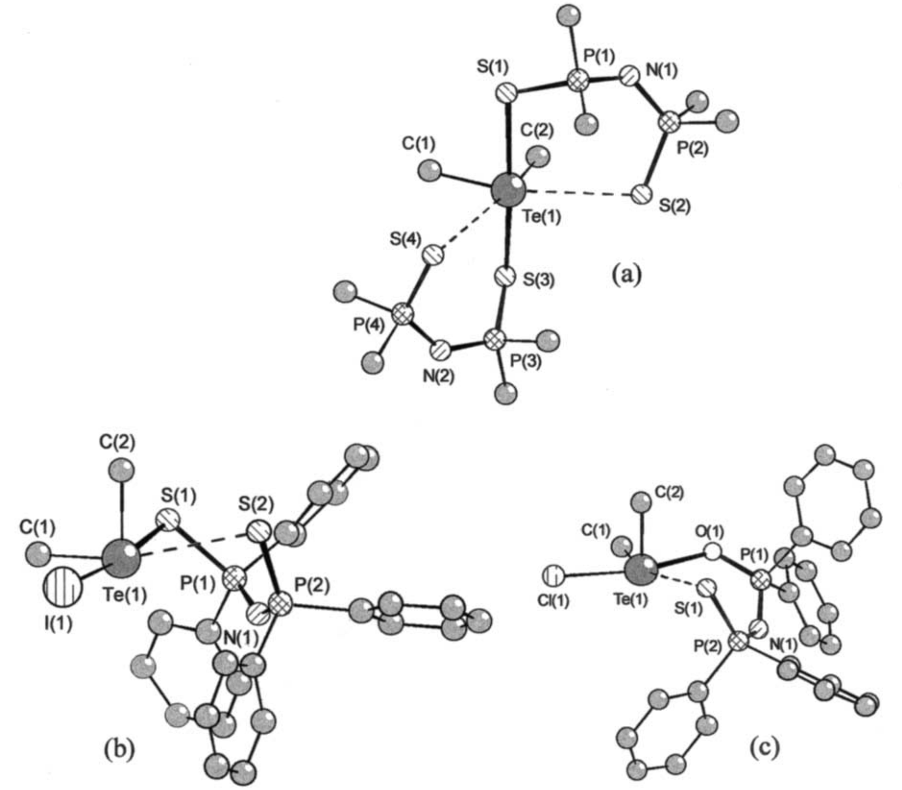

Fig. 43. The molecular structure of (a) $Me_2Te[(SPPh_2)_2N]_2$ (for clarity, only *ipso* carbons of the phenyl groups attached to phosphorus atoms are shown), (b) $Me_2TeI[(SPPh_2)_2N]$, and (c) $Me_2TeCl[(OPPh_2)(SPPh_2)N]$ [152].

halo-complexes, as with $Me_2Te[(SPPh_2)_2N]_2$, the dithioimidodiphosphinato group can be treated as an asymmetric bidentate ligand by assuming that the pendant S(2) atom is part of the coordinating sphere to give weak Te···S intramolecular interactions [Te(1)···S(2) 3.367(2) and 3.361(8) Å for X = Cl and I, respectively]. The orientation of the phosphorus ligand is identical, giving rise to a distorted square pyramidal arrangement about tellurium in both cases or a distorted pseudo-octahedral arrangement if the lone pair is now assumed to be occupying the position *trans* to the C(2) atom.

In all three dimethyltellurium(IV) dithioimidodiphosphinato complexes the short and long tellurium–sulfur distances can be correlated with the long and short phosphorus–sulfur bond lengths which are typical for single P–S and double P=S bonds. Consequently, the phosphorus–nitrogen bond lengths are also different, i.e. coresponding to double P=N and single P–N bonds [152].

The resulting TeS_2P_2N rings display different conformations. Thus in $Me_2Te[(SPPh_2)_2N]_2$ both six-membered rings may be discussed in terms of a boat with a variable degree of distortion, while in both halo derivatives the TeS_2P_2N rings are folded along the S(1)···S(2) axis [dihedral angle of 104.9 and 104.0° for X = Cl and I, respectively] [152].

The overall molecular structure of $Me_2TeCl[(OPPh_2)(SPPh_2)N]$ (Fig. 43c) is very similar to that described above for the dithio complexes [152]. However, in contrast to the halo-dithioimidodiphosphinato derivatives, the oxygen atom of the monothio ligand forms the primary bond to tellurium [Cl(1)–Te(1)–O(1) 168.9(4)°] and the S(1) atom establishes only a weak Te(1)···S(1) [3.413(7) Å] intramolecular interaction *trans* to the C(1) atom. This is contrary to what was observed in $Ph_3Te[(SPPh_2)(OPPh_2)N]$ where neither chalcogen forms a short bond (see subsequent discussion) [153]. The primary coordination of the monothioimidodiphosphinato ligand through the oxygen atom is consistent with the length of the P(1)–O(1) bond [1.56(1) Å], which is typical of a single phosphorus–oxygen bond. On the other hand, the P(2)–S(1) bond length [1.973(8) Å] is of a similar magnitude to those of the aniso-bonded sulfur atom in the dithio derivatives described above, and typical for a P=S double bond. Consequently, the phosphorus–nitrogen bond lengths are also different; their lengths being consistent with double P=N and single P–N bonds, and thus with the asymmetric monometallic biconnective pattern of the monothio ligand. The conformation of the $TeOSP_2N$ ring is similar to those displayed by the $Me_2TeX[(SPPh_2)_2N]$ derivatives, i.e. folded along the O(1)···S(1) axis [152].

Several triphenyltellurium(IV) complexes, $Ph_3Te[(XPR_2)(YPR'_2)N]$, have been described [153,154]. In some cases they were identified unequivocally by multinuclear NMR spectroscopy, but attempts to isolate them failed due to decomposition. However, the molecular structures of $Ph_3Te[(XPPh_2)_2N]$ (X = O (Fig. 44a) [153], S (Fig. 44b) [154]) and $Ph_3Te[(OPPh_2)(SPPh_2)_2N]$ (Fig. 44c) [153] were established by X-ray diffraction and reveal some interesting patterns. The compounds are monomeric with long tellurium–chalcogen interactions [Te(1)···O(1) 2.926(6) and Te(1)···O(2) 2.654(6) Å in $Ph_3Te[(OPPh_2)_2N]$, Te(1)···S(1) 3.264 and Te(1)···S(2) 3.451 Å in $Ph_3Te[(SPPh_2)_2N]$, and Te(1)···O(1) 2.77(1) and Te(1)···S(1) 3.282(4) in $Ph_3Te[(OPPh_2)(SPPh_2)_2N]$, respectively]. A question arises as to whether these weak tellurium–chalcogen interactions should be considered in discussing the coordination number and geometry of the central tellurium atom. If such interactions are ignored, the coordination geometry around tellurium, determined by the three phenyl groups, is trigonal pyramidal, with C–Te–C bond angles slightly larger than 90°. However, a comparison with the molecular dimensions observed for other organotellurium compounds [153,154] suggest that the chalcogens should be considered as part of the coordination sphere around tellurium. As a consequence, the immediate environment about tellurium can be described as pseudo-octahedral with the apparently stereochemically active lone pair occupying the axial position *trans* to a phenyl group from the Ph_3Te moiety. The other two phenyl groups and two long tellurium–chalcogen interactions complete the equatorial plane around tellurium.

The chelate rings normally formed by coordination of the bidentate imidodiphosphorus ligand to a metal center, can be considered in the case of

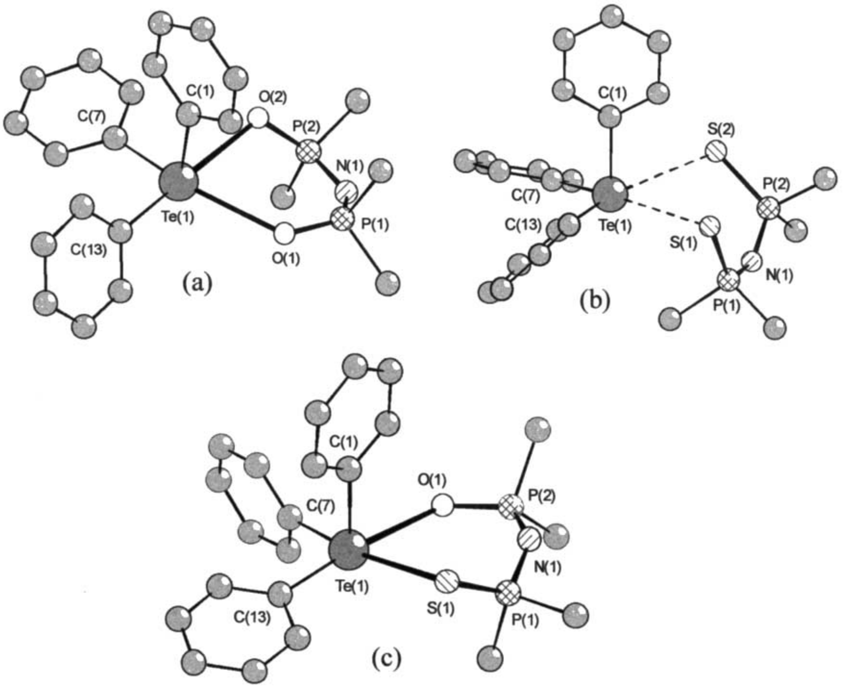

Fig. 44. The molecular structure of (a) $Ph_3Te[(OPPh_2)_2N]$ [153], (b) $Ph_3Te[(SPPh_2)_2N]$ [154], and (c) $Ph_3Te[(OPPh_2)(SPPh_2)N]$ [153] (for clarity, only *ipso* carbons of the phenyl groups attached to phosphorus atoms are shown).

$Ph_3Te[(XPR_2)(YPR'_2)N]$ complexes to be cation–anion association through Te···chalcogen secondary bonds, additional to electrostatic interactions. The resulting $TeXYP_2N$ rings may be discussed in terms of boat conformations with different degrees of distortion.

5. Concluding remarks

The increase in the number of relevant publications in the last few years is evidence of the current interest in the coordination chemistry of imidodiphosphorus ligands. This has resulted in the development of improved methods of synthesis and a larger diversity of $(XPR_2)(YPR'_2)NH$ compounds. Two common structural features in the molecular unit of imidodiphosphorus acids are the angular P–N–P system and the acidic hydrogen linked to nitrogen in the P_2NH fragment. Basically, the conformation of the X–P–N–P–Y skeleton can be discussed in terms of *anti* or *syn* with respect to the relative orientation of the phosphorus–chalcogen bonds. With few exceptions in the solid state, the molecules are linked through N–H···X=P hydrogen bonding, into dimeric or polymeric associations.

The coordination patterns of the $[(XPR_2)(YPR'_2)N]^-$ anions observed so far in complexes formed with main group metals, reflect the versatility of this type of ligand. Usually the two chalcogen atoms attached to the phosphorus atoms of the imidodiphosphorus ligand moiety are involved in coordination to the metal center, resulting in either *symmetric* (**24**) or *asymmetric* (**25**) *monometallic biconnective* ligand units. When different chalcogens are present, the asymmetric chelating behavior can be discussed in terms of primary bonds involving X or Y, as is found for example, in the case of the $PhSb[(OPPh_2)(SPPh_2)N]_2$ derivative (Section 4.6.1).

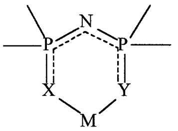

(24)

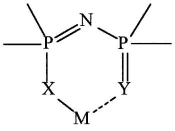

(25)

Although by far the most common behavior observed for the $[(XPR_2)(YPR'_2)N]^-$ ligands involves X,Y-chelation, several other coordination patterns occur to accommodate the requirements of the metal center, at least in the solid state. Thus, a few monomeric complexes containing a *monometallic monoconnective* (**26**) ligand unit, in which attachment to the metal is through only one chalcogen atom, were recently reported, i.e. $Me_3Sb[(OPPh_2)(SPPh_2)N]_2$ or $[2\text{-}(Me_2NCH_2)C_6H_4]Te[(SPPh_2)_2N]$.

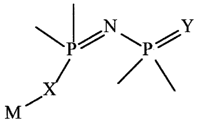

(26)

The use of both of the terminal chalcogen atoms in coordination of an $[(XPR_2)(YPR'_2)N]^-$ ligand is not limited to the formation of chelate structures, because *bimetallic biconnective* (bridging) (**27**) patterns are also possible, which result in both dimers and polymers, as illustrated by $[RTe\{(SPPh_2)_2N\}]_2$ and $[Me_3Sn\{(SPPh_2)_2N\}]_n$. An unusual biconnective pattern (**28**) is found in the lithium dimer $[Li\{(OPPh_2)(SPMe_2)N\}\cdot 2H_2O]_2$, in which only the oxygen atom of the ligand is involved in a bridge between two metal atoms.

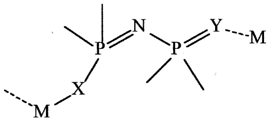

(27)

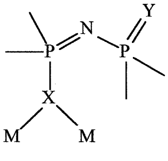

(28)

Bimetallic triconnective (**29**) and *trimetallic tetraconnective* (**30**) coordination, in which only the terminal chalcogen atoms are involved, results in dimers, as in

$[Na\{(OPPh_2)(SPPh_2)N\} \cdot 2THF]_2$, $[Cd\{(OPMe_2)(SPPh_2)N\}]_2$ and $[PhHg\{(OPR_2)(SPPh_2)N\}]_2$ (R = Me, Ph), hexamers, as in $[Na\{OP(OPh)_2\}_2N]_6$, or the trinuclear $K[Cd_2\{(OPPh_2)_2N\}_5]$.

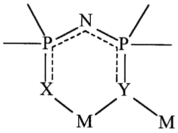

(29)

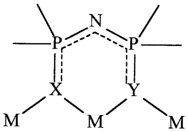

(30)

In some less common cases, the nitrogen atom of the X–P–N–P–Y skeleton is also used in coordination to the metal center. Thus, *O,N-bimetallic biconnective* (**31**) coordination occurs in the dimer, $[PhHg\{OP(OPh)_2\}_2N]_2$, in contrast to the *X,X,Y-bimetallic triconnective* (**29**) pattern observed in the monothioimidodiphosphinato analogs, $[PhHg\{(OPR_2)(SPPh_2)N\}]_2$ (R = Me, Ph). In other cases, the nitrogen appears to be involved in coordination in addition to both of the chalcogen atoms. Thus, consideration of a weak, transanular Bi···N interaction in the $[\{2\text{-}(Me_2NCH_2)C_6H_4\}Bi\{(XPPh_2)_2N\}]_2$ (X = S, Se) dimers suggests *X,X,N-monometallic triconnectivity* (**32**), while *S,S′,S′,S′,N-tetrametallic pentaconnectivity* (**33**) is found in the polymeric $[K\{(SPMe)_2N\}]_n$.

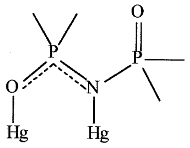

(31)

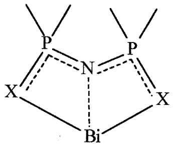

(32)

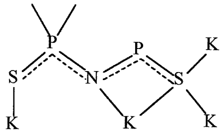

(33)

When phenyl groups are attached to phosphorus atoms, the coordination sphere around the central metal atom can be completed by π M···Ph interactions, thereby increasing the overall connectivity of the imidodiphosphorus ligand unit. Thus, one π Pb···Ph intramolecular interaction (**34**) is achieved in the dimer, $[Pb\{(OPPh_2)(SPPh_2)N\}_2]_2$, while two π Pb···Ph intramolecular interactions (**35**), which involve one aromatic group of each of the phosphorus atoms, occur in the monomer, $Pb[(SPPh_2)_2N]_2$. In contrast, two bridging π K···Ph interactions (**36**) are established by a dithio ligand unit in the polymeric $[K\{(SPPh)_2N\}]_n$. Moreover, polymeric associations in crystals of $[K(18\text{-crown-}6)][(XPPh_2)_2N]$ (X = S, Se) are realized only through π K···Ph interactions; none of the chalcogen atoms of the ligand unit being involved in coordination to the metal atoms (**37**).

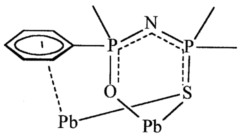

(34)

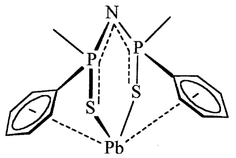

(35)

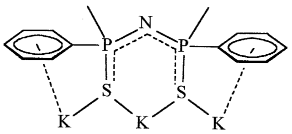

(36)

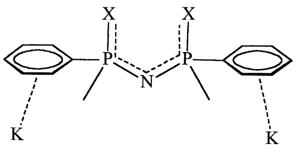

(37)

The presence of alkoxy or aryloxy groups on one or both of the phosphorus atoms in the $[(XPR_2)(YPR'_2)N]^-$ ligand provides new potential donor atoms since the oxygen atoms of these groups may also be involved in coordination to the metal center. Thus, in the polymeric association of $[K[\{OP(OEt)_2\}(SPPh_2)N] \cdot H_2O]_n$, the monothio ligand involves one oxygen atom of an ethoxy group in coordination to potassium, in addition to the terminal chalcogen atoms. This results in *O,O$_{ethoxy}$,S-bimetallic triconnectivity* (**38**) for one type of ligand unit, while the other one is also involved in a π K···Ph bridging interaction (**39**). An even more complicated pattern is found for some of the imidodiphosphorus ligand moieties in the $[Na\{OP(OPh)_2\}_2N]_6$ hexamer, i.e. *O,O′,O′,O$_{phenoxy}$,-trimetallic tetraconnective* (**40**) and *O,O,O,O′,O′,O′,O$_{phenoxy}$,-pentametallic heptaconnective* (**41**), respectively.

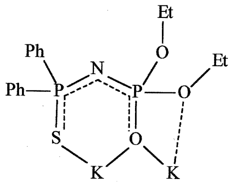

(38)

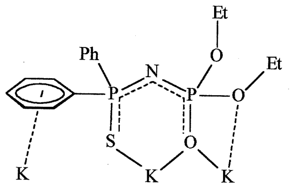

(39)

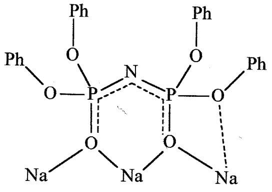

(40)

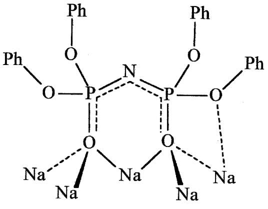

(41)

Structural investigations of main group metal complexes containing imidodiphosphorus ligands have also provided unusual examples of *isomerism*, e.g. molecules of $Sn[(SePPh_2)_2N]_2$ exhibiting square pyramidal or square-planar $SnSe_4$ cores, and *heterogeometrism*, e.g. $[K\{(SPMe)_2N\}]_n$ and $[K\{(SPPh)_2N\}]_n$.

In conclusion, the use of imidodiphosphorus ligands, $[(XPR_2)(YPR'_2)N]^-$, in research involving the coordination chemistry of main group metals is becoming an increasingly attractive field of investigation. This arises because the potential for variations in structures appears to be enormous and could lead to a wide range of applications. Changes in the nature of the organic groups and/or the chalcogen atoms attached to the phosphorus atoms can provide interesting results and this is especially true in the case of asymmetric chalcogen ligands and/or alkoxy/aryloxy ligands, where unusual supramolecular associations can be anticipated.

References

[1] J.R. Wasson, G.M. Woltermann, H.J. Stoklosa, Fortschr. Chem. Forsch. (Top. Curr. Chem.) 35 (1973) 65.
[2] I. Haiduc, Rev. Inorg. Chem. 3 (1981) 353.
[3] R.C. Mehrotra, G. Srivastava, B.P.S. Chauhan, Coord. Chem. Rev. 55 (1984) 207.
[4] E.R.T. Tiekink, Main Group Metal Chem. 15 (1992) 161.
[5] V.K. Jain, Coord. Chem. Rev. 135/136 (1994) 809.
[6] I. Haiduc, Phosphorus, Sulfur Silicon 93–94 (1994) 345.
[7] I. Haiduc, D.B. Sowerby, S.-F. Lu, Polyhedron 14 (1995) 3389.
[8] I. Haiduc, D.B. Sowerby, Polyhedron 15 (1996) 2469.
[9] C. Silvestru, I. Haiduc, Coord. Chem. Rev. 147 (1996) 117.
[10] I. Haiduc, Coord. Chem. Rev. 158 (1997) 325.
[11] A.V. Kirsanov, I.N. Zhmurova, Zh. Obshch. Khim. 28 (1958) 2478 (Chem. Abstr. 53 (1959) 3118).
[12] A. Schmidpeter, R. Böhm, H. Groeger, Angew. Chem. 76 (1964) 860.
[13] A. Schmidpeter, H. Groeger, Z. Anorg. Allg. Chem. 345 (1966) 106.
[14] A. Schmidpeter, K. Stoll, Angew. Chem. 79 (1967) 242 (Angew. Chem. Int. Ed. Engl. 6 (1967) 252).
[15] A. Schmidpeter, H. Brecht, H. Groeger, Chem. Ber. 100 (1967) 3063.
[16] A. Schmidpeter, H. Groeger, Chem. Ber. 100 (1967) 3979.
[17] A. Schmidpeter, K. Stoll, Angew. Chem. 80 (1968) 558 (Angew. Chem. Int. Ed. Engl. 7 (1968) 549).
[18] A. Schmidpeter, J. Ebeling, Chem. Ber. 101 (1968) 815.
[19] A. Schmidpeter, H. Brecht, J. Ebeling, Chem. Ber. 101 (1968) 3902.
[20] I. Haiduc, I. Silaghi-Dumitrescu, Coord. Chem. Rev. 74 (1986) 127.
[21] T.S. Lobana, Prog. Inorg. Chem. 37 (1989) 495.
[22] J.D. Woollins, J. Chem. Soc. Dalton Trans. (1996) 2893.
[23] J.D. Woollins, Main Group Chem. News 4 (1996) 12.
[24] C. Silvestru, J.E. Drake, R. Rösler, J. Yang, A. Silvestru, I. Haiduc, Phosphorus, Sulfur Silicon 124–125 (1997) 63.
[25] O. Navratil, M. Fofana, J. Smola, Z. Chem. 24 (1984) 30.
[26] E. Herrmann, O. Navratil, H. Nang, J. Smola, J. Friedrich, J. Prihoda, R. Dreyer, V.A. Chalkin, S. Kulpe, Collect. Czech. Chem. Commun. 49 (1984) 201.
[27] O. Navratil, E. Herrmann, P. Slezak, Collect. Czech. Chem. Commun. 52 (1987) 1708.
[28] O. Navratil, E. Herrmann, G. Grossmann, J. Teply, Collect. Czech. Chem. Commun. 55 (1990) 364.

[29] O. Navratil, E. Herrmann, Collect. Czech. Chem. Commun. 57 (1992) 1655.

[30] J.G.H. du Preez, K.U. Knabl, L. Krüger, B.J.A.M. van Brecht, Solvent Extr. Ion Exch. 10 (1992) 729.

[31] E. Herrmann, O. Navratil, P. Sladek, Phosphorus, Sulfur Silicon 109–110 (1996) 201.

[32] I. Rodriguez, C. Alvarez, J. Gomez-Lara, R.A. Toscano, N. Platzer, C. Mulheim, H. Rudler, J. Chem. Soc. Chem. Commun. (1987) 1502.

[33] C. Alvarez, L. Barhaoui, N. Goasdoue, J.C. Daran, N. Platzer, H. Rudler, J. Vaissermann, J. Chem. Soc. Chem. Commun. (1989) 1507.

[34] N. Platzer, H. Rudler, C. Alvarez, L. Barkaoui, B. Denise, N. Goasdoue, M.-N. Rager, J. Vaissermann, J.C. Daran, Bull. Soc. Chim. Fr. 132 (1995) 95.

[35] H. Witt, W. Kläui, in: The XVIII International Conference on Organometallic Chemistry, Munchen, Germany, Abstract B196, August 1998.

[36] S.W. Magennis, S. Parsons, A. Corval, J.D. Woollins, Z. Pikramenou, Chem. Commun. (1999) 61.

[37] H. Ishikawa, T. Kido, T. Umeda, H. Ohyama, Biosci. Biotech. Biochem. 56 (1992) 1882.

[38] P. Bhattacharyya, J.D. Woollins, Polyhedron 14 (1995) 3367.

[39] T.Q. Ly, J.D. Woollins, Coord. Chem. Rev. 176 (1998) 451.

[40] DIAMOND — Visual Crystal Structure Information System, CRYSTAL IMPACT, Postfach 1251, D-53002 Bonn.

[41] M.L. Nielsen, J.V. Pustinger Jr., J. Phys. Chem. 68 (1964) 152.

[42] B. Jirjahn, H. Hildebrandt, G. Heller, Z. Naturforsch. Teil. B 52 (1997) 95.

[43] N.V. Pavlenko, G.I. Matyushecheva, V.Ya. Semenii, L.M. Yagupol'skii, Zh. Obshch. Khim. 55 (1985) 1586 (Engl. Transl., p. 1411; Chem. Abstr. 105 (1986) 42926).

[44] D. Cupertino, D.J. Birdsall, A.M.Z. Slawin, J.D. Woollins, Inorg. Chim. Acta 287 (1999) 61.

[45] V.A. Gilyarov, E.N. Tsvetkov, M.I. Kabachnik, Zh. Obshch. Khim. 36 (1966) 274 (Chem. Abstr. 64 (1966) 17408).

[46] O.A. Mukhaceva, A.I. Razumov, Zh. Obshch. Khim. 32 (1962) 2696 (Chem. Abstr. 58 (1963) 9119).

[47] E.I. Matrosov, V.A. Gilyarov, M.I. Kabachnik, Izv. Akad. Nauk. SSSR Ser. Khim. (1965) 1331 (Chem. Abstr. 65 (1966) 16262).

[48] E. Fluck, F.L. Goldmann, Chem. Ber. 96 (1963) 3091.

[49] F.T. Wang, J. Najdzionek, K.L. Leneker, H. Wasserman, D.M. Braitsch, Synth. React. Inorg. Met.-Org. Chem. 8 (1978) 119.

[50] D.J. Williams, Inorg. Nucl. Chem. Lett. 16 (1980) 189.

[51] P. Bhattacharyya, A.M.Z. Slawin, M.B. Smith, J.D. Woollins, Inorg. Chem. 35 (1996) 3675.

[52] H. Nöth, Z. Naturforsch. Teil. B 37 (1982) 1491.

[53] K.L. Paciorek, Inorg. Chem. 3 (1964) 96.

[54] I.T. Gilson, H.H. Sisler, Inorg. Chem. 4 (1965) 273.

[55] K.I. Paciorek, R.H. Kratzer, Inorg. Chem. 5 (1966) 538.

[56] C. Silvestru, R. Rösler, A. Silvestru, J.E. Drake, unpublished results.

[57] C. Silvestru, J.E. Drake, R. Rösler, J. Yang, in preparation.

[58] E. Fluck, H. Richter, W. Schwarz, Z. Anorg. Allg. Chem. 498 (1983) 161.

[59] H. Nöth, E. Fluck, Z. Naturforsch. Teil. B 39 (1984) 744.

[60] G. Balazs, J.E. Drake, C. Silvestru, I. Haiduc, Inorg. Chim. Acta 287 (1999) 61.

[61] L. Riesel, G. Pich, C. Ruby, Z. Anorg. Allg. Chem. 430 (1977) 227.

[62] M.I. Kabachnik, V.A. Gilyarov, Izv. Akad. Nauk. SSSR Ser. Khim. (1961) 819 (Chem. Abstr. 55 (1961) 27014).

[63] V.V. Kireev, G.S. Kolesnikov, S.S. Titov, Zh. Obshch. Khim. 40 (1970) 2015.

[64] H. Richter, E. Fluck, H. Riffel, H. Hess, Z. Anorg. Allg. Chem. 496 (1983) 109.

[65] H. Richter, E. Fluck, W. Schwarz, Z. Naturforsch. Teil. B 35 (1980) 578.

[66] E. Herrmann, M. Nouaman, Z. Zak, G. Grossmann, G. Ohms, Z. Anorg. Allg. Chem. 620 (1994) 1879.

[67] S. Kulpe, I. Seidel, E. Hermann, Cryst. Res. Technol. 19 (1984) 661.

[68] M.L. Nielsen, J.V. Pustinger Jr., J. Strobel, J. Chem. Eng. Data 9 (1964) 167.

[69] H. Steinberger, W. Kuchen, Z. Naturforsch. Teil. B 29 (1974) 611.

[70] C. Silvestru, R. Rösler, I. Haiduc, R. Cea-Olivares, G. Espinosa-Perez, Inorg. Chem. 34 (1995) 3352.

[71] O. Siiman, J. Vetuskey, Inorg. Chem. 19 (1980) 1672.

[72] J. Bödeker, H. Zärtner, J. Prakt. Chem. 318 (1976) 149.

[73] D. Cupertino, R. Keyte, A.M.Z. Slawin, D.J. Williams, J.D. Woollins, Inorg. Chem. 35 (1996) 2695.

[74] D. Cupertino, R. Keyte, A.M.Z. Slawin, D.J. Williams, J.D. Woollins, Phosphorus, Sulfur Silicon 109–110 (1996) 193.

[75] D.C. Cupertino, R.W. Keyte, A.M.Z. Slawin, J.D. Woollins, Polyhedron 18 (1998) 707.

[76] R.A. Shaw, E.H.M. Ibrahim, Angew. Chem. Int. Ed. Engl. 6 (1967) 556.

[77] S. Husebye, K. Maartmann-Moe, Acta Chem. Scand. A 37 (1983) 439.

[78] P.B. Hitchcock, J.F. Nixon, I. Silaghi-Dumitrescu, I. Haiduc, Inorg. Chim. Acta 96 (1985) 77.

[79] G.P. McQuillan, I.A. Oxton, Inorg. Chim. Acta 29 (1978) 69.

[80] A.M.Z. Slawin, J. Ward, D.J. Williams, J.D. Woolins, Chem. Commun. (1994) 421.

[81] R. Rösler, J.E. Drake, C. Silvestru, J. Yang, I. Haiduc, G. Espinosa-Perez, J. Chem. Soc. Dalton Trans. (1998) 73.

[82] D.C. Cupertino, R.W. Keyte, A.M.Z. Slawin, J.D. Woollins, Polyhedron 18 (1998) 311.

[83] M. Nouaman, Z. Zak, E. Herrmann, O. Navratil, Z. Anorg. Allg. Chem. 619 (1993) 1147.

[84] L.M. Gilby, B. Piggott, Polyhedron 18 (1999) 1077.

[85] P. Bahttacharyya, J. Novasad, J. Phillips, A.M.Z. Slawin, D.J. Williams, J.D. Woollins, J. Chem. Soc. Dalton Trans. (1995) 1607.

[86] P. Bahttacharyya, A.M.Z. Slawin, D.J. Williams, J.D. Woollins, J. Chem. Soc. Dalton Trans. (1995) 2489.

[87] C.G. Pernin, J.A. Ibers, Acta Crystallogr. C 56 (2000) 376.

[88] R. Rösler, M. Stanciu, J. Yang, J.E. Drake, C. Silvestru, I. Haiduc, Phosphorus, Sulfur Silicon 132 (1998) 231.

[89] A.M.Z. Slawin, M.B. Smith, J.D. Woollins, J. Chem. Soc. Dalton Trans. (1996) 3659.

[90] J. Yang, J.E. Drake, S. Hernandez-Ortega, R. Rösler, C. Silvestru, Polyhedron 16 (1997) 4061.

[91] R. Rösler, J.E. Drake, C. Silvestru, J. Yang, I. Haiduc, J. Chem. Soc. Dalton Trans. (1996) 391.

[92] D.C. Cupertino, R.W. Keyte, A.M.Z. Slawin, J.D. Woollins, Polyhedron 17 (1998) 4216.

[93] P. Bhattacharyya, A.M.Z. Slawin, M.B. Smith, J. Chem. Soc. Dalton Trans. (1998) 2467.

[94] V.V. Korshak, I.A. Gribova, T.V. Artamonova, A.N. Bushmarina, Vysokomol. Soed. 2 (1960) 377.

[95] C.D. Schmulbach, Prog. Inorg. Chem. 4 (1962) 275.

[96] M.L. Nielsen, Inorg. Chem. 3 (1964) 1760.

[97] I. Ghesner, I. Negru-Pavel, J.E. Drake, C. Silvestru, I. Haiduc, in: The XVIII International Conference on Organometallic Chemistry, Munchen, Germany, Abstract A93, August 1998.

[98] S. Pohl, Chem. Ber. 109 (1976) 3122.

[99] C. Silvestru, H.J. Breunig, R. Rösler, O. Stanga, I. Haiduc, in: The XIII FECHEM Conference on Organometallic Chemistry, Lisbon, Portugal, Abstract P250, August–September 1999, p. 321.

[100] R.O. Day, R.R. Holmes, A. Schmidpeter, K. Stoll, L. Howe, Chem. Ber. 124 (1991) 2443.

[101] M. Rietzel, H.W. Roesky, K.V. Katti, H.G. Schmidt, R. Herbst-Irmer, M. Noltemeyer, G.M. Sheldrick, M.C.R. Symons, A. Abu-Raqabah, J. Chem. Soc. Dalton Trans. (1990) 2387.

[102] D. Fenske, R. Mattes, J. Löns, K.-F. Tebbe, Chem. Ber. 106 (1973) 1139.

[103] I. Ghesner, C. Palotas, A. Silvestru, C. Silvestru, J.E. Drake, Polyhedron 20 (2001) 1101.

[104] H. Bock, H. Schödel, Z. Havlas, E. Herrmann, Angew. Chem. 107 (1995) 1441.

[105] B.M. Dillard, PhD Dissertation, The University of Georgia, 1975; cited in Ref. [50].

[106] R. Cea-Olivares, M.A. Muñoz, Monatsh. Chem. 124 (1993) 471.

[107] R. Czernuszewicz, E. Maslowsky Jr., K. Nakamoto, Inorg. Chim. Acta 40 (1980) 199.

[108] R. Cea-Olivares, H. Nöth, Z. Naturforsch. Teil. B 42 (1987) 1507.

[109] R. Rösler, C. Silvestru, G. Espinosa-Perez, I. Haiduc, R. Cea-Olivares, Inorg. Chim. Acta 241 (1996) 47.

[110] K.H. Ebert, R. Cea-Olivares, V. Garcia-Montalvo, G. Espinosa-Perez, M.R. Estrada, J. Novosad, J.D. Woollins, Z. Naturforsch. Teil. B 51 (1996) 1145.

[111] I. Haiduc, R. Cea-Olivares, S. Hernandez-Ortega, C. Silvestru, Polyhedron 14 (1995) 2041.

[112] I. Haiduc, J. Zukerman-Schpector, E. Castellano, R. Cea-Olivares, Heteroatom Chem. 11 (2000) 244.

[113] G. Kräuter, S.K. Sunny, W.S. Rees Jr., Polyhedron 17 (1998) 391.

[114] V. Garcia-Montalvo, J. Novosad, P. Kilian, J.D. Woollins, A.M.Z. Slawin, P. Garcia y Garcia, M. Lopez-Cardoso, G. Espinosa-Perez, R. Cea-Olivares, J. Chem. Soc. Dalton Trans. (1997) 1025.

[115] M. Ghesner, O. Bumbu, A. Silvestru, J.E. Drake, C. Silvestru, in preparation.

[116] H. Richter, E. Fluck, H. Riffel, H. Hess, Z. Anorg. Allg. Chem. 491 (1982) 266.

[117] V. Garcia-Montalvo, R. Cea-Olivares, D.J. Williams, G. Espinosa-Perez, Inorg. Chem. 35 (1996) 3948.

[118] R.A. Toscano, G. Carreon, J. Valdes-Martinez, Monatsh. Chem. 123 (1992) 391.

[119] R. Cea-Olivares, V. Garcia-Montalvo, J. Novosad, J.D. Woollins, R.A. Toscano, G. Espinosa-Perez, Chem. Ber. 129 (1996) 919.

[120] R. Cea-Olivares, R.A. Toscano, S. Hernandez-Ortega, J. Novosad, V. Garcia-Montalvo, Eur. J. Inorg. Chem. (1999) 1613.

[121] K. Darwin, L.M. Gilby, P.R. Hodge, B. Piggott, Polyhedron 18 (1999) 3729.

[122] M.A. Muñoz-Hernandez, A. Singer, D.A. Atwood, R. Cea-Olivares, J. Organomet. Chem. 571 (1998) 15.

[123] J.S. Casas, A. Castineiras, I. Haiduc, A. Sanchez, J. Sordo, E.M. Vazquez-Lopez, Polyhedron 14 (1995) 805.

[124] R. Cea-Olivares, J. Novosad, J.D. Woollins, A.M.Z. Slawin, V. Garcia-Montalvo, G. Espinosa-Perez, P. Garcia y Garcia, Chem. Commun. (1996) 519.

[125] J.S. Casas, A. Castineiras, I. Haiduc, A. Sanchez, J. Sordo, E.M. Vazquez-Lopez, Polyhedron 13 (1994) 2873.

[126] V. Garcia-Montalvo, R. Cea-Olivares, G. Espinosa-Perez, Polyhedron 15 (1996) 829.

[127] C. Silvestru, I. Haiduc, R. Cea-Olivares, A. Zimbron, Polyhedron 13 (1994) 3159.

[128] R. Rösler, C. Silvestru, I. Haiduc, M. Gielen, F. Kayser, B. Mahieu, Main Group Metal Chem. 16 (1993) 435.

[129] I. Haiduc, C. Silvestru, H.W. Roesky, H.-G. Schmidt, M. Noltemeyer, Polyhedron 12 (1993) 69.

[130] L. Flores-Santos, R. Cea-Olivares, S. Hernandez-Ortega, R.A. Toscano, V. Garcia-Montalvo, J. Novosad, J.D. Woollins, J. Organomet. Chem. 544 (1997) 37.

[131] K.C. Molloy, M.F. Mahon, I. Haiduc, C. Silvestru, Polyhedron 14 (1995) 1169.

[132] R. Varga, J.E. Drake, C. Silvestru, Phosphorus, Sulfur Silicon (2001), in press.

[133] R. Varga, J.E. Drake, C. Silvestru, I. Haiduc, in: The XIII FECHEM Conference on Organometallic Chemistry, Lisbon, Portugal, Abstract P309, August–September 1999, p. 396.

[134] I. Silaghi-Dumitrescu, L. Silaghi-Dumitrescu, R. Cea-Olivares, Main Group Metal Chem. 22 (1999) 5.

[135] C. Silvestru, I. Haiduc, S. Klima, U. Thewalt, M. Gielen, J.J. Zuckerman, J. Organomet. Chem. 327 (1987) 181.

[136] I. Haiduc, C. Silvestru, F. Caruso, M. Rossi, M. Gielen, Rev. Roum. Chim. 39 (1994) 53.

[137] N.W. Alcock, J. Culver, S.M. Roe, J. Chem. Soc. Dalton Trans. (1992) 1477.

[138] C. Sreelatha, D.K. Srivastava, V.D. Gupta, H. Nöth, J. Chem. Soc. Dalton Trans. (1988) 407.

[139] M. Arca, A. Garau, F.A. Devillanova, F. Isaia, V. Lippolis, G. Verani, Z. Anorg. Allg. Chem. 625 (1999) 517.

[140] D.J. Williams, J.B. Travis, K.L. Bergbauer, J. Coord. Chem. 16 (1987) 315.

[141] D.J. Williams, C.O. Quicksall, K.M. Barkigia, Inorg. Chem. 21 (1982) 2097.

[142] G. Balazs, H.J. Breunig, J.E. Drake, I. Ghesner, A. Silvestru, Phosphorus, Sulfur Silicon (2001), in press.

[143] C. Silvestru, R. Rösler, I. Haiduc, R.A. Toscano, D.B. Sowerby, J. Organomet. Chem. 515 (1996) 131.

[144] S. Husebye, K. Maartmann-Moe, Acta Chem. Scand. A 37 (1983) 219.

[145] R. Cea-Olivares, G. Canseco-Melchor, V. Garcia-Montalvo, S. Hernandez-Ortega, J. Novosad, Eur. J. Inorg. Chem. (1998) 1573.

[146] D.J. Birdsall, J. Novosad, A.M.Z. Slawin, J.D. Woollins, J. Chem. Soc. Dalton Trans. (2000) 438.

[147] S. Bjoernevag, S. Husebye, K. Maartmann-Moe, Acta Chem. Scand. A 36 (1982) 195.
[148] J. Novosad, S.V. Lindeman, J. Marek, J.D. Woollins, S. Husebye, Heteroatom Chem. 9 (1998) 615.
[149] J. Novosad, K.W. Törnroos, M. Necas, A.M.Z. Slawin, J.D. Woollins, S. Husebye, Polyhedron 18 (1999) 2861.
[150] S. Husebye, K. Maartmann-Moe, O. Mikalsen, Acta Chem. Scand. 44 (1990) 802.
[151] J.E. Drake, M.B. Hursthouse, M. Kulcsar, M.E. Light, A. Silvestru, J. Organomet. Chem. 623 (2001) 153.
[152] J.E. Drake, R.J. Drake, A. Silvestru, J. Yang, Can. J. Chem. 77 (1999) 356.
[153] J.E. Drake, A. Silvestru, J. Yang, I. Haiduc, Inorg. Chim. Acta 271 (1998) 75.
[154] A. Silvestru, I. Haiduc, R.A. Toscano, H.J. Breunig, Polyhedron 14 (1995) 2047.